UNIVERSITY OF AMSTERDAM

UvA-DARE (Digital Academic Repository)

A search for new resonances in multiple final states with a high transverse momentum Z boson in √s = 13 TeV pp collisions with the ATLAS detector

The ATLAS collaboration

DOI
10.1007/JHEP06(2023)036

Publication date
2023

Document Version
Final published version

Published in
Journal of High Energy Physics

License
CC BY

Link to publication

Citation for published version (APA):
The ATLAS collaboration (2023). A search for new resonances in multiple final states with a high transverse momentum *Z* boson in √s = 13 TeV *pp* collisions with the ATLAS detector. *Journal of High Energy Physics*, *2023*(6), Article 036. https://doi.org/10.1007/JHEP06(2023)036

General rights
It is not permitted to download or to forward/distribute the text or part of it without the consent of the author(s) and/or copyright holder(s), other than for strictly personal, individual use, unless the work is under an open content license (like Creative Commons).

Disclaimer/Complaints regulations
If you believe that digital publication of certain material infringes any of your rights or (privacy) interests, please let the Library know, stating your reasons. In case of a legitimate complaint, the Library will make the material inaccessible and/or remove it from the website. Please Ask the Library: https://uba.uva.nl/en/contact, or a letter to: Library of the University of Amsterdam, Secretariat, P.O. Box 19185, 1000 GD Amsterdam, The Netherlands. You will be contacted as soon as possible.

UvA-DARE is a service provided by the library of the University of Amsterdam (https://dare.uva.nl)

Download date:07 Sept 2026

Published for SISSA by Springer

Received: October 3, 2022
Accepted: April 11, 2023
Published: June 7, 2023

A search for new resonances in multiple final states with a high transverse momentum Z boson in $\sqrt{s} = 13$ TeV pp collisions with the ATLAS detector

The ATLAS collaboration

E-mail: atlas.publications@cern.ch

Abstract: A generic search for resonances is performed with events containing a Z boson with transverse momentum greater than 100 GeV, decaying into e^+e^- or $\mu^+\mu^-$. The analysed data collected with the ATLAS detector in proton-proton collisions at a centre-of-mass energy of 13 TeV at the Large Hadron Collider correspond to an integrated luminosity of 139 fb^{-1}. Two invariant mass distributions are examined for a localised excess relative to the expected Standard Model background in six independent event categories (and their inclusive sum) to increase the sensitivity. No significant excess is observed. Exclusion limits at 95% confidence level are derived for two cases: a model-independent interpretation of Gaussian-shaped resonances with the mass width between 3% and 10% of the resonance mass, and a specific heavy vector triplet model with the decay mode $W' \to ZW \to \ell\ell qq$.

Keywords: Beyond Standard Model, Hadron-Hadron Scattering, Particle and Resonance Production

ArXiv ePrint: 2209.15345

Open Access, Copyright CERN,
for the benefit of the ATLAS Collaboration.
Article funded by SCOAP^3.

https://doi.org/10.1007/JHEP06(2023)036

JHEP06(2023)036

Contents

1 Introduction **1**

2 ATLAS detector **3**

3 Data and simulated event samples **4**

4 Object selection **6**

5 Event selection and classification **8**

6 Search for narrow resonances **8**
- 6.1 Background modelling 8
- 6.2 Search strategy 9
- 6.3 BumpHunter search results 11

7 Model-independent and model-dependent interpretations **16**
- 7.1 Systematic uncertainty and statistical methodology 16
- 7.2 Constraints on a generic Gaussian-shaped signal for a model-independent interpretation 16
- 7.3 Constraint on a $W' \to ZW$ signal in an HVT model 17

8 Conclusion **20**

A Merged-e^+e^- identification **25**

B Signal-sensitive mass range **26**

C Limit-sensitive mass range **28**

The ATLAS collaboration **38**

JHEP06(2023)036

1 Introduction

One of the key components of the Large Hadron Collider (LHC) physics programme is the search for new resonances predicted by hypotheses for physics beyond the Standard Model (BSM) [1–9]. A large number of searches have been performed in proton-proton (pp) collisions at the LHC. Most searches are optimised for some specific final states motivated by a particular BSM model, or a class of models, and are therefore model-dependent, e.g. those associated with a Z boson [10–31]. No new physics has been found so far by these model-specific searches. To expand the search program, generic searches can be sensitive to

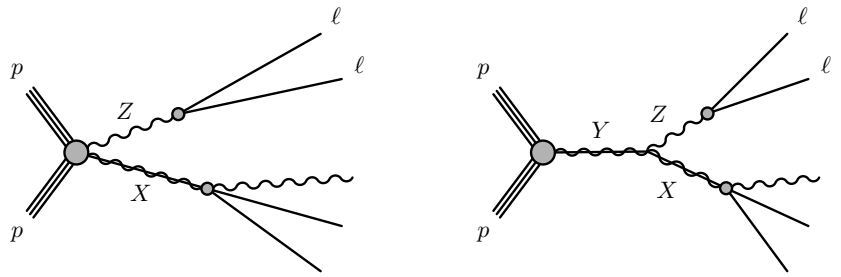

Figure 1. Schematic diagrams for (a) $pp \to ZX$ and (b) $pp \to Y \to ZX$ where Y is a new resonance to be searched for while X can be a new resonance or SM particle.

models that do not have the same characteristics of those already searched for and give more ability for reinterpretation for theories yet to be proposed.

This article presents a generic resonance search with both model-independent and model-dependent interpretations in events with a leptonically decaying Z boson with high transverse momentum, p_{T}. It is generic since the search is performed in multiple final states and it is sensitive to new particles in various production and decay modes. It is also model-independent since minimal features of BSM physics are assumed. Specifically, BSM processes are assumed to produce a resonance decaying into high-transverse-momentum objects, in association with, or including, a Z boson, whereas the SM background is assumed to be smoothly falling over the observables of interest. Two generic cases are considered, as shown schematically in figure 1: $pp \to ZX$, where the new resonance, represented as X, decays to a final state of SM particles, and $pp \to Y \to ZX$, where the resonance appears in production as an intermediate state Y that subsequently decays into a Z boson and SM particles, possibly via another intermediate resonance X. To probe a variety of possible BSM processes in a single analysis, events are separated into six exclusive categories according to the identity of the leading-p_{T} object in X. The leading-p_{T} object can be an electron, a muon, a photon, a small-R jet reconstructed with a radius parameter of $R = 0.4$ containing a b-hadron, a small-R jet without a b-hadron, or a large-R jet with $R = 1$. Invariant mass distributions of all the visible objects in the final state, either excluding the leptons from the Z boson decay (m_X) or including the leptons from the Z decay (m_{ZX}) in each of the six event categories, are defined as observables of interest. The distributions are examined with the BumpHunter algorithm [32, 33] for local excesses above a data-driven estimate of the smoothly falling SM background. Depending on the event categories and mass observables, the search is performed so as to be sensitive to a large mass range from around 200 GeV up to 6 TeV.

Generic searches with minimal beyond-the-SM signal assumptions were performed by the D0 Collaboration [34–37] and the CDF Collaboration [32, 38] at the Tevatron, and by the H1 Collaboration [39, 40] at HERA. At the LHC, a general search was performed by each of the ATLAS [41] and CMS [42] collaborations, using 3.2 fb^{-1} and 35.9 fb^{-1} of data at a centre-of-mass energy ($\sqrt{s}$) of 13 TeV, respectively. ATLAS also performed searches in final states containing two-leptons as well as in three- and four-leptons [43, 44]. However, final

JHEP06(2023)036

states including a Z resonance were not explicitly considered in general searches although decays through weak bosons are often possible in BSM models. Requiring a high-p_{T} Z boson may reduce the background enough to reveal signals which are not visible in an inclusive sample and also explores a signature not explicitly considered in previous general searches. Furthermore, a leptonically decaying Z boson is a fully reconstructable final state with straightforward ways to reduce the multijet background which is challenging to model.

The analysis uses the full data sample from $\sqrt{s} = 13\,\mathrm{TeV}$ pp collisions recorded by the ATLAS detector in Run 2 at the LHC, corresponding to an integrated luminosity of $139\,\mathrm{fb}^{-1}$. The results are interpreted in a model-independent way in terms of Gaussian-shaped signals with relative mass widths of 3%, 5%, and 10% for all the event categories. Furthermore, the results from the dominant leading large-R-jet event category are interpreted in a Heavy Vector Triplet (HVT) model [45, 46] in order to demonstrate the sensitivity of the analysis.

2 ATLAS detector

The ATLAS detector [47] covers nearly the entire solid angle around the collision point.[1] It consists of an inner tracking detector (ID) surrounded by a thin superconducting solenoid providing a 2 T axial magnetic field, electromagnetic (EM) and hadronic calorimeters, and a muon spectrometer (MS).

The ID provides charged-particle tracking in the range $|\eta| < 2.5$. It consists of silicon pixel, silicon microstrip, and transition radiation tracking detectors. The high-granularity silicon pixel detector covers the vertex region and typically provides four measurements per track, the first hit normally being in the insertable B-layer [48, 49]. It is followed by the silicon microstrip tracker, which usually provides eight measurements per track. These silicon detectors are complemented by the transition radiation tracker, which enables radially extended track reconstruction up to $|\eta| = 2.0$ and contributes to electron identification.

Lead/liquid-argon (LAr) sampling calorimeters provide EM energy measurements with high granularity. A steel/scintillator-tile hadronic calorimeter covers the central pseudorapidity range ($|\eta| < 1.7$). The end-cap and forward regions are instrumented with LAr calorimeters for both the EM and hadronic energy measurements up to $|\eta| = 4.9$. For $|\eta| < 2.5$, the EM calorimeter is divided into three layers longitudinal in shower depth, which are finely segmented in η and ϕ, particularly in the first layer. This segmentation allows measurements of the lateral and longitudinal shower profile, and the calculation of shower shapes [50] used for particle identification and background rejection. The longitudinal segmentation of the EM calorimeter is also exploited to calibrate the energy response to electron and photon candidates [50].

The MS comprises separate trigger and high-precision tracking chambers measuring the deflection of muons in a magnetic field generated by superconducting air-core toroids. The

[1] The ATLAS experiment uses a right-handed coordinate system with its origin at the nominal interaction point (IP) in the centre of the detector and the z-axis along the beam pipe. The x-axis points from the IP to the centre of the LHC ring, and the y-axis points upwards. Cylindrical coordinates (r, ϕ) are used in the transverse plane. The polar angle (θ) is measured from the positive z-axis and the azimuthal angle (ϕ) is measured from the positive x-axis in the transverse plane. The pseudorapidity is defined as $\eta = -\ln\tan(\theta/2)$. Angular distance is measured in units of $\Delta R \equiv \sqrt{(\Delta\eta)^2 + (\Delta\phi)^2}$.

JHEP06(2023)036

precision chamber system covers the region $|\eta| < 2.7$ with three layers of monitored drift tubes, complemented by cathode-strip chambers in the forward region, where the background is highest. The muon trigger system covers the range $|\eta| < 2.4$ with resistive-plate chambers in the barrel, and thin-gap chambers in the end-cap regions.

A two-level trigger system [51] was used during the 2015–2018 data-taking period. The first-level trigger (L1) is implemented in hardware and uses a subset of the detector information. This is followed by a software-based high-level trigger, which runs algorithms similar to those in the offline reconstruction software, reducing the event rate to approximately 1 kHz from the maximum L1 rate of 100 kHz.

An extensive software suite [52] is used in data simulation, in the reconstruction and analysis of real and simulated data, in detector operations, and in the trigger and data acquisition systems of the experiment.

3 Data and simulated event samples

The analysed data comprise the full ATLAS pp collisions at $\sqrt{s} = 13$ TeV collected from 2015 to 2018, corresponding to an integrated luminosity of 139 fb^{-1} after data quality requirements [53] were imposed to ensure that all the subdetectors were operating normally.

Candidate signal events are selected using triggers [54, 55] that require either a single isolated lepton or a pair of isolated leptons, targeting leptonic decays of the Z bosons. Selecting Z bosons with p_{T} greater than 100 GeV, decaying into e^+e^- or $\mu^+\mu^-$, reduces the SM background contribution and provides a clean sample with high trigger efficiencies. For the single-lepton triggers, the minimum p_{T} thresholds vary between 24 GeV and 26 GeV for electrons and between 20 GeV and 26 GeV for muons, depending on the data-taking period. For the dilepton triggers, the minimum p_{T} thresholds vary between 12 GeV and 17 GeV for electrons and between 10 GeV and 14 GeV for muons. These triggers are complemented with jet triggers [56] with minimum p_{T} thresholds of 360 GeV for events with relatively small angular separation between two electron candidates (merged-e^+e^- candidates, discussed in section 4). The overall trigger efficiency per event as measured in simulated $Z+$jets events is about 96% at low p_{T}^Z down to 100 GeV and increases to above 99% for $p_{\mathrm{T}}^Z \gtrsim 600$ GeV in the muon channel, and it is above 99% for the entire considered p_{T}^Z range in the electron channel.

The SM background originates mainly from production of $Z+$jets, dibosons (ZZ, ZW, $Z\gamma$), top-quark pairs ($t\bar{t}$), and single top quarks. The combination of the SM background processes is expected to yield smoothly falling spectra in the considered mass observables. A data-driven method using a functional fit is employed to model the contributions from the SM background in the invariant mass distributions. However, simulated Monte Carlo (MC) samples are used to optimise the analysis, to select fit functions for both observables, and to determine the corresponding fitting ranges.

The production of a Z boson in association with jets was modelled by the Sherpa 2.2.1 [57] generator with the NNPDF3.0nnlo parton distribution function (PDF) set [58]. Diagrams with up to two additional parton emissions were simulated at next-to-leading-order (NLO) accuracy in QCD, and with three or four additional parton emissions at leading-order (LO) accuracy [59]. Matrix elements were merged with the Sherpa

JHEP06(2023)036

parton shower using the MEPS@NLO formalism [59]. An alternative sample was generated with POWHEG BOX v1 [60–63] at NLO accuracy in QCD, and it was interfaced to PYTHIA 8.186 [64] for the modelling of the parton shower, hadronisation, and underlying event, with a set of tuned parameters called to the AZNLO tune [65]. The CT10NLO PDF set [66] was used for the hard-scattering processes, whereas the CTEQ6L1 PDF set [67] was used for the parton shower.

Diboson production with leptonic final states was simulated using SHERPA 2.2.2. The matrix elements were calculated using the NNPDF3.0NNLO PDF set. Processes with up to one additional parton emission were calculated at NLO accuracy in QCD, while processes with two or three parton emissions were modelled at LO accuracy. The various jet-multiplicity final states were merged using the MEPS@NLO formalism. Diboson production with semileptonic decays was modelled using SHERPA 2.2.1 and the same PDF set.

The production of a top-quark pair $t\bar{t}$ and the associated production of a single top quark and a W boson (Wt) were modelled using POWHEG BOX v2 [68] interfaced to PYTHIA 8.210 with the A14 parton shower tune [69]. The matrix elements were calculated at NLO precision in QCD using the NNPDF3.0NLO PDF set and assuming a top-quark mass of 172.5 GeV. The $t\bar{t}$ production cross section is normalised to the prediction from the TOP++ 2.0 program at next-to-next-to-leading order (NNLO) in perturbative QCD, including soft-gluon resummation calculated to next-to-next-to-leading-logarithm (NNLL) precision [70].

Contributions from multi-jet and $W+$jets processes, which cannot be estimated reliably from simulations, are found to be negligible when using data-driven techniques similar to those applied in ref. [71].

For the model-dependent interpretation, HVT signal samples with the coupling strength to SM gauge bosons, g_V, set to 1, referred to as model A, and $g_V = 3$, referred to as model B, are used. Both of them have the same decay channel, $W' \to ZW \to \ell\ell qq$. The sample was generated using MADGRAPH5_AMC@NLO [72] interfaced to PYTHIA 8.186 with the NNPDF2.3LO PDF set [73]. Thirteen signal mass points were simulated, ranging from 500 GeV to 6 TeV. The reconstructed W' resonance mass can be modelled by a double-sided Crystal Ball function [74, 75]. Acceptance times efficiency, $\mathcal{A} \times \epsilon$, values of up to 50% are found for these signal models in the dominant leading large-R-jet category.

All background and signal samples were processed through a GEANT4-based simulation [76, 77] of the ATLAS detector. The effect of multiple interactions in the same and neighbouring bunch crossings (pile-up) was modelled by overlaying the simulated hard-scattering event with inelastic pp collision events generated with PYTHIA 8.186 using the NNPDF2.3LO PDF set and the A3 tune [78]. The MC simulated events are weighted to match the distribution of the number of reconstructed pile-up vertices observed in different data-taking periods. Scale factors are applied to the simulated events to account for any remaining differences between observed and simulated data.

JHEP06(2023)036

4 Object selection

Selected events are required to have at least one primary vertex [79] with at least two associated tracks, each with $p_{\mathrm{T}} > 500\,\mathrm{MeV}$. In each event, only the primary vertex with the highest sum of squared transverse momenta of contributing tracks, hereafter denoted by $\sum p_{\mathrm{T}}^2$, is considered.

Muons are reconstructed either by combining ID and MS tracks that have consistent trajectories and curvatures or as stand-alone MS tracks [80, 81]. The muon candidates used in this analysis are required to have $p_{\mathrm{T}} > 25\,\mathrm{GeV}$ and $|\eta| < 2.7$. They are also required to pass the 'Medium' selection for $p_{\mathrm{T}} > 25\,\mathrm{GeV}$ and the 'HighPt' selection for $p_{\mathrm{T}} > 300\,\mathrm{GeV}$. The efficiency for identifying a single muon is about 99% for $p_{\mathrm{T}} < 300\,\mathrm{GeV}$ and around 80% for $p_{\mathrm{T}} > 300\,\mathrm{GeV}$.

Electrons are reconstructed from clusters of energy deposits in the EM calorimeter that match a track reconstructed in the ID. Reconstructed electrons are identified using likelihood identification criteria [50, 82]. The electron candidates are required to have $p_{\mathrm{T}} > 25\,\mathrm{GeV}$. They are also required to pass the 'MediumLH' selection and be within $|\eta| < 2.47$, excluding the transition region between the barrel and end-caps in the LAr calorimeter ($1.37 < |\eta| < 1.52$).

To ensure that lepton candidates originate from the interaction point, the likelihood-based electrons (muons) must satisfy $|d_0|/\sigma_{d_0} < 5\,(3)$, and both lepton types must satisfy $|z_0 \sin\theta| < 0.5$ mm. Here, d_0 is the transverse impact parameter of the lepton measured relative to the primary vertex, σ_{d_0} is the uncertainty in d_0, and z_0 is the longitudinal distance between the position of the primary vertex and the position of the track at the point of closest approach. In addition, electron and muon candidates are required to be isolated from other tracks and calorimetric activity by applying p_{T}- and η-dependent isolation criteria. For both the electron and muon candidates, the calorimeter isolation is based on the sum of the transverse energies of topological clusters [83] within a cone of size $\Delta R = 0.2$ around each lepton. The track isolation is computed by summing the transverse momenta of selected tracks within a cone of p_{T}^{ℓ}-dependent size around the lepton track. The efficiency of the isolation requirements is 95% for muons from Z bosons with $p_{\mathrm{T}} > 100\,\mathrm{GeV}$. For electrons, it is 90% but decreases for Z bosons with $p_{\mathrm{T}} > 450\,\mathrm{GeV}$ as the electron signatures begin to overlap.

If a $Z \to e^+e^-$ decay has a sufficiently large Lorentz boost, the e^+e^- angular separation becomes small enough for the e^+e^- pair to merge and fail the electron isolation requirements. The merged e^+e^- pairs are then reconstructed as jets, and a boosted decision tree (BDT) algorithm [84, 85] is used to separate merged-e^+e^- candidates from hadronic jets. This BDT identification is only applied when there is no Z boson candidate from either an e^+e^- pair or a $\mu^+\mu^-$ pair in the event. The input variables for the BDT include the jet's calorimeter- and ID-track-related properties and kinematic information. More details are given in appendix A. The combined efficiency of the resolved and merged identification for an e^+e^- pair forming a Z boson candidate is around 80% with weak p_{T} dependence.

Photon candidates are reconstructed from dynamic, variable-size topological clusters of cells with significant energy in the EM calorimeter and, possibly, matching tracks

JHEP06(2023)036

reconstructed in the inner detector [86]. The photon candidates are classified as 'converted' if two tracks forming a conversion vertex, or one track with the signature of an electron track but without hits in the innermost pixel layer, are matched to the cluster; otherwise, they are labelled as 'unconverted'. They are identified by using variables that characterise the lateral and longitudinal shower development in the EM calorimeter and the energy fraction leaking into the hadronic calorimeter. Photons used in this analysis are required to pass the 'Tight' selection [50, 53] for transverse energy $E_{\mathrm{T}} > 25\,\mathrm{GeV}$ and be within $|\eta| < 2.37$, excluding the same transition region between the barrel and end-caps in the LAr calorimeter as for electrons. The selection has an efficiency of 82%–92% (75%–92%) for unconverted (converted) photon candidates depending on E_{T} and η. The fractions of the unconverted and converted photon candidates are about 68% and 32%, respectively. The photon isolation requirement is based on the amount of transverse energy inside a cone of size $\Delta R = 0.4$. The efficiency of the isolation requirement is 75%–90% (∼70%) for unconverted (converted) photon candidates.

Small-R jets are reconstructed using the particle-flow algorithm [87], which considers both tracker and calorimeter information, using the anti-k_t algorithm [88] with a radius parameter of $R = 0.4$ implemented in the FastJet package [89]. The four-momenta of these small-R jets are calculated as the sum of the four-momenta of their constituents. Jets are corrected using p_{T}- and η-dependent scale factors to account for the calorimeter's non-compensating response, signal losses due to noise-threshold effects, energy lost in passive material, and contributions from pile-up interactions, as described in ref. [90].

The jets are required to have $p_{\mathrm{T}} > 30\,\mathrm{GeV}$ and $|\eta| < 2.4$. To suppress jets that originate from pile-up, a jet-vertex tagger using the 'Tight' working point [91] is applied to jets with $p_{\mathrm{T}} < 60\,\mathrm{GeV}$ and $|\eta| < 2.4$. To avoid double counting, jets of any transverse momentum are discarded if they are within a cone of size $\Delta R = 0.2$ around an electron or a photon, or if they have fewer than three associated tracks and are within a cone of size $\Delta R = 0.2$ around a muon. However, jets discarded due to an overlap with a reconstructed electron are still considered when testing for a merged-e^+e^- candidate. If a remaining jet with three or more associated tracks is within a cone of size $\Delta R = 0.4$ around a muon candidate, or the separation between an electron or a photon and any jet is within $0.2 < \Delta R < 0.4$, the corresponding muon, electron, or photon candidate is rejected.

Small-R jets containing a b-hadron are identified using the DL1r b-tagging algorithm [92] at the 77% b-tagging efficiency operating point. The misidentification rate for jets which originate from a light quark or a gluon is less than 1%, while it is approximately 20% for c-jets, as measured in simulated $t\bar{t}$ events.

Large-R jets are reconstructed from topological clusters [83] in the calorimeter, using the anti-k_t algorithm with a radius parameter $R = 1.0$. To reduce contributions to the jet's transverse momentum and mass that arise from pile-up, a trimming procedure [93] is applied to remove $R = 0.2$ subjets with less than 5% of the original p_{T} of the jet. Corrections are applied to restore the jet's energy to that of jets reconstructed at the particle-level energy scale [94]. Jet candidates are required to have p_{T} above 200 GeV and $|\eta| < 2.0$. The energy resolution for large-R jets with p_{T} between 200 GeV and 1 TeV is ∼7% [94]. The jet's mass is computed as a weighted combination of calorimetric mass and track-assisted mass [95].

JHEP06(2023)036

Category	LeadJ	LeadB	LeadFatJ	LeadP	LeadE	LeadM
e^+e^-	979 074	77 625	181 561	2 601	565	530
$\mu^+\mu^-$	1 307 187	99 927	228 986	3 418	790	766

Table 1. Data yields of the six event categories in the $Z \to e^+e^-$ and $\mu^+\mu^-$ decay channels. The merged-e^+e^- events are included in the e^+e^- channel, increasing the event yield, mainly in the leading large-R-jet category, by 0.6%.

To avoid double counting, the small-R jets are discarded if they are within a cone of size $\Delta R = 1.0$ around the large-R jets. The large-R jets are discarded if they are within a cone of size $\Delta R = 1.0$ around an electron or a photon.

5 Event selection and classification

The Z boson candidates are selected by requiring two oppositely charged, same-flavour leptons (e^+e^- or $\mu^+\mu^-$). Both leptons must satisfy the minimal quality criteria discussed in section 4. If no Z boson candidate can be formed from a pair of two isolated leptons, merged-e^+e^- candidates are checked. The Z boson candidates are required to have an invariant mass between 66 and 116 GeV. If there are multiple Z boson candidates, the one with the mass closest to the Z boson mass is chosen. To suppress the large SM background contributions at low p_{T} and to be more sensitive to high p_{T} final states expected from new heavy particles, the selected Z boson candidate is also required to have $p_{\mathrm{T}}^Z > 100$ GeV. The choice of this p_{T}^Z threshold is a compromise between suppressing the SM background contribution and keeping the data event yields high enough for data-driven background estimations in all search categories.

For a given event, all objects satisfying the selections described in section 4, except the lepton pair from the Z boson decay, are assumed to belong to the recoil system (X). The objects in X are ordered in p_{T}. The leading-p_{T} object type is used to assign an event to one of six independent event categories: a small-R (non-b) jet (LeadJ), a small-R b-jet (LeadB), a large-R jet (LeadFatJ), a photon (LeadP), an electron (LeadE) or a muon (LeadM). An inclusive category is formed by summing the six exclusive categories. This category can be useful when the signal is distributed over several considered event categories. The data yields in the six categories are shown in table 1. The invariant mass of the recoil system, m_X, and the invariant mass of the recoil system and the Z boson, m_{ZX}, are the observables of the search.

6 Search for narrow resonances

6.1 Background modelling

The SM background is modelled by a fit to the binned distribution of m_X or m_{ZX} after combining the e^+e^- and $\mu^+\mu^-$ channels in each event category. MC samples are used in selecting the varying bin size for each mass distribution, $\mathcal{M}$ (m_X or m_{ZX}). The bin widths

JHEP06(2023)036

for a mass spectrum are chosen to approximate the mass resolution, which broadens with increasing mass. Two functional forms are considered for the estimation of the background and are defined as:

$$f_1(x) = p_0 \left(\mathrm{e}^{-p_1 x} + p_2 \mathrm{e}^{-(p_1+p_3)x} + p_4 \mathrm{e}^{-(p_1+p_3+p_5)x} + \cdots \right) \tag{6.1}$$

or

$$f_2(x) = p_0 (1-x)^{p_1} x^{p_2 + p_3 \ln x + p_4 \ln^2 x + \cdots} \tag{6.2}$$

where $x = (\mathcal{M} - \mathcal{M}_{\mathrm{min}})/(\mathcal{M}_{\mathrm{max}} - \mathcal{M}_{\mathrm{min}})$ in eq. (6.1) and $x = \mathcal{M}/\sqrt{s}$ in eq. (6.2), p_0 is a free normalisation factor and p_i are a number of other free parameters controlling the shape of a mass distribution, and $\mathcal{M}_{\mathrm{min}}$ and $\mathcal{M}_{\mathrm{max}}$ are the lower and upper fit boundaries of the distribution. For a given mass bin, the integral of the function is fit to the selected number of events in the bin. The number of free parameters depends on the mass spectrum and event category. Mass spectra that cover a larger range usually have higher yields and need more parameters than those with a smaller range.

The choice of functional form, number of free parameters, and fit range is based on two criteria for the fits initially performed on the simulated SM mass spectrum. The statistics of the MC samples is category dependent and varies typically from a few times up to an order of magnitude larger than that of the data sample. The global χ^2 p-value of the background-only fit has to be greater than 0.05 for the modelling to be good enough over the considered mass range, and the significance of the spurious-signal yields over the fit range must typically be below 20%–50% to ensure a discovery will not be claimed falsely. The spurious signal is evaluated by fitting the simulated background's mass spectrum with signal-plus-background models. The statistical uncertainty of the mass spectrum corresponds to that of data. The signal significance is defined as the ratio of the absolute value of the signal yield to its fitted uncertainty. The upper fit boundary is dictated by the number of events in the high mass tail of the mass spectrum. In most cases, the lower fit boundary is a direct consequence of the event selection. However, in some cases, it has to be increased slightly to satisfy the requirements of a small spurious-signal significance and a global χ^2 p-value larger than 0.05 for the background fit. The spurious signal for the model-independent interpretation is evaluated by fitting the simulated background mass spectrum with a Gaussian-shaped signal function together with the selected background functional form. The detector resolution, with relative values typically around 5% for the mass observables, is also taken into account for the Gaussian-shaped signals with intrinsic relative width values of 3%, 5%, and 10%. It widens the reconstructed peak from the intrinsic width. For a model-dependent interpretation with an HVT signal, the spurious signal is evaluated with a double-sided Crystal Ball function whose parameter values are determined from the HVT MC sample.

6.2 Search strategy

The strategy applied in this search is diagrammed in figure 2. The mass spectrum in data in each category is fitted with a functional form within the fit range. Both the functional form and the fit range are chosen for each mass spectrum, as discussed in section 6.1. To

JHEP06(2023)036

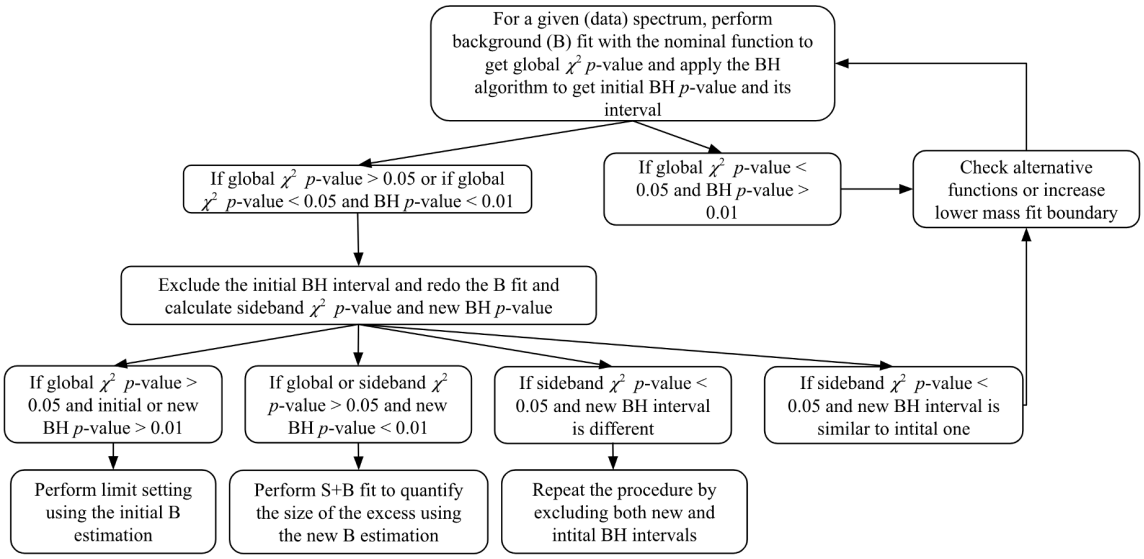

Figure 2. Workflow for the search strategy.

search for local excesses over the background, the BumpHunter (BH) algorithm is then applied to the mass spectrum within a signal-sensitive mass range, which lies within the fit range (see below).

The BH algorithm calculates the significance of any excess found in continuous mass intervals of varying size at various locations in the spectrum. The size of the search window varies from a minimum of two mass bins up to half of the bins in the sensitive mass range. For each interval in the scan, the BH algorithm computes the significance of the difference between the data and the background estimate. The interval where the data deviates most significantly from the background estimate is defined as the set of bins that have the smallest probability of arising from a Poisson background fluctuation. The probability of random fluctuations in the background-only hypothesis to create an excess at least as significant as the one observed anywhere in the spectrum defines the BH p-value. It is determined by performing a series of pseudo-experiments drawn from the background estimate, with the look-elsewhere effect considered.

The signal-sensitive mass range for each signal depends on the assumed shape and width. The sensitive range is derived using the procedures described in appendix B. A signal at a given mass point within the fit range is injected on top of a set of 100 pseudo-experiments generated by fluctuating the fitted background mass spectrum within a Poisson distribution. The injected number of signal events has a signal significance of 5σ, calculated over the full mass spectrum using a definition recommended in ref. [96]. A mass point is considered to be sensitive if the signal is correctly located with a BH p-value below 0.01 in more than 50% of the pseudo-experiments. In general, the procedure is more sensitive for narrow signals, so the signal-sensitive range corresponding to the 3% width value is used in the BH search and it is wider than the signal-sensitive mass ranges for other width values. For Gaussian-shaped signals, the largest considered width is 10% because wider signals are often absorbed into the estimated background.

JHEP06(2023)036

To ensure that the global fitting method is sensitive to potential signal resonances and the background functional form is appropriate, an alternative signal injection test has been performed and it was found that the injected signal can be recovered by the procedure.

The search strategy depends on the global χ^2 p-value and the BH p-value. If the global χ^2 p-value is above the threshold of 0.05 and the BH p-value is above the threshold of 0.01, it indicates that this functional form can model the SM background for the examined mass spectrum and there is no significant excess above the background. In this case, upper limits are set on the signal models within a limit-sensitive mass range which is derived for each signal using a procedure, described in appendix C, based on the coverage of the expected exclusion limit.

If the global χ^2 p-value is below 0.05 and the BH p-value is above 0.01, it indicates that the initial functional form validated on the simulated SM mass spectrum does not fit the corresponding data spectrum. Alternative functional forms are then tested against the nominal one. Two alternative functional forms are considered: the same functional form as the nominal one but with more free parameters and the other functional form defined in eq. (6.1) or (6.2). In the first case, the test is performed using an F-test [97]:

$$F = \frac{\left(\chi^2_{\text{nom}} - \chi^2_{\text{alt}}\right)/(n_{\text{alt}} - n_{\text{nom}})}{\chi^2_{\text{alt}}/(n - n_{\text{alt}})}$$

where χ^2_{nom} and χ^2_{alt} are the χ^2 values for fits to the spectrum using, respectively, the nominal or alternative model, n_{nom} and n_{alt} are the number of free parameters in each model, and n is the number of bins used for the χ^2 computation. The value of F is larger if the alternative model provides a significantly better fit to the spectrum than the nominal model. The alternative model is retained if the p-value of the F-test satisfies $p(F) > 0.05$. If the test is not successful, the other functional form is considered with up to six (eight) free parameters for $f_2(x)$ ($f_1(x)$). If both functional forms fail to describe the background, the lower fit boundary is raised until the global χ^2 p-value is above the threshold of 0.05.

If the BH p-value is below 0.01 for any global χ^2 p-value, a new global fit is performed while excluding the BH interval corresponding to the most significant excess relative to the background estimated by the fit in the full fit range. This gives the sideband χ^2 p-value. The BH algorithm is then applied using the newly fitted background estimate to get a new BH p-value. If the new BH interval is at the same mass location as the initial one, the new BH p-value is expected to be smaller than the initial one because more events from the excess may be absorbed in the background fit in the initial step. If the new BH interval is at a different location, the procedure is repeated while excluding both intervals. If the global χ^2 p-value is above 0.05, the excess is to be further quantified by performing a signal-plus-background fit to the mass spectrum. On the other hand, if the global χ^2 p-value is smaller than 0.05, the global fit is to be improved using alternative models described above and the procedure is then repeated.

6.3 BumpHunter search results

The functional forms given in section 6.1 are applied to mass spectra in data for the six exclusive event categories and the inclusive one to get the initial data-driven background estimate. The upper fit boundaries for some of the event categories have to be lowered from their initial

JHEP06(2023)036

Spectrum	Category	Fit range [GeV]	Function	$N_{\text{parameters}}$	χ^2 p-value
m_X	LeadJ	[350, 5270]	$f_1(x)$	6	0.68
m_X	LeadB	[350, 3340]	$f_1(x)$	6	0.69
m_X	LeadFatJ	[630, 5670]	$f_2(x)$	4	0.58
m_X	LeadP	[150, 1800]	$f_1(x)$	4	0.98
m_X	LeadE	[150, 1515]	$f_1(x)$	4	0.67
m_X	LeadM	[150, 1230]	$f_1(x)$	4	0.12
m_X	Inclusive	[550, 6455]	$f_2(x)$	6	0.58
m_{ZX}	LeadJ	[730, 6050]	$f_1(x)$	6	0.63
m_{ZX}	LeadB	[580, 4185]	$f_1(x)$	6	0.52
m_{ZX}	LeadFatJ	[830, 6650]	$f_1(x)$	4	0.05
m_{ZX}	LeadP	[280, 2200]	$f_1(x)$	4	0.84
m_{ZX}	LeadE	[325, 2185]	$f_1(x)$	4	0.85
m_{ZX}	LeadM	[290, 1900]	$f_2(x)$	4	0.11
m_{ZX}	Inclusive	[800, 6830]	$f_1(x)$	6	0.11

Table 2. A list of mass spectra, event categories and their corresponding fit ranges, functional forms, numbers of free parameters and global χ^2 p-values from background-only fits. The fit range values are rounded to the nearest 5 GeV.

MC-based values because there are fewer high-mass data events than expected. The lower fit boundaries are driven by the kinematic selection except for the m_{ZX} spectra in the leading large-R-jet and inclusive categories, where the search strategy requires them to be raised a little. The fit range and nominal functional form for each mass spectrum are shown in table 2.

Using the fitted background estimate, the BH algorithm is applied to all the spectra within the signal-sensitive mass ranges. The signal-sensitive mass ranges and the resulting BH p-values are given in table 3. The BH results using the backgrounds estimated by the fit in the full fitting range are also shown graphically in figures 3 and 4 for the m_X and m_{ZX} spectra, respectively, in the six exclusive event categories. Figure 5 shows the mass spectra of the inclusive event category. Gaussian-shaped signals with three different widths at mass values around 1, 2 and 3 TeV in the m_X and m_{ZX} spectra are shown as examples in the leading small-R-jet category. The signal yields are normalised to correspond to a cross-section value of 1 fb. An HVT signal at 3 TeV is also shown in the relevant m_{ZX} mass spectrum of the leading large-R-jet category. The largest excesses are at around 280 GeV in the m_X spectrum of the leading muon category and at around 1.6 TeV in the m_{ZX} spectrum of the leading large-R-jet category with a BH p-value of 0.48 and 0.46, respectively. With updated background estimates after excluding the initial BH interval, the corresponding new BH p-values are 0.08 and 0.10, respectively. They are still above the threshold value of 0.01, meaning that there is no significant excess in any of the mass spectra and event categories.

JHEP06(2023)036

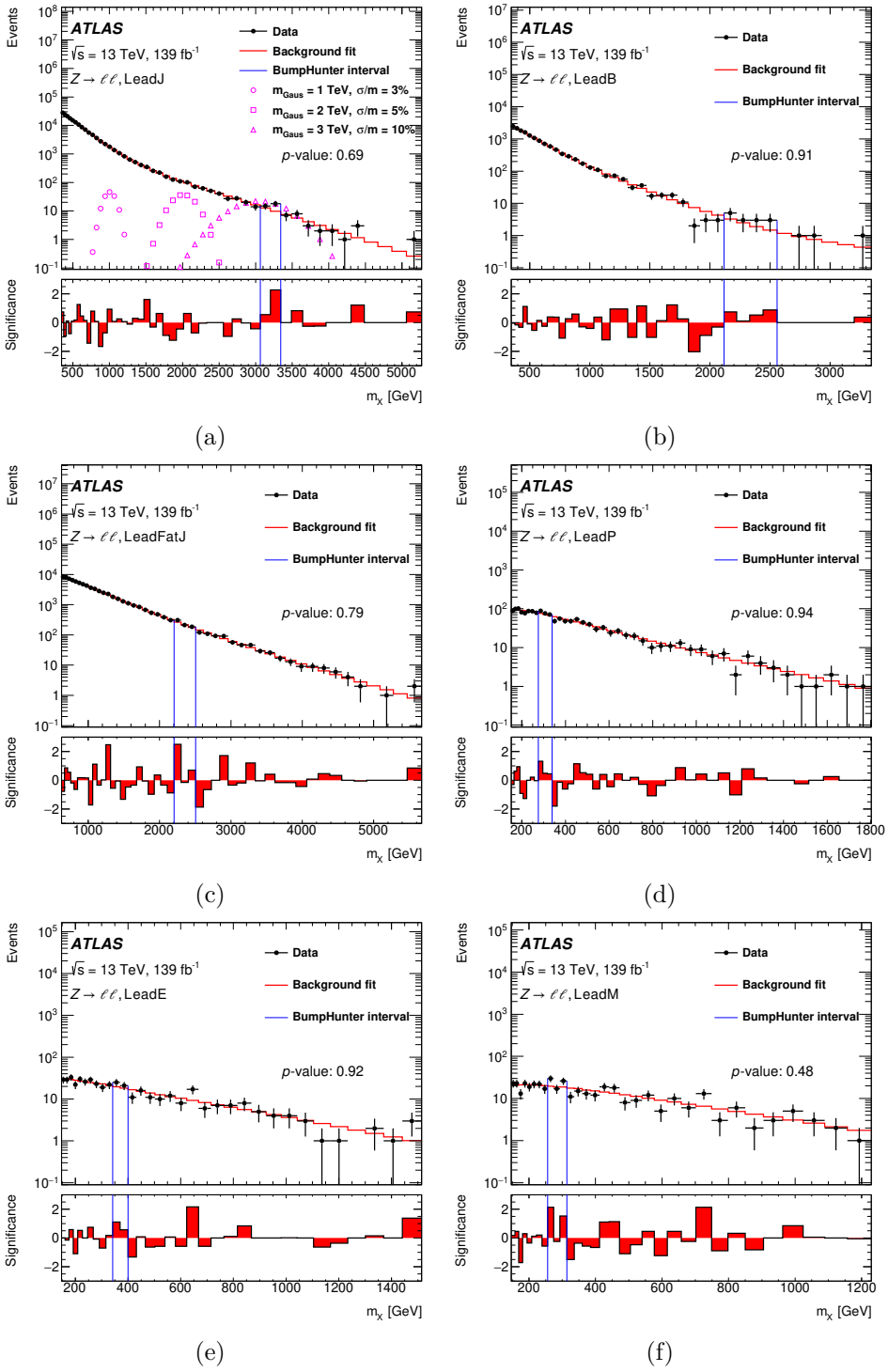

Figure 3. The m_X spectra in the six exclusive categories: (a) leading small-R jet, where Gaussian-shaped signals at mass values around 1, 2, and 3 TeV with relative widths of 3%, 5% and 10% corresponding to a cross section of 1 fb each are also shown, (b) leading b-jet, (c) leading large-R-jet, (d) leading photon, (e) leading electron, and (f) leading muon. The vertical lines indicate the most discrepant interval identified by the BH test from the initial step and the p-values correspond to those shown in the fourth column in table 3.

JHEP06(2023)036

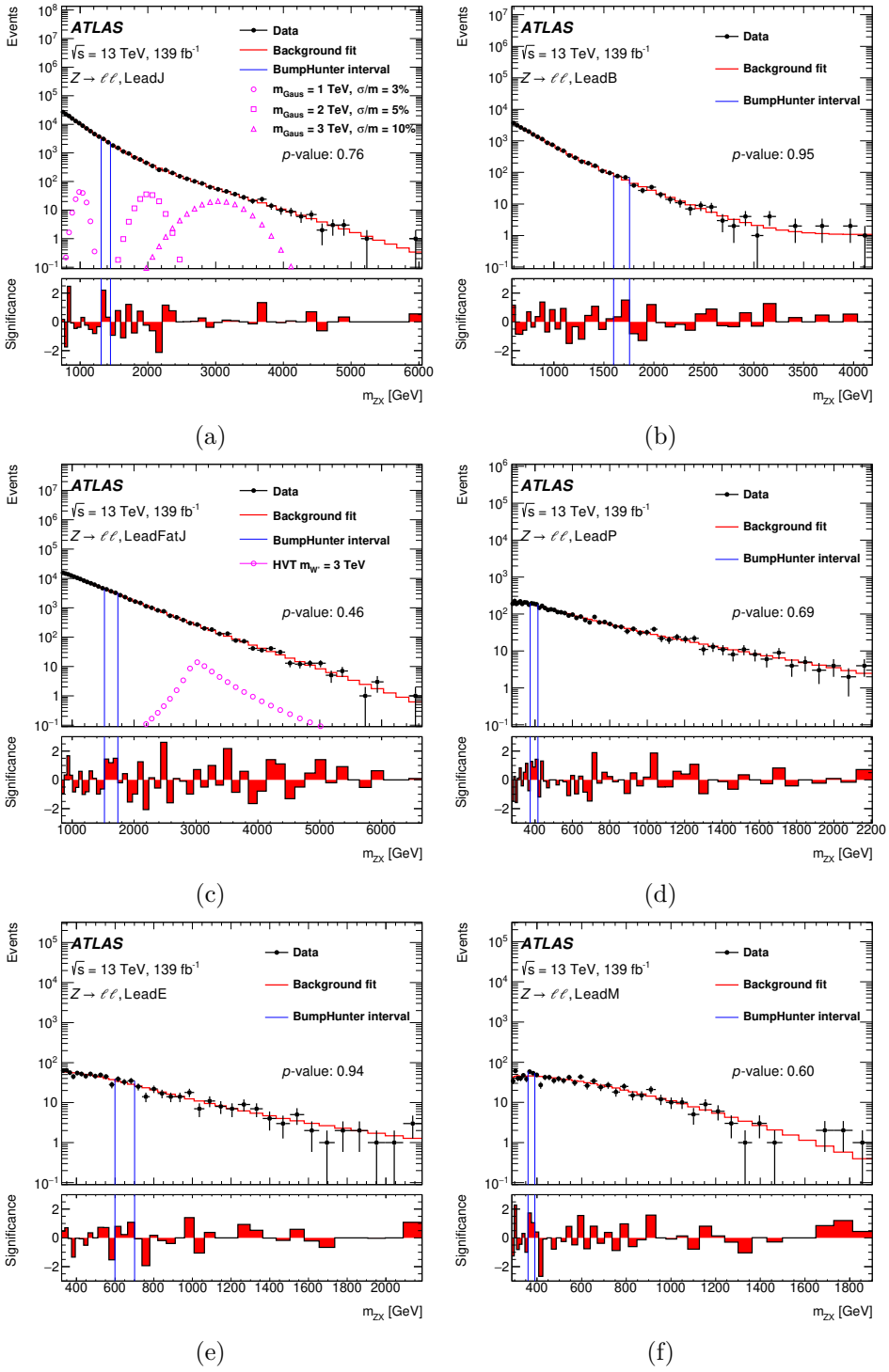

Figure 4. The m_{ZX} spectra in the six exclusive categories: (a) leading small-R jet (Gaussian-shaped signals similar to those in the m_X spectrum are also shown), (b) leading b-jet, (c) leading large-R jet, where an HVT signal at 3 TeV corresponding to a cross section of 1 fb is also shown, (d) leading photon, (e) leading electron, and (f) leading muon. The vertical lines indicate the most discrepant interval identified by the BH test from the initial step and the p-values correspond to those shown in the fourth column in table 3.

JHEP06(2023)036

Spectrum	Category	Sensitive range [GeV]	Initial BH p-value	New BH p-value
m_X	LeadJ	[350, 5270]	0.69	0.30
m_X	LeadB	[350, 2800]	0.91	0.39
m_X	LeadFatJ	[630, 5670]	0.79	0.61
m_X	LeadP	[150, 1580]	0.94	0.69
m_X	LeadE	[150, 1300]	0.92	0.65
m_X	LeadM	[150, 1025]	0.48	0.08
m_X	Inclusive	[675, 6450]	0.71	0.30
m_{ZX}	LeadJ	[860, 6050]	0.76	0.27
m_{ZX}	LeadB	[580, 3615]	0.95	0.72
m_{ZX}	LeadFatJ	[830, 6650]	0.46	0.10
m_{ZX}	LeadP	[280, 2200]	0.69	0.45
m_{ZX}	LeadE	[325, 1905]	0.94	0.85
m_{ZX}	LeadM	[290, 1650]	0.60	0.40
m_{ZX}	Inclusive	[800, 6830]	0.74	0.29

Table 3. A list of mass spectra, event categories and their corresponding signal-sensitive mass ranges. The initial BH p-value is obtained by using the background derived from the background-only fit in the full fit range, whereas the new BH p-value uses the background derived from the background-only fit in the range excluding the initial BH interval.

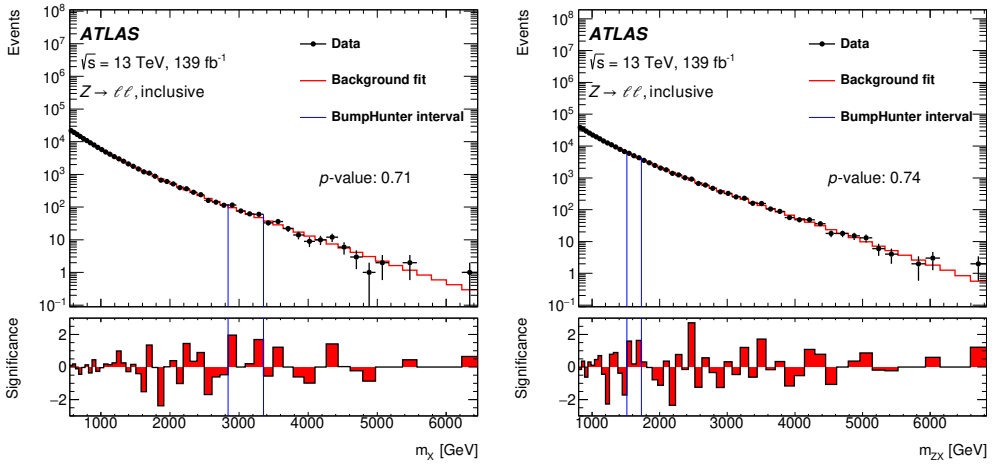

(a) (b)

Figure 5. Mass spectra of (a) m_X and (b) m_{ZX} in the inclusive category. The vertical lines indicate the most discrepant interval identified by the BH test from the initial step and the p-values correspond to those shown in the fourth column in table 3.

JHEP06(2023)036

7 Model-independent and model-dependent interpretations

Since no significant excesses are observed in any of the mass spectra, exclusion upper limits are derived at 95% confidence level (CL) for model-independent results based on Gaussian-shaped signals with relative width values of 3%, 5% and 10%, as well as for HVT signal interpretations.

7.1 Systematic uncertainty and statistical methodology

The statistical uncertainty of the fit due to the limited size of the data sample is considered as a systematic uncertainty affecting the data-driven background determination.

For signals, the spurious-signal uncertainty corresponds to an envelope of absolute spurious-signal yields over the mass spectrum under consideration. The envelope is obtained from a smooth parameterisation passing through the local maxima of the spurious-signal yields. However, given the differences in the shape and normalisation of the mass spectra between data and simulation, the implementation uses the absolute uncertainty scaled to keep the relative uncertainty unchanged.

The spurious signal's systematic uncertainty and the statistical uncertainty of the background function fit are the dominant sources of uncertainty. Additional systematic uncertainties for the HVT signal modelling include experimental, theoretical and luminosity uncertainties. The large-R-jet-related uncertainties are the dominant source of experimental uncertainty. The theoretical uncertainties include contributions due to missing higher-order corrections, PDF uncertainties, and the uncertainty in the strong coupling constant α_s. The effect of missing higher-order corrections is estimated by varying the renormalisation and factorisation scales by factors of 0.5 and 2. Similarly, the PDF and α_s are varied to estimate the effect of their uncertainties. The uncertainty in the combined 2015–2018 integrated luminosity is 1.7% [98], obtained using the LUCID-2 detector [99] for the primary luminosity measurement.

For each mass spectrum, a likelihood function is constructed as a product of Poisson distributions corresponding to different mass bins. Upper limits on the signal strength μ_s in terms of the cross-section times acceptance times branching ratio, $\sigma \times \mathcal{B} \times \mathcal{A}$, are extracted at 95% CL using the CLs method [100] with a binned profile likelihood ratio as the test statistic. The free parameters of the background functional forms described in section 6 are treated as nuisance parameters, which are optmised for each resonance mass value by the likelihood function without constraints during the fit [101]. The systematic uncertainties are also included as nuisance parameters, each with a Gaussian constraint except for the integrated luminosity, which has a log-normal constraint. Generally, each of the two dominant uncertainties mentioned above degrades the expected upper limits by around 10−20% but can reach up to 50% at low mass regions.

7.2 Constraints on a generic Gaussian-shaped signal for a model-independent interpretation

For a model-independent interpretation, Gaussian-shaped signals with relative width values of 3%, 5% and 10% are studied. The cross section value of the signals is normalised to

JHEP06(2023)036

1 fb. The exclusion upper limits are obtained by adjusting the normalisation of the signal strength μ_s of a template representing the Gaussian signal in question until a CL_s p-value of 0.05 is reached. The obtained μ_s value is thus the 95% CL upper limit on the event yield of the Gaussian-shaped portion of a signal in an appropriately chosen BSM model. This μ_s value is then divided by the integrated luminosity $\mathcal{L}$ to obtain the upper limit on $\sigma \times \mathcal{B} \times \mathcal{A}$. For the Gaussian-shaped signals, the $\mathcal{B} \times \mathcal{A}$ value cannot be specified as those must be determined in the context of a specific BSM model.

The resulting expected and observed limits at 95% CL on the Gaussian-shaped signal with a relative width value of 3% are shown as a function of m_X in figure 6 and m_{ZX} in figure 7 for the six exclusive event categories and in figure 8 for the inclusive event category. Similar limits are also derived for width values of 5% and 10%. Comparisons between the observed limits for the three width values are presented in figures 9–11 for each category. They show the general feature that the limits for the smallest width are the most stringent and cover the largest mass range. Depending on the event categories, the upper limits on $\sigma \times \mathcal{B} \times \mathcal{A}$ for a Gaussian-shaped signal with a relative width of 3% are 0.16 fb and 0.03 fb for m_X values of 200 GeV and 5.9 TeV, respectively. The upper limits are 0.3 fb and 0.04 fb for m_{ZX} values of 300 GeV and 6 TeV, respectively. The limits are calculated with the asymptotic approximation to the distribution of the test statistic [102]. The results are compared with the alternative approach using pseudo-experiments and the difference is found to be well below 15%, much smaller than the other dominant uncertainties. The limits are not corrected for efficiencies. Typical values of acceptance times efficiency can be found in [103].

These limits should be used when long low-mass off-shell tails from PDFs and non-perturbative effects on the narrow resonance signal shape can be safely truncated or neglected and, after applying the selection described in sections 4 and 5 (the main selection being $66 < m_{\ell\ell} < 116$ GeV and $p_T^Z > 100$ GeV), the reconstructed mass distribution approximates a Gaussian distribution. All reconstructed objects passing the object selection including initial-state radiation (ISR) must be included in m_X and m_{ZX}. ISR broadens the reconstructed mass, reducing sensitivity as outlined for the HVT model in the next section. A detailed description of how to use these limits is given in ref. [104].

7.3 Constraint on a $W' \to ZW$ signal in an HVT model

Although this generic analysis is not optimised for a particular model, it can also be used to constrain a specific model, for example the $W' \to ZW \to \ell\ell qq$ signal in the HVT model. The leptonic final state of the W boson decays is not used — the presence of the neutrino causes the reconstructed mass to be significantly shifted from the generated value and does not improve the analysis sensitivity. The acceptance times efficiency values as a function of m_{ZX} in the dominant leading large-R-jet category are shown in figure 12.

The derived observed and expected upper limits at 95% CL on the cross section times the branching fraction of the $W' \to ZW \to \ell\ell qq$ decay for the HVT signal are shown in figure 13. The limits exclude an HVT signal lighter than 1.2 TeV for both models A and B. The two models differ in their coupling parameter g_V to the SM gauge bosons, with a value of 1 and 3, respectively [46]. These limits are weaker than those in ref. [12], where boson

JHEP06(2023)036

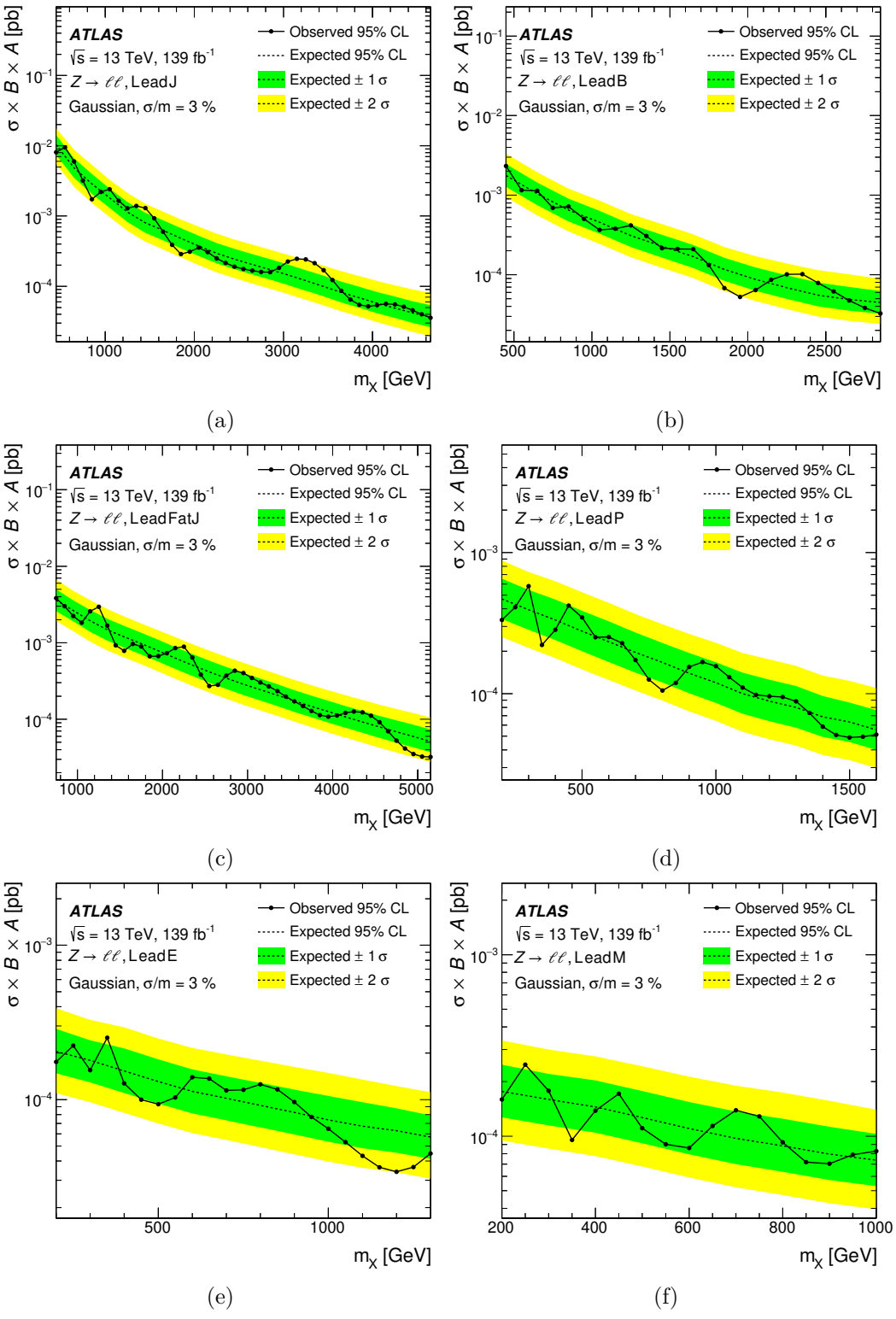

Figure 6. Upper limits at 95% CL on the cross section times branching fraction times acceptance for a Gaussian-shaped signal with a relative width value of 3% as a function of m_X in the (a) leading small-R-jet, (b) leading b-jet, (c) leading large-R-jet, (d) leading photon, (e) leading electron, and (f) leading muon categories.

JHEP06(2023)036

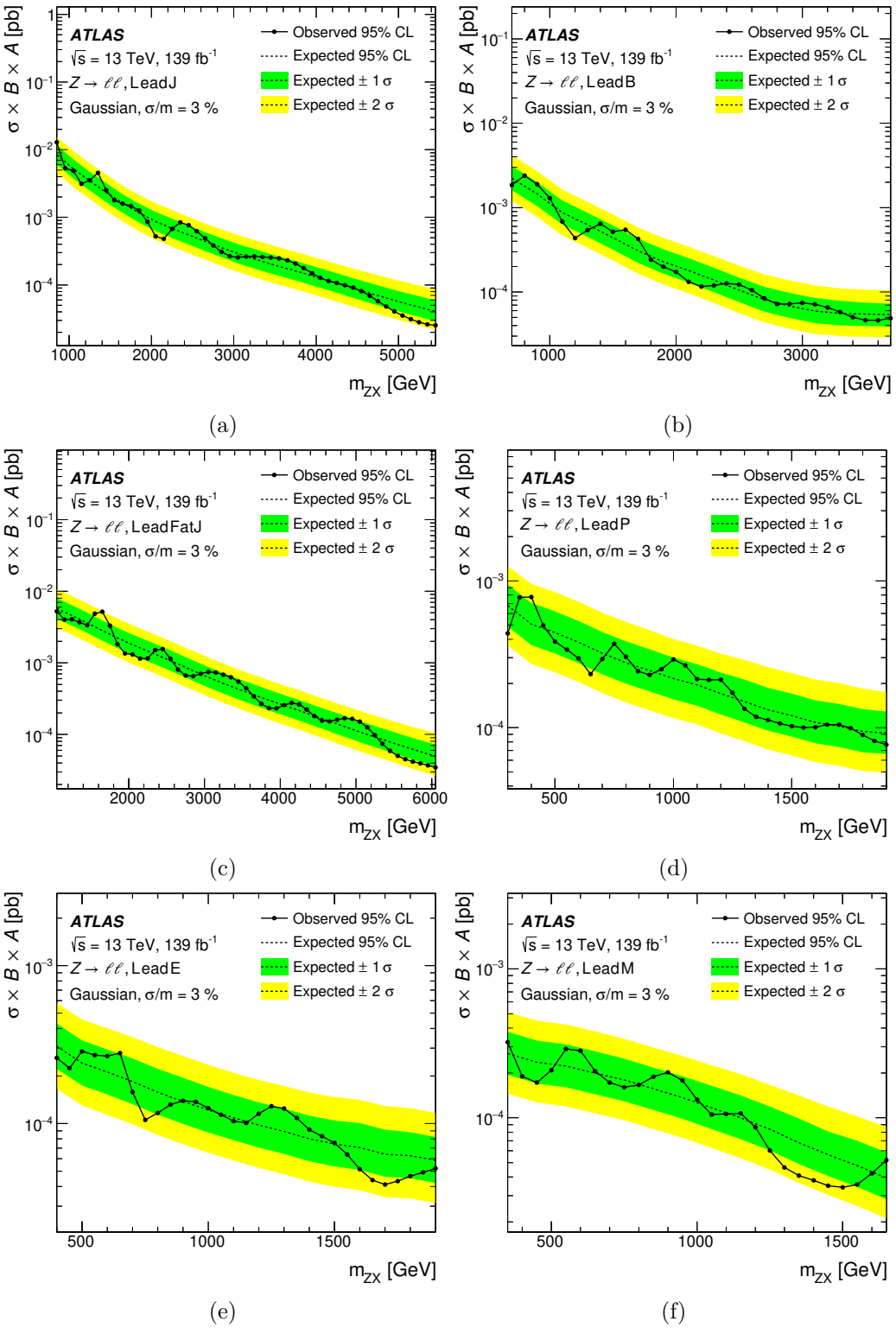

Figure 7. Upper limits at 95% CL on the cross section times branching fraction times acceptance for a Gaussian-shaped signal with a relative width value of 3% as a function of m_{ZX} in the (a) leading small-R-jet, (b) leading b-jet, (c) leading large-R-jet, (d) leading photon, (e) leading electron, and (f) leading muon categories.

JHEP06(2023)036

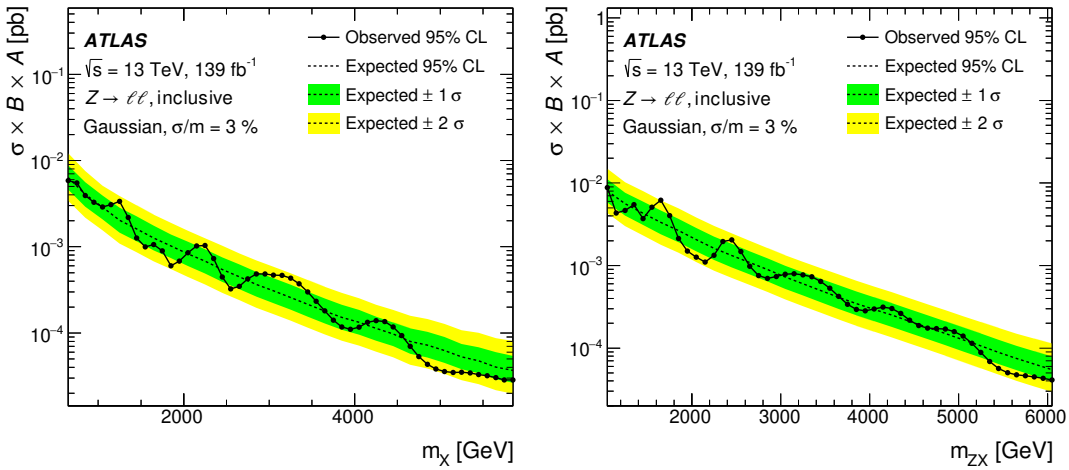

(a) (b)

Figure 8. Upper limits at 95% CL on the cross section times branching fraction times acceptance for a Gaussian-shaped signal with a relative width value of 3% as functions of (a) m_X and (b) m_{ZX} in the inclusive category.

tagging was applied to increase the signal sensitivity, illustrating the trade-off between generality and sensitivity.

When constructing m_{ZX}, all reconstructed objects passing the object selection are included, even those arising from ISR. For the HVT signal, the expected cross section limits from reinterpreting the limits on a Gaussian-shaped signal are about 20% stronger if ISR objects are excluded from the invariant mass calculation using generator-level information.

8 Conclusion

This article reports a novel generic search for resonances produced in association with, or decaying to, a Z boson with $p_{\mathrm{T}}^{Z} > 100\,\mathrm{GeV}$ and a subsequent decay into an e^+e^- or $\mu^+\mu^-$ pair, using $139\,\mathrm{fb}^{-1}$ of proton-proton collisions recorded at $\sqrt{s} = 13\,\mathrm{TeV}$ with the ATLAS detector at the Large Hadron Collider between 2015 and 2018. The invariant mass spectra of the system recoiling against the Z boson and of the full final state including the Z boson in six independent event categories, as well as the inclusive category, are analysed simultaneously. No significant excess is observed above the data-driven estimates of the smoothly falling distributions of the Standard Model background. Constraints on Gaussian-shaped signals with relative width values between 3% and 10% are derived. Depending on the event category, the search covers the mass range down to 200 GeV and up to 6 TeV, and the most stringent upper limits on the visible cross sections for a Gaussian-shaped signal with a relative width value of 3% are about 0.16 fb at the low mass boundary and 0.03 fb at high mass boundary. In a model-dependent interpretation of a $W' \to ZW$ signal in a heavy vector triplet model, signal mass values below 1.2 TeV are excluded using the leading large-R-jet event category.

JHEP06(2023)036

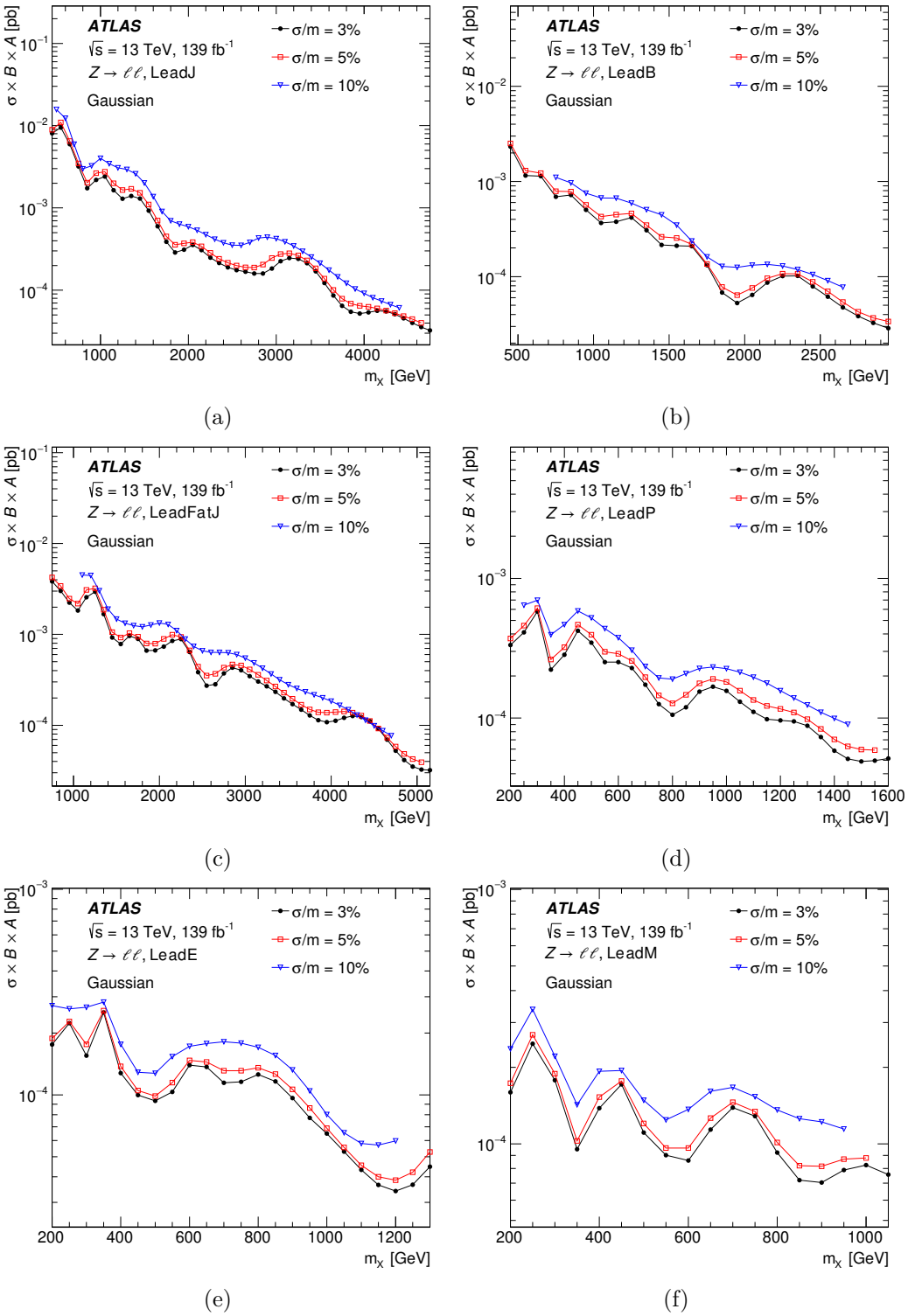

Figure 9. Comparison of observed upper limits at 95% CL on the cross section times branching fraction times acceptance for a Gaussian-shaped signals with relative width values of 3%, 5% and 10% as a function of m_X in the (a) leading small-R-jet, (b) leading b-jet, (c) leading large-R-jet, (d) leading photon, (e) leading electron, and (f) leading muon categories.

JHEP06(2023)036

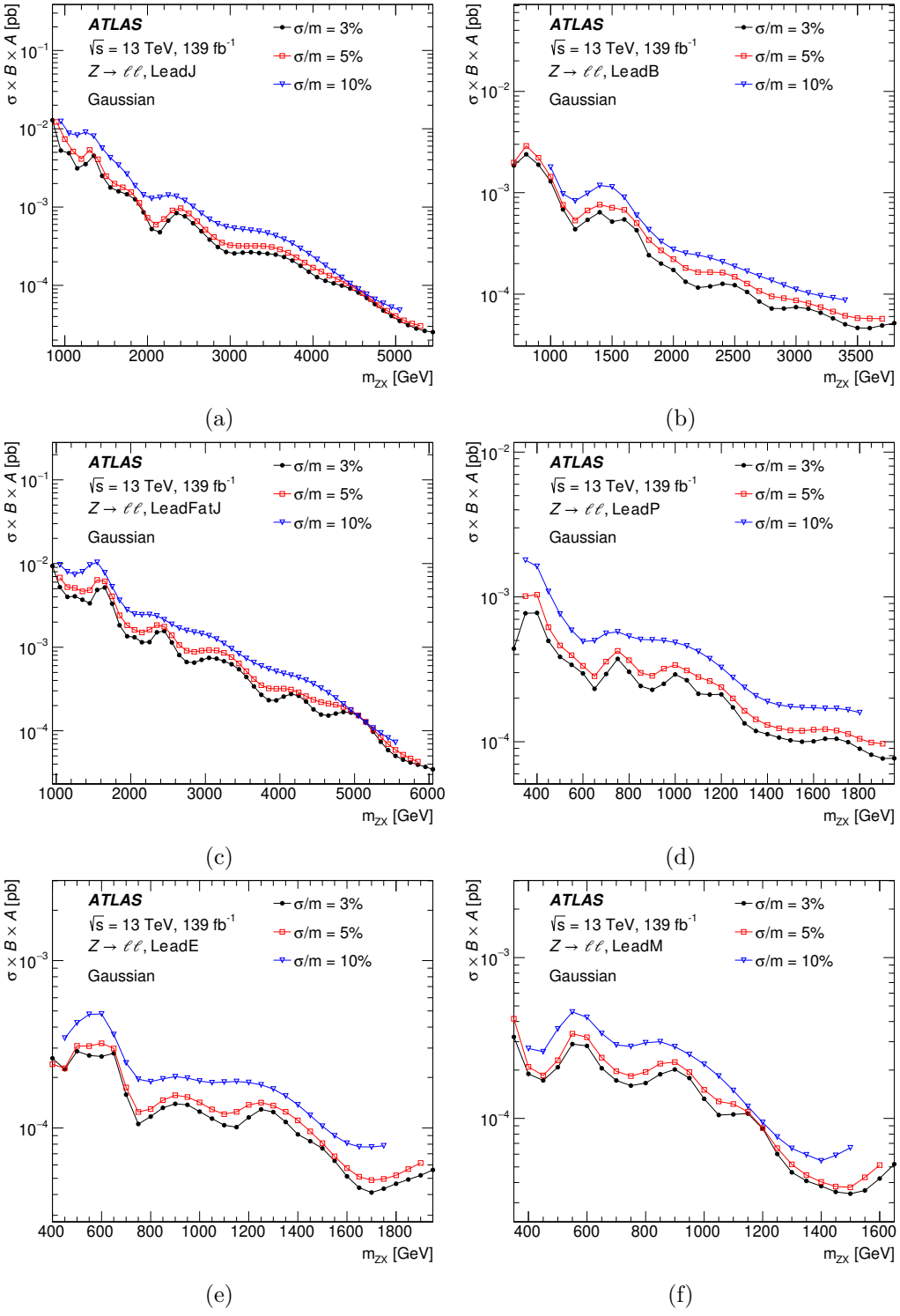

Figure 10. Comparison of observed upper limits at 95% CL on the cross section times branching fraction times acceptance for a Gaussian-shaped signals with relative width values of 3%, 5% and 10% as a function of m_{ZX} in the (a) leading small-R-jet, (b) leading b-jet, (c) leading large-R-jet, (d) leading photon, (e) leading electron, and (f) leading muon categories.

JHEP06(2023)036

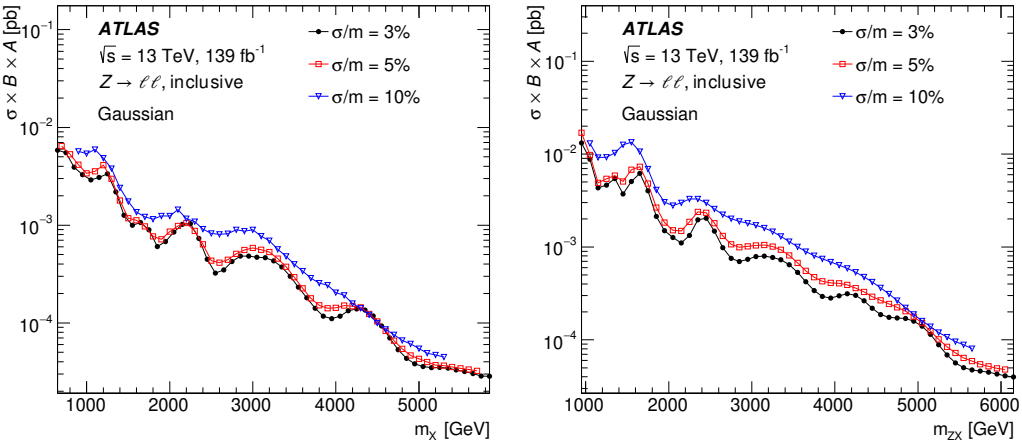

(a) (b)

Figure 11. Comparison of observed upper limits at 95% CL on the cross section times branching fraction times acceptance for a Gaussian-shaped signals with relative width values of 3%, 5% and 10% as a function of (a) m_X and (b) m_{ZX} in the inclusive category.

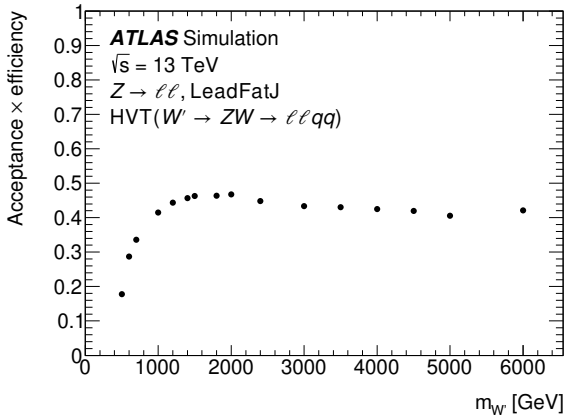

Figure 12. Acceptance times efficiency for a $W' \to ZW \to \ell\ell qq$ signal in an HVT model as a function of $m_{W'}$ in the leading large-R-jet category.

JHEP06(2023)036

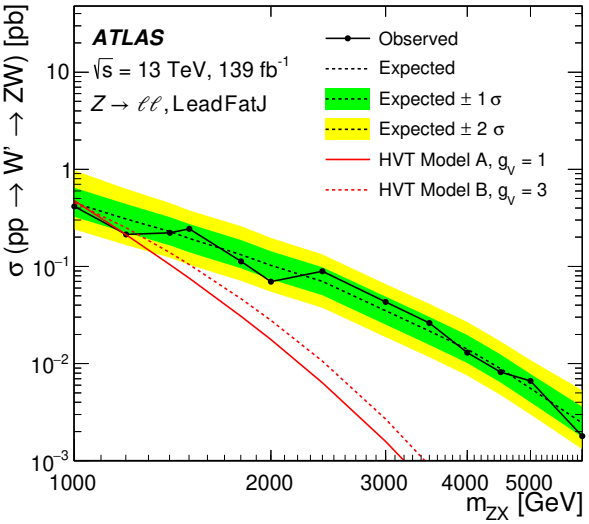

Figure 13. Upper limits at 95% CL on the cross section times the branching fraction ($W' \to ZW$) for the HVT signal as a function of m_{ZX} in the lead-R-jet event category. The full (dashed) red curves correspond to the theoretical predictions of HVT model A (B).

Acknowledgments

We thank CERN for the very successful operation of the LHC, as well as the support staff from our institutions without whom ATLAS could not be operated efficiently.

We acknowledge the support of ANPCyT, Argentina; YerPhI, Armenia; ARC, Australia; BMWFW and FWF, Austria; ANAS, Azerbaijan; CNPq and FAPESP, Brazil; NSERC, NRC and CFI, Canada; CERN; ANID, Chile; CAS, MOST and NSFC, China; Minciencias, Colombia; MEYS CR, Czech Republic; DNRF and DNSRC, Denmark; IN2P3-CNRS and CEA-DRF/IRFU, France; SRNSFG, Georgia; BMBF, HGF and MPG, Germany; GSRI, Greece; RGC and Hong Kong SAR, China; ISF and Benoziyo Center, Israel; INFN, Italy; MEXT and JSPS, Japan; CNRST, Morocco; NWO, Netherlands; RCN, Norway; MEiN, Poland; FCT, Portugal; MNE/IFA, Romania; MESTD, Serbia; MSSR, Slovakia; ARRS and MIZŠ, Slovenia; DSI/NRF, South Africa; MICINN, Spain; SRC and Wallenberg Foundation, Sweden; SERI, SNSF and Cantons of Bern and Geneva, Switzerland; MOST, Taiwan; TENMAK, Türkiye; STFC, United Kingdom; DOE and NSF, United States of America. In addition, individual groups and members have received support from BCKDF, CANARIE, Compute Canada and CRC, Canada; PRIMUS 21/SCI/017 and UNCE SCI/013, Czech Republic; COST, ERC, ERDF, Horizon 2020 and Marie Skłodowska-Curie Actions, European Union; Investissements d'Avenir Labex, Investissements d'Avenir Idex and ANR, France; DFG and AvH Foundation, Germany; Herakleitos, Thales and Aristeia programmes co-financed by EU-ESF and the Greek NSRF, Greece; BSF-NSF and MINERVA, Israel; Norwegian Financial Mechanism 2014–2021, Norway; NCN and NAWA, Poland; La Caixa Banking Foundation, CERCA Programme Generalitat de Catalunya and PROMETEO and GenT Programmes Generalitat Valenciana, Spain; Göran Gustafssons Stiftelse, Sweden; The Royal Society and Leverhulme Trust, United Kingdom.

JHEP06(2023)036

The crucial computing support from all WLCG partners is acknowledged gratefully, in particular from CERN, the ATLAS Tier-1 facilities at TRIUMF (Canada), NDGF (Denmark, Norway, Sweden), CC-IN2P3 (France), KIT/GridKA (Germany), INFN-CNAF (Italy), NL-T1 (Netherlands), PIC (Spain), ASGC (Taiwan), RAL (U.K.) and BNL (U.S.A.), the Tier-2 facilities worldwide and large non-WLCG resource providers. Major contributors of computing resources are listed in ref. [105].

A Merged-e^+e^- identification

The electrons from a boosted Z boson corresponding to the merged-e^+e^- topology appear as a reconstructed small-R jet in the EM calorimeter, which differs, however, from a hadronic jet. Therefore, the key idea of the BDT analysis is to separate the merged-e^+e^- system from hadronic jets. The following variables are selected as inputs for the BDT analysis (the requirements, where indicated, are applied prior to BDT training):

- $p_{\mathrm{T}}^{\mathrm{jet}}$: the transverse momentum of a jet (requiring $p_{\mathrm{T}}^{\mathrm{jet}} > 450\,\mathrm{GeV}$),
- η^{jet}: the pseudorapidity of a jet (requiring $|\eta^{\mathrm{jet}}| < 2.47$),
- m_{jet}: the invariant mass of a jet (requiring the expected jet mass for a $Z \to e^+e^-$ decay to be around the Z boson mass: $60 < m_{\mathrm{jet}} < 120\,\mathrm{GeV}$),
- $f_{\mathrm{jet}}^{\mathrm{EM}}$: the jet energy fraction deposited in the EM calorimeter, satisfying a p_{T}-dependent selection,
- $\max(E_{\mathrm{layer}}/E_{\mathrm{jet}})$: the maximum jet energy fraction deposited in a calorimeter layer,
- $N_{\mathrm{jet}}^{\mathrm{track}}$: the number of tracks, with $p_{\mathrm{T}} > 500\,\mathrm{MeV}$, associated to a jet using the ghost-association [106] (requiring $1 \leq N_{\mathrm{jet}}^{\mathrm{track}} \leq 7$),
- $\overline{\Delta R} \cdot p_{\mathrm{T}}/m_{\mathrm{jet}}$: where $\overline{\Delta R}$ is defined as $\sum(\Delta R(\mathrm{jet}, \mathrm{constituent}) \cdot p_{\mathrm{T}}(\mathrm{constituent}))/\sum p_{\mathrm{T}}(\mathrm{constituent})$,
- $n_{\mathrm{jet}}^{\mathrm{constituent}}$: the number of constituents of a jet,
- $n_{\mathrm{GSF\ tracks}}$: the number of Gaussian Sum Filter (GSF) [107]) tracks inside the jet cone $\Delta R(\mathrm{jet}, \mathrm{track}) < 0.4$, which satisfy $p_{\mathrm{T}} > 50\,\mathrm{GeV}$,
- $\Sigma \mathrm{Q}_{\mathrm{GSF\ tracks}}$: the total charge of the GSF tracks satisfying the selections,
- $n_{e/\gamma\ \mathrm{clusters}}$: the number of e/γ clusters inside the jet cone which satisfy $p_{\mathrm{T}} > 25\,\mathrm{GeV}$.

In this study, signal events are based on $Z(\to e^+e^-)+\mathrm{jets}$ MC samples requiring the merged-e^+e^- candidate to match the true Z boson within $\Delta R < 0.1$. The SM background events correspond to combined MC samples of $\gamma+\mathrm{jets}$, $W(\to e\nu)+\mathrm{jets}$ and $W(\to e\nu)+\gamma$. Background processes containing only hadronic jets, e.g. the dijet background, are efficiently suppressed to a negligible level by the selection listed above, in particular by a p_{T}-dependent $f_{\mathrm{jet}}^{\mathrm{EM}}$ requirement. The raw number of selected signal and background jets is 102 593 and

JHEP06(2023)036

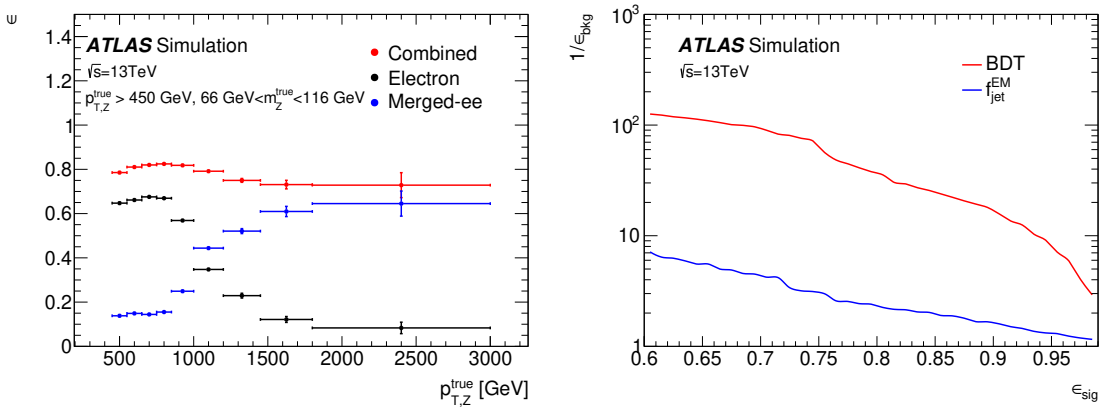

(a) (b)

Figure 14. (a) Comparison of the identification efficiencies using standard and merged-e^+e^- reconstruction as a function of true p_{T}^Z. (b) Background rejection factor as a function of signal efficiency. The red curve shows the BDT performance whereas the blue curve corresponds to that of a cut-based analysis relying only on the jet energy fraction deposited in the EM calorimeter.

8572, respectively. Events are required to fire either jet triggers or electron triggers. Events with two oppositely charged same-flavour leptons are vetoed since those events are analysed using the standard likelihood-based electron identification. The jet energy fraction in the EM calorimeter must satisfy a p_{T}-dependent selection, and at least one but no more than seven tracks must be found in the jet cone. The candidate must match with at least one GSF track, and satisfy $N_{\mathrm{PFO}} - N_{\mathrm{GSF\ tracks}} < 2$ to suppress $\gamma+$jets background, where N_{PFO} is the number of particle-flow tracks with $p_{\mathrm{T}} > 1\,\mathrm{GeV}$. At least one e/γ cluster [50] must also be matched with the jet. The cluster-based mass, m_{cls}, different from m_{jet}, is defined using the matched e/γ cluster information. It is constructed with the leading-p_{T} e/γ cluster in the jet, to show the two-body decay property of the $Z \to e^+e^-$ process. The cluster-based mass is defined as $m_{\mathrm{cls}} = \frac{1}{2}\overline{\Delta R} p_{\mathrm{T}}^2/\sqrt{z(1-z)}$, where z is the ratio of leading-cluster energy to jet energy. The jet must satisfy $m_{\mathrm{cls}} > 60\,\mathrm{GeV}$.

Using a p_{T}-dependent BDT-score selection, the merged-e^+e^- identification efficiency as a function of p_{T}^Z is determined using the $Z(\to e^+e^-)+$jets MC samples and compared with that of the standard electron identification in figure 14(a). The decrease in the efficiency of the standard electron identification at high p_{T}^Z is recovered with the BDT-based merged-e^+e^- identification, reaching a combined efficiency of 80%. The background rejection factor for three types of processes surviving the analysis preselection is shown in figure 14(b), illustrating the better performance of the BDT method in comparison with a cut-based method using $f_{\mathrm{jet}}^{\mathrm{EM}}$ at the same signal efficiency.

B Signal-sensitive mass range

To obtain a mass range in a given event category in which the search is able to detect a signal, a set of 100 pseudo-experiments are generated using the fitted background functional form with Poisson fluctuations. Gaussian-shaped signals with intrinsic relative width values

JHEP06(2023)036

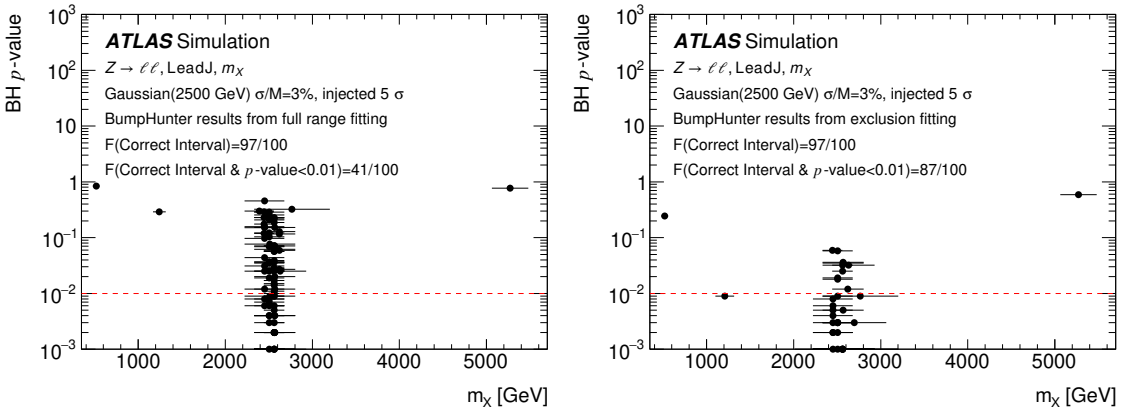

(a) (b)

Figure 15. BH p-values of the 100 pseudo-experiments as a function of m_X in the leading small-R-jet category for a 5σ injected Gaussian-shaped signal with a mass of 2.5 TeV and a relative width value of 3%. The fractions (F) of the pseudo-experiments that have the correctly identified interval and BH p-values below the threshold of 0.01 (red dashed horizontal line) are indicated. (a) The background is derived by the background-only fit in the full fitting range. (b) The background is derived by the background-only fit in the range excluding the BH interval.

varying between 3% and 10% are injected, after taking into account detector resolution effects, on top of each pseudo-experiment. The injected signals correspond to a signal strength of 5σ and are spaced every 250 GeV in m_X and m_{ZX}. Each of the 100 resulting mass spectra is treated as data and is studied following the search strategy described in section 6.2 in two steps.

As an example, the sensitive range of the m_X spectrum in the leading small-R-jet category was found as follows. A Gaussian-shaped signal with a width value of 3% is injected centred at 2.5 TeV with the number of signal events corresponding to a signal significance equal to 5σ. In 97 of the 100 pseudo-experiments, the BH algorithm correctly identifies the location of the injected signal. However, only 41 pseudo-experiments yield a BH p-value below the threshold of 0.01 since the signal is partially absorbed in the background-only fit which is performed in the full fitting range. But if the BH interval which is derived using the background-only fit in the full fitting range is excluded from the fit range, the number of pseudo-experiments with a BH p-value below 0.01 increases to 87. For signal width values of 5% and 10%, this number is 76 and 57 respectively, showing the lower sensitivity for signals with larger widths. The results for a signal width value of 3% are shown in figure 15.

The study is also performed at other mass points for both the m_X and m_{ZX} spectra in all event categories. The fractions from the right panel of figure 15 for the leading small-R-jet category are presented in figure 16. It shows that the sensitivity of the BH algorithm is best in the intermediate mass range and decreases at low and high mass values. The signal-sensitive mass range in this analysis is defined by requiring at least 50% of the pseudo-experiments to have a correctly identified BH interval and a BH p-value below 0.01.

JHEP06(2023)036

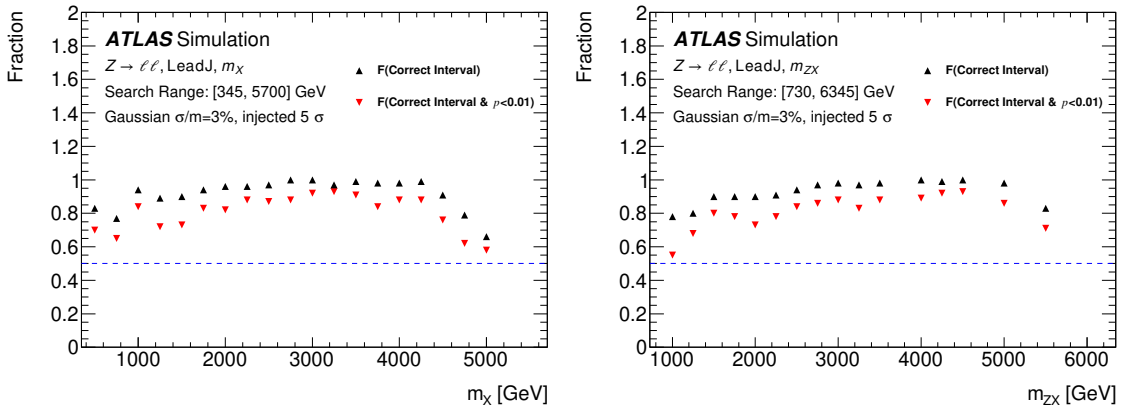

(a) (b)

Figure 16. Fractions (F) of pseudo-experiments in which the detected BH interval agrees with the injected mass point and the BH p-value is below 0.01 as a function of (a) m_X and (b) m_{ZX} in the leading small-R-jet category for a 5σ injected Gaussian-shaped signal with a relative width of 3%. The blue dashed horizontal line at 0.5 is used to define the signal-sensitive mass range.

C Limit-sensitive mass range

For a given event category, a background mass spectrum based on MC simulations can be used to derive an expected exclusion upper limit at 95% CL for a Gaussian-shaped signal of a certain given width in a model-independent way. This is referred to as nominal exclusion limit in the following. A set of 1000 pseudo-experiments are generated from the MC estimates with both the background and a signal with a signal strength set to the nominal exclusion limit value. For each pseudo-experiment, a signal+background fit is performed and an exclusion upper limit at 95% CL is extracted. The distribution of the cross-section exclusion upper limits from the 1000 pseudo-experiments is compared with the nominal limit derived directly from the MC mass spectrum. The fraction of pseudo-experiments that have a higher upper limit is calculated. If it is larger than 95%, the background modelling is sensible for the mass point under study and the corresponding exclusion upper limit is conservative. Given the limited size of each pseudo-experiment, a fraction larger than 90% is considered acceptable. One example is shown in figure 17 for mass points at the lower and upper boundaries of the limit-sensitive mass range for the m_{ZX} mass spectrum in the leading small-R-jet category for Gaussian-shaped signals with relative width values of 3%, 5% and 10%. The results for all the mass spectra and event categories are summarised in table 4. As expected, the limit-sensitive mass range is largest for signals with small widths. Most of these mass ranges can be applied directly to data when setting limits; an adjustment is only needed when the limit-sensitive mass range extends beyond the corresponding fit range in data.

JHEP06(2023)036

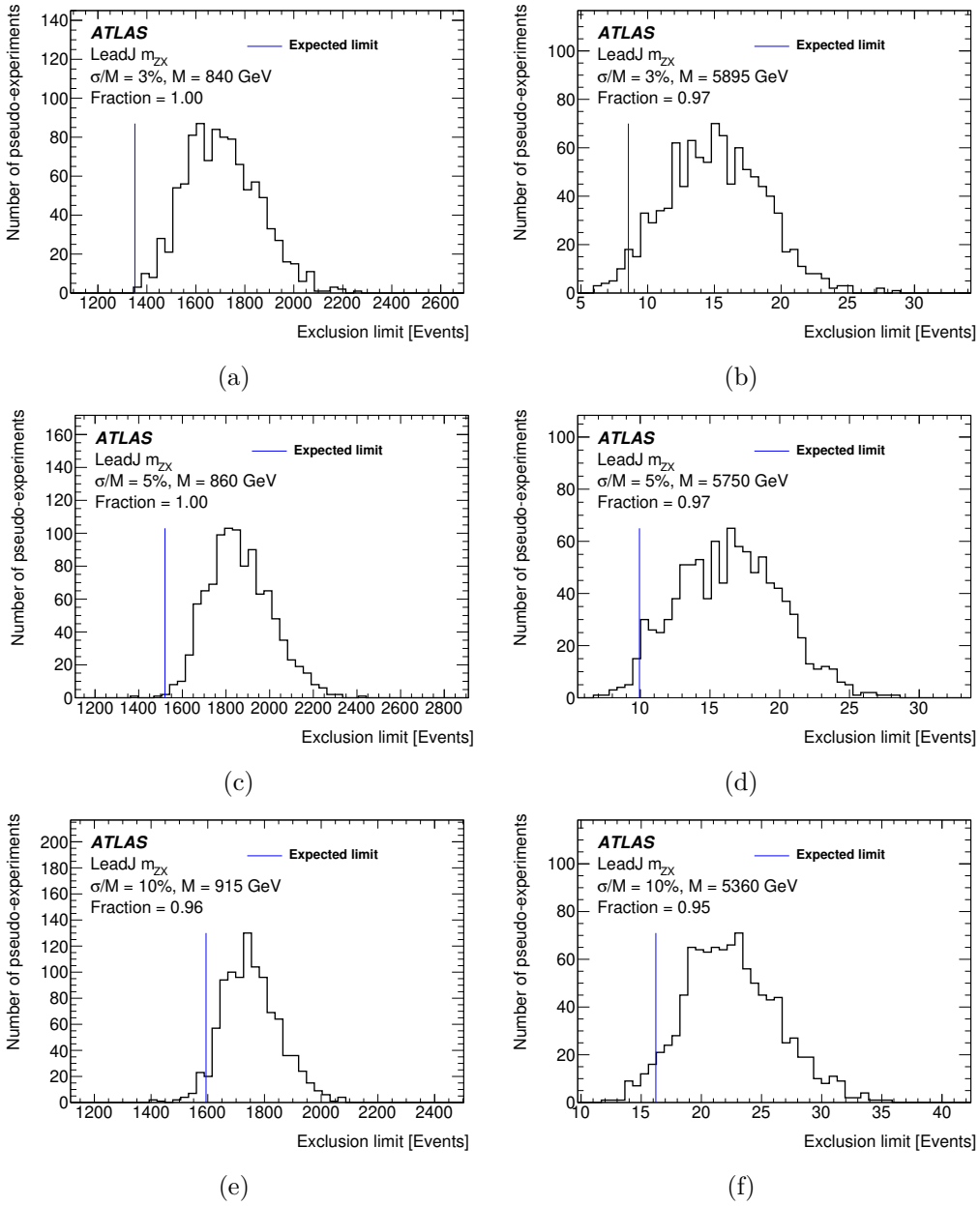

Figure 17. Distribution of exclusion upper limits on signal event yields at 95% CL from 1000 pseudo-experiments for Gaussian-shaped signals with relative width values of (a)–(b) 3%, (c)–(d) 5% and (e)–(f) 10% at the (a), (c), (e) lower and (b), (d), (f) upper boundaries of the limit-sensitive mass range for the m_{ZX} spectrum of the leading small-R-jet category. The vertical line corresponds to the expected nominal exclusion limit at 95% CL.

JHEP06(2023)036

Spectrum	Category	Width [%]	Limit range [GeV]	Fractions
m_X	LeadJ	3	[430, 5195]	0.986, 0.968
		5	[435, 5065]	0.980, 0.972
		10	[470, 4750]	0.936, 0.967
m_X	LeadB	3	[420, 3050]	0.930, 0.949
		5	[430, 2960]	0.926, 0.948
		10	[750, 2750]	0.919, 0.941
m_X	LeadFatJ	3	[730, 5580]	0.964, 0.976
		5	[745, 5540]	0.903, 0.981
		10	[1100, 5070]	0.917, 0.959
m_X	LeadP	3	[185, 1620]	0.984, 0.960
		5	[190, 1580]	0.990, 0.955
		10	[205, 1475]	0.996, 0.951
m_X	LeadE	3	[180, 1350]	0.946, 0.953
		5	[180, 1315]	0.946, 0.947
		10	[200, 1230]	0.948, 0.945
m_X	LeadM	3	[175, 1065]	0.937, 0.944
		5	[180, 1045]	0.956, 0.944
		10	[195, 980]	0.961, 0.937
m_X	Inclusive	3	[650, 5940]	0.923, 0.982
		5	[665, 5795]	0.936, 0.978
		10	[900, 5375]	0.906, 0.956
m_{ZX}	LeadJ	3	[840, 5895]	1.000, 0.971
		5	[860, 5750]	0.997, 0.974
		10	[915, 5360]	0.956, 0.955
m_{ZX}	LeadB	3	[665, 3815]	0.932, 0.953
		5	[680, 3705]	0.901, 0.931
		10	[1000, 3460]	0.921, 0.926
m_{ZX}	LeadFatJ	3	[730, 6505]	0.964, 0.969
		5	[750, 6345]	0.957, 0.971
		10	[815, 5910]	0.953, 0.966
m_{ZX}	LeadP	3	[300, 2255]	0.960, 0.962
		5	[310, 2190]	0.958, 0.954
		10	[350, 2035]	0.991, 0.942
m_{ZX}	LeadE	3	[360, 1960]	0.967, 0.947
		5	[370, 1910]	0.934, 0.948
		10	[410, 1785]	0.953, 0.930
m_{ZX}	LeadM	3	[320, 1680]	0.957, 0.949
		5	[325, 1645]	0.941, 0.956
		10	[365, 1530]	0.940, 0.960
m_{ZX}	Inclusive	3	[740, 7230]	0.954, 0.983
		5	[755, 7040]	0.943, 0.980
		10	[815, 6550]	0.935, 0.982

Table 4. A list of mass spectra, event categories, relative width values of Gaussian-shaped signals and limit-sensitive mass ranges and fractions, corresponding to the mass values in the previous column, of pseudo-experiments having exclusion upper limits higher than the nominal exclusion limit at 95% CL.

JHEP06(2023)036

Open Access. This article is distributed under the terms of the Creative Commons Attribution License (CC-BY 4.0), which permits any use, distribution and reproduction in any medium, provided the original author(s) and source are credited. SCOAP^3 supports the goals of the International Year of Basic Sciences for Sustainable Development.

References

[1] P. Langacker, R.W. Robinett and J.L. Rosner, *New heavy gauge bosons in pp and $p\bar{p}$ collisions*, *Phys. Rev. D* **30** (1984) 1470 [INSPIRE].

[2] H.E. Haber and G.L. Kane, *The search for supersymmetry: probing physics beyond the standard model*, *Phys. Rept.* **117** (1985) 75 [INSPIRE].

[3] G. Altarelli, B. Mele and M. Ruiz-Altaba, *Searching for new heavy vector bosons in $p\bar{p}$ colliders*, *Z. Phys. C* **45** (1989) 109 [*Erratum ibid.* **47** (1990) 676] [INSPIRE].

[4] N. Arkani-Hamed, S. Dimopoulos and G.R. Dvali, *The hierarchy problem and new dimensions at a millimeter*, *Phys. Lett. B* **429** (1998) 263 [hep-ph/9803315] [INSPIRE].

[5] L. Randall and R. Sundrum, *A Large Mass Hierarchy from a Small Extra Dimension*, *Phys. Rev. Lett.* **83** (1999) 3370 [hep-ph/9905221] [INSPIRE].

[6] H. Davoudiasl, J.L. Hewett and T.G. Rizzo, *Bulk gauge fields in the Randall-Sundrum model*, *Phys. Lett. B* **473** (2000) 43 [hep-ph/9911262] [INSPIRE].

[7] G.F. Giudice, *Naturally speaking: the naturalness criterion and physics at the lhc*, arXiv:0801.2562 [DOI:10.1142/9789812779762_0010] [INSPIRE].

[8] I. Low, J. Lykken and G. Shaughnessy, *Singlet scalars as Higgs boson imposters at the Large Hadron Collider*, *Phys. Rev. D* **84** (2011) 035027 [arXiv:1105.4587] [INSPIRE].

[9] R.L. Delgado et al., *Production of vector resonances at the LHC via WZ-scattering: a unitarized EChL analysis*, *JHEP* **11** (2017) 098 [arXiv:1707.04580] [INSPIRE].

[10] ATLAS collaboration, *Search for Higgs bosons decaying into new spin-0 or spin-1 particles in four-lepton final states with the ATLAS detector with 139 fb^{-1} of pp collision data at $\sqrt{s} = 13$ TeV*, *JHEP* **03** (2022) 041 [arXiv:2110.13673] [INSPIRE].

[11] ATLAS collaboration, *Search for a heavy Higgs boson decaying into a Z boson and another heavy Higgs boson in the $\ell\ell bb$ and $\ell\ell WW$ final states in pp collisions at $\sqrt{s} = 13$ TeV with the ATLAS detector*, *Eur. Phys. J. C* **81** (2021) 396 [arXiv:2011.05639] [INSPIRE].

[12] ATLAS collaboration, *Search for heavy diboson resonances in semileptonic final states in pp collisions at $\sqrt{s} = 13$ TeV with the ATLAS detector*, *Eur. Phys. J. C* **80** (2020) 1165 [arXiv:2004.14636] [INSPIRE].

[13] ATLAS collaboration, *Search for exotic decays of the Higgs boson into $b\bar{b}$ and missing transverse momentum in pp collisions at $\sqrt{s} = 13$ TeV with the ATLAS detector*, *JHEP* **01** (2022) 063 [arXiv:2109.02447] [INSPIRE].

[14] ATLAS collaboration, *Search for heavy resonances decaying into a pair of Z bosons in the $\ell^+\ell^-\ell'^+\ell'^-$ and $\ell^+\ell^-\nu\bar{\nu}$ final states using 139 fb^{-1} of proton-proton collisions at $\sqrt{s} = 13$ TeV with the ATLAS detector*, *Eur. Phys. J. C* **81** (2021) 332 [arXiv:2009.14791] [INSPIRE].

JHEP06(2023)036

[15] ATLAS collaboration, *Search for top squarks in events with a Higgs or Z boson using 139 fb^{-1} of pp collision data at $\sqrt{s} = 13$ TeV with the ATLAS detector*, *Eur. Phys. J. C* **80** (2020) 1080 [arXiv:2006.05880] [INSPIRE].

[16] CMS collaboration, *Search for dark matter produced in association with a leptonically decaying Z boson in proton-proton collisions at $\sqrt{s} = 13$ TeV*, *Eur. Phys. J. C* **81** (2021) 13 [*Erratum ibid.* **81** (2021) 333] [arXiv:2008.04735] [INSPIRE].

[17] ATLAS collaboration, *Search for the Production of a Long-Lived Neutral Particle Decaying within the ATLAS Hadronic Calorimeter in Association with a Z Boson from pp Collisions at $\sqrt{s} = 13$ TeV*, *Phys. Rev. Lett.* **122** (2019) 151801 [arXiv:1811.02542] [INSPIRE].

[18] CMS collaboration, *Search for a heavy pseudoscalar Higgs boson decaying into a 125 GeV Higgs boson and a Z boson in final states with two tau and two light leptons at $\sqrt{s} = 13$ TeV*, *JHEP* **03** (2020) 065 [arXiv:1910.11634] [INSPIRE].

[19] CMS collaboration, *Search for new neutral Higgs bosons through the $H \to ZA \to \ell^+\ell^- b\bar{b}$ process in pp collisions at $\sqrt{s} = 13$ TeV*, *JHEP* **03** (2020) 055 [arXiv:1911.03781] [INSPIRE].

[20] CMS collaboration, *Search for dark photons in decays of Higgs bosons produced in association with Z bosons in proton-proton collisions at $\sqrt{s} = 13$ TeV*, *JHEP* **10** (2019) 139 [arXiv:1908.02699] [INSPIRE].

[21] CMS collaboration, *Search for a heavy vector resonance decaying to a Z boson and a Higgs boson in proton-proton collisions at $\sqrt{s} = 13$ TeV*, *Eur. Phys. J. C* **81** (2021) 688 [arXiv:2102.08198] [INSPIRE].

[22] CMS collaboration, *Search for a heavy resonance decaying into a Z boson and a Z or W boson in $2\ell 2q$ final states at $\sqrt{s} = 13$ TeV*, *JHEP* **09** (2018) 101 [arXiv:1803.10093] [INSPIRE].

[23] CMS collaboration, *Search for $Z\gamma$ resonances using leptonic and hadronic final states in proton-proton collisions at $\sqrt{s} = 13$ TeV*, *JHEP* **09** (2018) 148 [arXiv:1712.03143] [INSPIRE].

[24] CMS collaboration, *Search for ZZ resonances in the $2\ell 2\nu$ final state in proton-proton collisions at 13 TeV*, *JHEP* **03** (2018) 003 [arXiv:1711.04370] [INSPIRE].

[25] CMS collaboration, *Search for heavy resonances decaying into a vector boson and a Higgs boson in final states with charged leptons, neutrinos and b quarks at $\sqrt{s} = 13$ TeV*, *JHEP* **11** (2018) 172 [arXiv:1807.02826] [INSPIRE].

[26] ATLAS collaboration, *Search for an invisibly decaying Higgs boson or dark matter candidates produced in association with a Z boson in pp collisions at $\sqrt{s} = 13$ TeV with the ATLAS detector*, *Phys. Lett. B* **776** (2018) 318 [arXiv:1708.09624] [INSPIRE].

[27] ATLAS collaboration, *Search for heavy ZZ resonances in the $\ell^+\ell^-\ell^+\ell^-$ and $\ell^+\ell^-\nu\bar{\nu}$ final states using proton-proton collisions at $\sqrt{s} = 13$ TeV with the ATLAS detector*, *Eur. Phys. J. C* **78** (2018) 293 [arXiv:1712.06386] [INSPIRE].

[28] ATLAS collaboration, *Search for a heavy Higgs boson decaying into a Z boson and another heavy Higgs boson in the $\ell\ell bb$ final state in pp collisions at $\sqrt{s} = 13$ TeV with the ATLAS detector*, *Phys. Lett. B* **783** (2018) 392 [arXiv:1804.01126] [INSPIRE].

[29] ATLAS collaboration, *Searches for heavy ZZ and ZW resonances in the $\ell\ell qq$ and $\nu\nu qq$ final states in pp collisions at $\sqrt{s} = 13$ TeV with the ATLAS detector*, *JHEP* **03** (2018) 009 [arXiv:1708.09638] [INSPIRE].

JHEP06(2023)036

[30] ATLAS collaboration, *Search for resonant WZ production in the fully leptonic final state in proton-proton collisions at $\sqrt{s} = 13$ TeV with the ATLAS detector*, *Phys. Lett. B* **787** (2018) 68 [arXiv:1806.01532] [INSPIRE].

[31] ATLAS collaboration, *Search for heavy resonances decaying into a W or Z boson and a Higgs boson in final states with leptons and b-jets in 36 fb^{-1} of $\sqrt{s} = 13$ TeV pp collisions with the ATLAS detector*, *JHEP* **03** (2018) 174 [*Erratum ibid.* **11** (2018) 051] [arXiv:1712.06518] [INSPIRE].

[32] CDF collaboration, *Global search for new physics with 2.0 fb^{-1} at CDF*, *Phys. Rev. D* **79** (2009) 011101 [arXiv:0809.3781] [INSPIRE].

[33] G. Choudalakis, *On hypothesis testing, trials factor, hypertests and the BumpHunter*, arXiv:1101.0390.

[34] D0 collaboration, *Search for new physics in $e\mu X$ data at DØ using SLEUTH: A quasi-model-independent search strategy for new physics*, *Phys. Rev. D* **62** (2000) 092004 [hep-ex/0006011] [INSPIRE].

[35] D0 collaboration, *Quasi-model-independent search for new physics at large transverse momentum*, *Phys. Rev. D* **64** (2001) 012004 [hep-ex/0011067] [INSPIRE].

[36] D0 collaboration, *Quasi-model-independent search for new high p_T physics at DØ* , *Phys. Rev. Lett.* **86** (2001) 3712 [hep-ex/0011071] [INSPIRE].

[37] D0 collaboration, *Model independent search for new phenomena in $p\bar{p}$ collisions at $\sqrt{s} = 1.96$ TeV*, *Phys. Rev. D* **85** (2012) 092015 [arXiv:1108.5362] [INSPIRE].

[38] CDF collaboration, *Model-independent and quasi-model-independent search for new physics at CDF*, *Phys. Rev. D* **78** (2008) 012002 [arXiv:0712.1311] [INSPIRE].

[39] H1 collaboration, *A general search for new phenomena in ep scattering at HERA*, *Phys. Lett. B* **602** (2004) 14 [hep-ex/0408044] [INSPIRE].

[40] H1 collaboration, *A general search for new phenomena at HERA*, *Phys. Lett. B* **674** (2009) 257 [arXiv:0901.0507] [INSPIRE].

[41] ATLAS collaboration, *A strategy for a general search for new phenomena using data-derived signal regions and its application within the ATLAS experiment*, *Eur. Phys. J. C* **79** (2019) 120 [arXiv:1807.07447] [INSPIRE].

[42] CMS collaboration, *MUSiC: a model-unspecific search for new physics in proton-proton collisions at $\sqrt{s} = 13$ TeV*, *Eur. Phys. J. C* **81** (2021) 629 [arXiv:2010.02984] [INSPIRE].

[43] ATLAS collaboration, *Search for high-mass dilepton resonances using 139 fb^{-1} of pp collision data collected at $\sqrt{s} = 13$ TeV with the ATLAS detector*, *Phys. Lett. B* **796** (2019) 68 [arXiv:1903.06248] [INSPIRE].

[44] ATLAS collaboration, *Search for new phenomena in three- or four-lepton events in pp collisions at $\sqrt{s} = 13$ TeV with the ATLAS detector*, *Phys. Lett. B* **824** (2022) 136832 [arXiv:2107.00404] [INSPIRE].

[45] J. de Blas, J.M. Lizana and M. Perez-Victoria, *Combining searches of Z' and W' bosons*, *JHEP* **01** (2013) 166 [arXiv:1211.2229] [INSPIRE].

[46] D. Pappadopulo, A. Thamm, R. Torre and A. Wulzer, *Heavy vector triplets: bridging theory and data*, *JHEP* **09** (2014) 060 [arXiv:1402.4431] [INSPIRE].

[47] ATLAS collaboration, *The ATLAS Experiment at the CERN Large Hadron Collider*, 2008 *JINST* **3** S08003 [INSPIRE].

JHEP06(2023)036

[48] ATLAS collaboration, *ATLAS Insertable B-Layer Technical Design Report*, ATLAS-TDR-2010-19, CERN, Geneva (2010) [ATLAS-TDR-2010-19-ADD-1].

[49] ATLAS IBL collaboration, *Production and integration of the ATLAS Insertable B-Layer*, 2018 *JINST* **13** T05008 [arXiv:1803.00844] [INSPIRE].

[50] ATLAS collaboration, *Electron and photon performance measurements with the ATLAS detector using the 2015–2017 LHC proton-proton collision data*, 2019 *JINST* **14** P12006 [arXiv:1908.00005] [INSPIRE].

[51] ATLAS collaboration, *Performance of the ATLAS trigger system in 2015*, *Eur. Phys. J. C* **77** (2017) 317 [arXiv:1611.09661] [INSPIRE].

[52] ATLAS collaboration, *The ATLAS Collaboration Software and Firmware*, ATL-SOFT-PUB-2021-001, CERN, Geneva (2021).

[53] ATLAS collaboration, *ATLAS data quality operations and performance for 2015–2018 data-taking*, 2020 *JINST* **15** P04003 [arXiv:1911.04632] [INSPIRE].

[54] ATLAS collaboration, *Performance of electron and photon triggers in ATLAS during LHC Run 2*, *Eur. Phys. J. C* **80** (2020) 47 [arXiv:1909.00761] [INSPIRE].

[55] ATLAS collaboration, *Performance of the ATLAS muon triggers in Run 2*, 2020 *JINST* **15** P09015 [arXiv:2004.13447] [INSPIRE].

[56] ATLAS collaboration, *The performance of the jet trigger for the ATLAS detector during 2011 data taking*, *Eur. Phys. J. C* **76** (2016) 526 [arXiv:1606.07759] [INSPIRE].

[57] SHERPA collaboration, *Event generation with Sherpa 2.2*, *SciPost Phys.* **7** (2019) 034 [arXiv:1905.09127] [INSPIRE].

[58] NNPDF collaboration, *Parton distributions for the LHC run II*, *JHEP* **04** (2015) 040 [arXiv:1410.8849] [INSPIRE].

[59] S. Hoeche, F. Krauss, M. Schonherr and F. Siegert, *QCD matrix elements + parton showers. The NLO case*, *JHEP* **04** (2013) 027 [arXiv:1207.5030] [INSPIRE].

[60] P. Nason, *A new method for combining NLO QCD with shower Monte Carlo algorithms*, *JHEP* **11** (2004) 040 [hep-ph/0409146] [INSPIRE].

[61] S. Frixione, P. Nason and C. Oleari, *Matching NLO QCD computations with parton shower simulations: the POWHEG method*, *JHEP* **11** (2007) 070 [arXiv:0709.2092] [INSPIRE].

[62] S. Alioli, P. Nason, C. Oleari and E. Re, *A general framework for implementing NLO calculations in shower Monte Carlo programs: the POWHEG BOX*, *JHEP* **06** (2010) 043 [arXiv:1002.2581] [INSPIRE].

[63] S. Alioli, P. Nason, C. Oleari and E. Re, *NLO vector-boson production matched with shower in POWHEG*, *JHEP* **07** (2008) 060 [arXiv:0805.4802] [INSPIRE].

[64] T. Sjöstrand et al., *An introduction to PYTHIA 8.2*, *Comput. Phys. Commun.* **191** (2015) 159 [arXiv:1410.3012] [INSPIRE].

[65] ATLAS collaboration, *Measurement of the Z/γ^* boson transverse momentum distribution in pp collisions at $\sqrt{s} = 7$ TeV with the ATLAS detector*, *JHEP* **09** (2014) 145 [arXiv:1406.3660] [INSPIRE].

[66] H.-L. Lai et al., *New parton distributions for collider physics*, *Phys. Rev. D* **82** (2010) 074024 [arXiv:1007.2241] [INSPIRE].

JHEP06(2023)036

[67] J. Pumplin et al., *New generation of parton distributions with uncertainties from global QCD analysis*, *JHEP* **07** (2002) 012 [hep-ph/0201195] [INSPIRE].

[68] S. Frixione, P. Nason and G. Ridolfi, *A Positive-weight next-to-leading-order Monte Carlo for heavy flavour hadroproduction*, *JHEP* **09** (2007) 126 [arXiv:0707.3088] [INSPIRE].

[69] ATLAS collaboration, *ATLAS Pythia 8 tunes to 7 TeV data*, ATL-PHYS-PUB-2014-021, CERN, Geneva (2014).

[70] M. Czakon and A. Mitov, *Top++: A program for the calculation of the top-pair cross-section at hadron colliders*, *Comput. Phys. Commun.* **185** (2014) 2930 [arXiv:1112.5675] [INSPIRE].

[71] ATLAS collaboration, *Measurement of the transverse momentum distribution of Drell-Yan lepton pairs in proton-proton collisions at* $\sqrt{s} = 13$ *TeV with the ATLAS detector*, *Eur. Phys. J. C* **80** (2020) 616 [arXiv:1912.02844] [INSPIRE].

[72] J. Alwall et al., *The automated computation of tree-level and next-to-leading order differential cross sections, and their matching to parton shower simulations*, *JHEP* **07** (2014) 079 [arXiv:1405.0301] [INSPIRE].

[73] S. Carrazza, S. Forte and J. Rojo, *Parton distributions and event generators*, arXiv:1311.5887.

[74] M. Oreglia, *A study of the reactions* $\psi' \to \gamma\gamma\psi$, SLAC-R-0236 (1980) [www.slac.stanford.edu/cgi-wrap/getdoc/slac-r-236.pdf [INSPIRE].

[75] ATLAS collaboration, *A search for the dimuon decay of the Standard Model Higgs boson with the ATLAS detector*, *Phys. Lett. B* **812** (2021) 135980 [arXiv:2007.07830] [INSPIRE].

[76] GEANT4 collaboration, *GEANT4 — a simulation toolkit*, *Nucl. Instrum. Meth. A* **506** (2003) 250 [INSPIRE].

[77] ATLAS collaboration, *The ATLAS Simulation Infrastructure*, *Eur. Phys. J. C* **70** (2010) 823 [arXiv:1005.4568] [INSPIRE].

[78] ATLAS collaboration, *The Pythia 8 A3 tune description of ATLAS minimum bias and inelastic measurements incorporating the Donnachie-Landshoff diffractive model*, ATL-PHYS-PUB-2016-017, CERN, Geneva (2016).

[79] ATLAS collaboration, *Vertex Reconstruction Performance of the ATLAS Detector at* $\sqrt{s} = 13$ *TeV*, ATL-PHYS-PUB-2015-026, CERN, Geneva (2015).

[80] ATLAS collaboration, *Muon reconstruction performance of the ATLAS detector in proton-proton collision data at* $\sqrt{s} = 13$ *TeV*, *Eur. Phys. J. C* **76** (2016) 292 [arXiv:1603.05598] [INSPIRE].

[81] ATLAS collaboration, *Muon reconstruction and identification efficiency in ATLAS using the full Run 2 pp collision data set at* $\sqrt{s} = 13$ *TeV*, *Eur. Phys. J. C* **81** (2021) 578 [arXiv:2012.00578] [INSPIRE].

[82] ATLAS collaboration, *Electron reconstruction and identification in the ATLAS experiment using the 2015 and 2016 LHC proton-proton collision data at* $\sqrt{s} = 13$ *TeV*, *Eur. Phys. J. C* **79** (2019) 639 [arXiv:1902.04655] [INSPIRE].

[83] ATLAS collaboration, *Topological cell clustering in the ATLAS calorimeters and its performance in LHC Run 1*, *Eur. Phys. J. C* **77** (2017) 490 [arXiv:1603.02934] [INSPIRE].

[84] L. Breiman, J.H. Friedman, R.A. Olshen and C.J. Stone, *Classification and regression trees*, Routledge (2017) [DOI:10.1201/9781315139470].

JHEP06(2023)036

[85] B.P. Roe et al., *Boosted decision trees as an alternative to artificial neural networks for particle identification*, *Nucl. Instrum. Meth. A* **543** (2005) 577 [physics/0408124] [INSPIRE].

[86] ATLAS collaboration, *Measurement of the photon identification efficiencies with the ATLAS detector using LHC Run 2 data collected in 2015 and 2016*, *Eur. Phys. J. C* **79** (2019) 205 [arXiv:1810.05087] [INSPIRE].

[87] ATLAS collaboration, *Jet reconstruction and performance using particle flow with the ATLAS Detector*, *Eur. Phys. J. C* **77** (2017) 466 [arXiv:1703.10485] [INSPIRE].

[88] M. Cacciari, G.P. Salam and G. Soyez, *The anti-k_t jet clustering algorithm*, *JHEP* **04** (2008) 063 [arXiv:0802.1189] [INSPIRE].

[89] M. Cacciari, G.P. Salam and G. Soyez, *FastJet user manual*, *Eur. Phys. J. C* **72** (2012) 1896 [arXiv:1111.6097] [INSPIRE].

[90] ATLAS collaboration, *Jet energy scale measurements and their systematic uncertainties in proton-proton collisions at $\sqrt{s} = 13$ TeV with the ATLAS detector*, *Phys. Rev. D* **96** (2017) 072002 [arXiv:1703.09665] [INSPIRE].

[91] ATLAS collaboration, *Performance of pile-up mitigation techniques for jets in pp collisions at $\sqrt{s} = 8$ TeV using the ATLAS detector*, *Eur. Phys. J. C* **76** (2016) 581 [arXiv:1510.03823] [INSPIRE].

[92] ATLAS collaboration, *ATLAS b-jet identification performance and efficiency measurement with $t\bar{t}$ events in pp collisions at $\sqrt{s} = 13$ TeV*, *Eur. Phys. J. C* **79** (2019) 970 [arXiv:1907.05120] [INSPIRE].

[93] D. Krohn, J. Thaler and L.-T. Wang, *Jet trimming*, *JHEP* **02** (2010) 084 [arXiv:0912.1342] [INSPIRE].

[94] ATLAS collaboration, *Optimisation of large-radius jet reconstruction for the ATLAS detector in 13 TeV proton-proton collisions*, *Eur. Phys. J. C* **81** (2021) 334 [arXiv:2009.04986] [INSPIRE].

[95] ATLAS collaboration, *Measurement of the ATLAS Detector Jet Mass Response using Forward Folding with 80 fb^{-1} of $\sqrt{s} = 13$ TeV pp data*, ATLAS-CONF-2020-022, CERN, Geneva (2020).

[96] ATLAS collaboration, *Formulae for Estimating Significance*, ATL-PHYS-PUB-2020-025, CERN, Geneva (2020).

[97] ATLAS collaboration, *Recommendations for the Modeling of Smooth Backgrounds*, ATL-PHYS-PUB-2020-028, CERN, Geneva (2020).

[98] ATLAS collaboration, *Luminosity determination in pp collisions at $\sqrt{s} = 13$ TeV using the ATLAS detector at the LHC*, ATLAS-CONF-2019-021, CERN, Geneva (2019).

[99] G. Avoni et al., *The new LUCID-2 detector for luminosity measurement and monitoring in ATLAS*, 2018 *JINST* **13** P07017 [INSPIRE].

[100] A.L. Read, *Presentation of search results: the CL_S technique*, *J. Phys. G* **28** (2002) 2693 [INSPIRE].

[101] CMS collaboration, *Search for narrow and broad dijet resonances in proton-proton collisions at $\sqrt{s} = 13$ TeV and constraints on dark matter mediators and other new particles*, *JHEP* **08** (2018) 130 [arXiv:1806.00843] [INSPIRE].

JHEP06(2023)036

[102] G. Cowan, K. Cranmer, E. Gross and O. Vitells, *Asymptotic formulae for likelihood-based tests of new physics*, *Eur. Phys. J. C* **71** (2011) 1554 [*Erratum ibid.* **73** (2013) 2501] [arXiv:1007.1727] [INSPIRE].

[103] ATLAS collaboration, *A search for new resonances in multiple final states with a high transverse Z momentum boson in $\sqrt{s} = 13$ TeV pp collisions with the ATLAS detector* HEPData collection, DOI:10.17182/hepdata.132793 (2022).

[104] ATLAS collaboration, *Search for new phenomena in the dijet mass distribution using pp collision data at $\sqrt{s} = 8$ TeV with the ATLAS detector*, *Phys. Rev. D* **91** (2015) 052007 [arXiv:1407.1376] [INSPIRE].

[105] ATLAS collaboration, *ATLAS Computing Acknowledgements*, ATL-SOFT-PUB-2021-003, CERN, Geneva (2021).

[106] M. Cacciari and G.P. Salam, *Pileup subtraction using jet areas*, *Phys. Lett. B* **659** (2008) 119 [arXiv:0707.1378] [INSPIRE].

[107] ATLAS collaboration, *Improved electron reconstruction in ATLAS using the Gaussian Sum Filter-based model for bremsstrahlung*, ATLAS-CONF-2012-047, CERN, Geneva (2012).

JHEP06(2023)036

The ATLAS collaboration

G. Aad[101], B. Abbott[119], D.C. Abbott[102], K. Abeling[55], S.H. Abidi[29], A. Aboulhorma[35e], H. Abramowicz[150], H. Abreu[149], Y. Abulaiti[116], A.C. Abusleme Hoffman[136a], B.S. Acharya[68a,68b,o], B. Achkar[55], C. Adam Bourdarios[4], L. Adamczyk[84a], L. Adamek[154], S.V. Addepalli[26], J. Adelman[114], A. Adiguzel[21c], S. Adorni[56], T. Adye[133], A.A. Affolder[135], Y. Afik[36], M.N. Agaras[13], J. Agarwala[72a,72b], A. Aggarwal[99], C. Agheorghiesei[27c], J.A. Aguilar-Saavedra[129f], A. Ahmad[36], F. Ahmadov[38,x], W.S. Ahmed[103], S. Ahuja[94], X. Ai[48], G. Aielli[75a,75b], I. Aizenberg[167], M. Akbiyik[99], T.P.A. Åkesson[97], A.V. Akimov[37], K. Al Khoury[41], G.L. Alberghi[23b], J. Albert[163], P. Albicocco[53], S. Alderweireldt[52], M. Aleksa[36], I.N. Aleksandrov[38], C. Alexa[27b], T. Alexopoulos[10], A. Alfonsi[113], F. Alfonsi[23b], M. Alhroob[119], B. Ali[131], S. Ali[147], M. Aliev[37], G. Alimonti[70a], W. Alkakhi[55], C. Allaire[66], B.M.M. Allbrooke[145], P.P. Allport[20], A. Aloisio[71a,71b], F. Alonso[89], C. Alpigiani[137], E. Alunno Camelia[75a,75b], M. Alvarez Estevez[98], M.G. Alviggi[71a,71b], M. Aly[100], Y. Amaral Coutinho[81b], A. Ambler[103], C. Amelung[36], M. Amerl[1], C.G. Ames[108], D. Amidei[105], S.P. Amor Dos Santos[129a], S. Amoroso[48], K.R. Amos[161], V. Ananiev[124], C. Anastopoulos[138], T. Andeen[11], J.K. Anders[36], S.Y. Andrean[47a,47b], A. Andreazza[70a,70b], S. Angelidakis[9], A. Angerami[41,z], A.V. Anisenkov[37], A. Annovi[73a], C. Antel[56], M.T. Anthony[138], E. Antipov[120], M. Antonelli[53], D.J.A. Antrim[17a], F. Anulli[74a], M. Aoki[82], T. Aoki[152], J.A. Aparisi Pozo[161], M.A. Aparo[145], L. Aperio Bella[48], C. Appelt[18], N. Aranzabal[36], V. Araujo Ferraz[81a], C. Arcangeletti[53], A.T.H. Arce[51], E. Arena[91], J-F. Arguin[107], S. Argyropoulos[54], J.-H. Arling[48], A.J. Armbruster[36], O. Arnaez[154], H. Arnold[113], Z.P. Arrubarrena Tame[108], G. Artoni[74a,74b], H. Asada[110], K. Asai[117], S. Asai[152], N.A. Asbah[61], J. Assahsah[35d], K. Assamagan[29], R. Astalos[28a], R.J. Atkin[33a], M. Atkinson[160], N.B. Atlay[18], H. Atmani[62b], P.A. Atmasiddha[105], K. Augsten[131], S. Auricchio[71a,71b], A.D. Auriol[20], V.A. Austrup[169], G. Avner[149], G. Avolio[36], K. Axiotis[56], M.K. Ayoub[14c], G. Azuelos[107,ac], D. Babal[28a], H. Bachacou[134], K. Bachas[151,q], A. Bachiu[34], F. Backman[47a,47b], A. Badea[61], P. Bagnaia[74a,74b], M. Bahmani[18], A.J. Bailey[161], V.R. Bailey[160], J.T. Baines[133], C. Bakalis[10], O.K. Baker[170], P.J. Bakker[113], E. Bakos[15], D. Bakshi Gupta[8], S. Balaji[146], R. Balasubramanian[113], E.M. Baldin[37], P. Balek[132], E. Ballabene[70a,70b], F. Balli[134], L.M. Baltes[63a], W.K. Balunas[32], J. Balz[99], E. Banas[85], M. Bandieramonte[128], A. Bandyopadhyay[24], S. Bansal[24], L. Barak[150], E.L. Barberio[104], D. Barberis[57b,57a], M. Barbero[101], G. Barbour[95], K.N. Barends[33a], T. Barillari[109], M-S. Barisits[36], T. Barklow[142], R.M. Barnett[17a], P. Baron[121], D.A. Baron Moreno[100], A. Baroncelli[62a], G. Barone[29], A.J. Barr[125], L. Barranco Navarro[47a,47b], F. Barreiro[98], J. Barreiro Guimarães da Costa[14a], U. Barron[150], M.G. Barros Teixeira[129a], S. Barsov[37], F. Bartels[63a], R. Bartoldus[142], A.E. Barton[90], P. Bartos[28a], A. Basalaev[48], A. Basan[99], M. Baselga[49], I. Bashta[76a,76b], A. Bassalat[66,ai], M.J. Basso[154], C.R. Basson[100], R.L. Bates[59], S. Batlamous[35e], J.R. Batley[32], B. Batool[140], M. Battaglia[135], D. Battulga[18], M. Bauce[74a,74b], P. Bauer[24], A. Bayirli[21a], J.B. Beacham[51], T. Beau[126], P.H. Beauchemin[157], F. Becherer[54], P. Bechtle[24],

JHEP06(2023)036

H.P. Beck[19,p], K. Becker[165], A.J. Beddall[21d], V.A. Bednyakov[38], C.P. Bee[144], L.J. Beemster[15], T.A. Beermann[36], M. Begalli[81d,81d], M. Begel[29], A. Behera[144], J.K. Behr[48], C. Beirao Da Cruz E Silva[36], J.F. Beirer[55,36], F. Beisiegel[24], M. Belfkir[115b], G. Bella[150], L. Bellagamba[23b], A. Bellerive[34], P. Bellos[20], K. Beloborodov[37], K. Belotskiy[37], N.L. Belyaev[37], D. Benchekroun[35a], F. Bendebba[35a], Y. Benhammou[150], D.P. Benjamin[29], M. Benoit[29], J.R. Bensinger[26], S. Bentvelsen[113], L. Beresford[36], M. Beretta[53], D. Berge[18], E. Bergeaas Kuutmann[159], N. Berger[4], B. Bergmann[131], J. Beringer[17a], S. Berlendis[7], G. Bernardi[5], C. Bernius[142], F.U. Bernlochner[24], T. Berry[94], P. Berta[132], A. Berthold[50], I.A. Bertram[90], S. Bethke[109], A. Betti[74a,74b], A.J. Bevan[93], M. Bhamjee[33c], S. Bhatta[144], D.S. Bhattacharya[164], P. Bhattarai[26], V.S. Bhopatkar[120], R. Bi[29,af], R.M. Bianchi[128], O. Biebel[108], R. Bielski[122], M. Biglietti[76a], T.R.V. Billoud[131], M. Bindi[55], A. Bingul[21b], C. Bini[74a,74b], S. Biondi[23b,23a], A. Biondini[91], C.J. Birch-sykes[100], G.A. Bird[20,133], M. Birman[167], T. Bisanz[36], E. Bisceglie[43b,43a], D. Biswas[168,k], A. Bitadze[100], K. Bjørke[124], I. Bloch[48], C. Blocker[26], A. Blue[59], U. Blumenschein[93], J. Blumenthal[99], G.J. Bobbink[113], V.S. Bobrovnikov[37], M. Boehler[54], D. Bogavac[36], A.G. Bogdanchikov[37], C. Bohm[47a], V. Boisvert[94], P. Bokan[48], T. Bold[84a], M. Bomben[5], M. Bona[93], M. Boonekamp[134], C.D. Booth[94], A.G. Borbély[59], H.M. Borecka-Bielska[107], L.S. Borgna[95], G. Borissov[90], D. Bortoletto[125], D. Boscherini[23b], M. Bosman[13], J.D. Bossio Sola[36], K. Bouaouda[35a], N. Bouchhar[161], J. Boudreau[128], E.V. Bouhova-Thacker[90], D. Boumediene[40], R. Bouquet[5], A. Boveia[118], J. Boyd[36], D. Boye[29], I.R. Boyko[38], J. Bracinik[20], N. Brahimi[62d], G. Brandt[169], O. Brandt[32], F. Braren[48], B. Brau[102], J.E. Brau[122], K. Brendlinger[48], R. Brener[167], L. Brenner[113], R. Brenner[159], S. Bressler[167], B. Brickwedde[99], D. Britton[59], D. Britzger[109], I. Brock[24], G. Brooijmans[41], W.K. Brooks[136f], E. Brost[29], T.L. Bruckler[125], P.A. Bruckman de Renstrom[85], B. Brüers[48], D. Bruncko[28b,*], A. Bruni[23b], G. Bruni[23b], M. Bruschi[23b], N. Bruscino[74a,74b], L. Bryngemark[142], T. Buanes[16], Q. Buat[137], P. Buchholz[140], A.G. Buckley[59], I.A. Budagov[38,*], M.K. Bugge[124], O. Bulekov[37], B.A. Bullard[61], S. Burdin[91], C.D. Burgard[48], A.M. Burger[40], B. Burghgrave[8], J.T.P. Burr[32], C.D. Burton[11], J.C. Burzynski[141], E.L. Busch[41], V. Büscher[99], P.J. Bussey[59], J.M. Butler[25], C.M. Buttar[59], J.M. Butterworth[95], W. Buttinger[133], C.J. Buxo Vazquez[106], A.R. Buzykaev[37], G. Cabras[23b], S. Cabrera Urbán[161], D. Caforio[58], H. Cai[128], Y. Cai[14a,14d], V.M.M. Cairo[36], O. Cakir[3a], N. Calace[36], P. Calafiura[17a], G. Calderini[126], P. Calfayan[67], G. Callea[59], L.P. Caloba[81b], D. Calvet[40], S. Calvet[40], T.P. Calvet[101], M. Calvetti[73a,73b], R. Camacho Toro[126], S. Camarda[36], D. Camarero Munoz[26], P. Camarri[75a,75b], M.T. Camerlingo[76a,76b], D. Cameron[124], C. Camincher[163], M. Campanelli[95], A. Camplani[42], V. Canale[71a,71b], A. Canesse[103], M. Cano Bret[79], J. Cantero[161], Y. Cao[160], F. Capocasa[26], M. Capua[43b,43a], A. Carbone[70a,70b], R. Cardarelli[75a], J.C.J. Cardenas[8], F. Cardillo[161], T. Carli[36], G. Carlino[71a], J.I. Carlotto[13], B.T. Carlson[128,r], E.M. Carlson[163,155a], L. Carminati[70a,70b], M. Carnesale[74a,74b], S. Caron[112], E. Carquin[136f], S. Carrá[70a,70b], G. Carratta[23b,23a], F. Carrio Argos[33g], J.W.S. Carter[154], T.M. Carter[52], M.P. Casado[13,h], A.F. Casha[154], E.G. Castiglia[170], F.L. Castillo[63a], L. Castillo Garcia[13],

JHEP06(2023)036

V. Castillo Gimenez[161], N.F. Castro[129a,129e], A. Catinaccio[36], J.R. Catmore[124], V. Cavaliere[29], N. Cavalli[23b,23a], V. Cavasinni[73a,73b], E. Celebi[21a], F. Celli[125], M.S. Centonze[69a,69b], K. Cerny[121], A.S. Cerqueira[81a], A. Cerri[145], L. Cerrito[75a,75b], F. Cerutti[17a], A. Cervelli[23b], S.A. Cetin[21d], Z. Chadi[35a], D. Chakraborty[114], M. Chala[129f], J. Chan[168], W.Y. Chan[152], J.D. Chapman[32], B. Chargeishvili[148b], D.G. Charlton[20], T.P. Charman[93], M. Chatterjee[19], S. Chekanov[6], S.V. Chekulaev[155a], G.A. Chelkov[38,a], A. Chen[105], B. Chen[150], B. Chen[163], H. Chen[14c], H. Chen[29], J. Chen[62c], J. Chen[26], S. Chen[152], S.J. Chen[14c], X. Chen[62c], X. Chen[14b,ab], Y. Chen[62a], C.L. Cheng[168], H.C. Cheng[64a], S. Cheong[142], A. Cheplakov[38], E. Cheremushkina[48], E. Cherepanova[113], R. Cherkaoui El Moursli[35e], E. Cheu[7], K. Cheung[65], L. Chevalier[134], V. Chiarella[53], G. Chiarelli[73a], N. Chiedde[101], G. Chiodini[69a], A.S. Chisholm[20], A. Chitan[27b], M. Chitishvili[161], Y.H. Chiu[163], M.V. Chizhov[38], K. Choi[11], A.R. Chomont[74a,74b], Y. Chou[102], E.Y.S. Chow[113], T. Chowdhury[33g], L.D. Christopher[33g], K.L. Chu[64a], M.C. Chu[64a], X. Chu[14a,14d], J. Chudoba[130], J.J. Chwastowski[85], D. Cieri[109], K.M. Ciesla[84a], V. Cindro[92], A. Ciocio[17a], F. Cirotto[71a,71b], Z.H. Citron[167,l], M. Citterio[70a], D.A. Ciubotaru[27b], B.M. Ciungu[154], A. Clark[56], P.J. Clark[52], J.M. Clavijo Columbie[48], S.E. Clawson[100], C. Clement[47a,47b], J. Clercx[48], L. Clissa[23b,23a], Y. Coadou[101], M. Cobal[68a,68c], A. Coccaro[57b], R.F. Coelho Barrue[129a], R. Coelho Lopes De Sa[102], S. Coelli[70a], H. Cohen[150], A.E.C. Coimbra[70a,70b], B. Cole[41], J. Collot[60], P. Conde Muiño[129a,129g], M.P. Connell[33c], S.H. Connell[33c], I.A. Connelly[59], E.I. Conroy[125], F. Conventi[71a,ad], H.G. Cooke[20], A.M. Cooper-Sarkar[125], F. Cormier[162], L.D. Corpe[36], M. Corradi[74a,74b], E.E. Corrigan[97], F. Corriveau[103,v], A. Cortes-Gonzalez[18], M.J. Costa[161], F. Costanza[4], D. Costanzo[138], B.M. Cote[118], G. Cowan[94], J.W. Cowley[32], K. Cranmer[116], S. Crépé-Renaudin[60], F. Crescioli[126], M. Cristinziani[140], M. Cristoforetti[77a,77b,c], V. Croft[157], G. Crosetti[43b,43a], A. Cueto[36], T. Cuhadar Donszelmann[158], H. Cui[14a,14d], Z. Cui[7], A.R. Cukierman[142], W.R. Cunningham[59], F. Curcio[43b,43a], P. Czodrowski[36], M.M. Czurylo[63b], M.J. Da Cunha Sargedas De Sousa[62a], J.V. Da Fonseca Pinto[81b], C. Da Via[100], W. Dabrowski[84a], T. Dado[49], S. Dahbi[33g], T. Dai[105], C. Dallapiccola[102], M. Dam[42], G. D'amen[29], V. D'Amico[108], J. Damp[99], J.R. Dandoy[127], M.F. Daneri[30], M. Danninger[141], V. Dao[36], G. Darbo[57b], S. Darmora[6], S.J. Das[29], S. D'Auria[70a,70b], C. David[155b], T. Davidek[132], D.R. Davis[51], B. Davis-Purcell[34], I. Dawson[93], K. De[8], R. De Asmundis[71a], M. De Beurs[113], N. De Biase[48], S. De Castro[23b,23a], N. De Groot[112], P. de Jong[113], H. De la Torre[106], A. De Maria[14c], A. De Salvo[74a], U. De Sanctis[75a,75b], A. De Santo[145], J.B. De Vivie De Regie[60], D.V. Dedovich[38], J. Degens[113], A.M. Deiana[44], F. Del Corso[23b,23a], J. Del Peso[98], F. Del Rio[63a], F. Deliot[134], C.M. Delitzsch[49], M. Della Pietra[71a,71b], D. Della Volpe[56], A. Dell'Acqua[36], L. Dell'Asta[70a,70b], M. Delmastro[4], P.A. Delsart[60], S. Demers[170], M. Demichev[38], S.P. Denisov[37], L. D'Eramo[114], D. Derendarz[85], F. Derue[126], P. Dervan[91], K. Desch[24], K. Dette[154], C. Deutsch[24], P.O. Deviveiros[36], F.A. Di Bello[57b,57a], A. Di Ciaccio[75a,75b], L. Di Ciaccio[4], A. Di Domenico[74a,74b], C. Di Donato[71a,71b], A. Di Girolamo[36], G. Di Gregorio[5], A. Di Luca[77a,77b], B. Di Micco[76a,76b], R. Di Nardo[76a,76b], C. Diaconu[101], F.A. Dias[113], T. Dias Do Vale[141], M.A. Diaz[136a,136b],

JHEP06(2023)036

F.G. Diaz Capriles[24], M. Didenko[161], E.B. Diehl[105], L. Diehl[54], S. Díez Cornell[48], C. Diez Pardos[140], C. Dimitriadi[24,159], A. Dimitrievska[17a], W. Ding[14b], J. Dingfelder[24], I-M. Dinu[27b], S.J. Dittmeier[63b], F. Dittus[36], F. Djama[101], T. Djobava[148b], J.I. Djuvsland[16], C. Doglioni[100,97], J. Dolejsi[132], Z. Dolezal[132], M. Donadelli[81c], B. Dong[62c], J. Donini[40], A. D'Onofrio[14c], M. D'Onofrio[91], J. Dopke[133], A. Doria[71a], M.T. Dova[89], A.T. Doyle[59], M.A. Draguet[125], E. Drechsler[141], E. Dreyer[167], I. Drivas-koulouris[10], A.S. Drobac[157], M. Drozdova[56], D. Du[62a], T.A. du Pree[113], F. Dubinin[37], M. Dubovsky[28a], E. Duchovni[167], G. Duckeck[108], O.A. Ducu[27b], D. Duda[109], A. Dudarev[36], M. D'uffizi[100], L. Duflot[66], M. Dührssen[36], C. Dülsen[169], A.E. Dumitriu[27b], M. Dunford[63a], S. Dungs[49], K. Dunne[47a,47b], A. Duperrin[101], H. Duran Yildiz[3a], M. Düren[58], A. Durglishvili[148b], B.L. Dwyer[114], G.I. Dyckes[17a], M. Dyndal[84a], S. Dysch[100], B.S. Dziedzic[85], Z.O. Earnshaw[145], B. Eckerova[28a], M.G. Eggleston[51], E. Egidio Purcino De Souza[81b], L.F. Ehrke[56], G. Eigen[16], K. Einsweiler[17a], T. Ekelof[159], P.A. Ekman[97], Y. El Ghazali[35b], H. El Jarrari[35e,147], A. El Moussaouy[35a], V. Ellajosyula[159], M. Ellert[159], F. Ellinghaus[169], A.A. Elliot[93], N. Ellis[36], J. Elmsheuser[29], M. Elsing[36], D. Emeliyanov[133], A. Emerman[41], Y. Enari[152], I. Ene[17a], S. Epari[13], J. Erdmann[49,aa], A. Ereditato[19], P.A. Erland[85], M. Errenst[169], M. Escalier[66], C. Escobar[161], E. Etzion[150], G. Evans[129a], H. Evans[67], M.O. Evans[145], A. Ezhilov[37], S. Ezzarqtouni[35a], F. Fabbri[59], L. Fabbri[23b,23a], G. Facini[95], V. Fadeyev[135], R.M. Fakhrutdinov[37], S. Falciano[74a], P.J. Falke[24], S. Falke[36], J. Faltova[132], Y. Fan[14a], Y. Fang[14a,14d], G. Fanourakis[46], M. Fanti[70a,70b], M. Faraj[68a,68b], Z. Farazpay[96], A. Farbin[8], A. Farilla[76a], T. Farooque[106], S.M. Farrington[52], F. Fassi[35e], D. Fassouliotis[9], M. Faucci Giannelli[75a,75b], W.J. Fawcett[32], L. Fayard[66], P. Federicova[130], O.L. Fedin[37,a], G. Fedotov[37], M. Feickert[168], L. Feligioni[101], A. Fell[138], D.E. Fellers[122], C. Feng[62b], M. Feng[14b], Z. Feng[113], M.J. Fenton[158], A.B. Fenyuk[37], L. Ferencz[48], S.W. Ferguson[45], J. Ferrando[48], A. Ferrari[159], P. Ferrari[113,112], R. Ferrari[72a], D. Ferrere[56], C. Ferretti[105], F. Fiedler[99], A. Filipčič[92], E.K. Filmer[1], F. Filthaut[112], M.C.N. Fiolhais[129a,129c,b], L. Fiorini[161], F. Fischer[140], W.C. Fisher[106], T. Fitschen[100], I. Fleck[140], P. Fleischmann[105], T. Flick[169], L. Flores[127], M. Flores[33d], L.R. Flores Castillo[64a], F.M. Follega[77a,77b], N. Fomin[16], J.H. Foo[154], B.C. Forland[67], A. Formica[134], A.C. Forti[100], E. Fortin[101], A.W. Fortman[61], M.G. Foti[17a], L. Fountas[9], D. Fournier[66], H. Fox[90], P. Francavilla[73a,73b], S. Francescato[61], S. Franchellucci[56], M. Franchini[23b,23a], S. Franchino[63a], D. Francis[36], L. Franco[112], L. Franconi[19], M. Franklin[61], G. Frattari[26], A.C. Freegard[93], P.M. Freeman[20], W.S. Freund[81b], N. Fritzsche[50], A. Froch[54], D. Froidevaux[36], J.A. Frost[125], Y. Fu[62a], M. Fujimoto[117], E. Fullana Torregrosa[161,*], J. Fuster[161], A. Gabrielli[23b,23a], A. Gabrielli[154], P. Gadow[48], G. Gagliardi[57b,57a], L.G. Gagnon[17a], G.E. Gallardo[125], E.J. Gallas[125], B.J. Gallop[133], R. Gamboa Goni[93], K.K. Gan[118], S. Ganguly[152], J. Gao[62a], Y. Gao[52], F.M. Garay Walls[136a,136b], B. Garcia[29,af], C. García[161], J.E. García Navarro[161], J.A. García Pascual[14a], M. Garcia-Sciveres[17a], R.W. Gardner[39], D. Garg[79], R.B. Garg[142], S. Gargiulo[54], C.A. Garner[154], V. Garonne[29], S.J. Gasiorowski[137], P. Gaspar[81b], G. Gaudio[72a], V. Gautam[13], P. Gauzzi[74a,74b],

JHEP06(2023)036

I.L. Gavrilenko[37], A. Gavrilyuk[37], C. Gay[162], G. Gaycken[48], E.N. Gazis[10], A.A. Geanta[27b,27e], C.M. Gee[135], J. Geisen[97], M. Geisen[99], C. Gemme[57b], M.H. Genest[60], S. Gentile[74a,74b], S. George[94], W.F. George[20], T. Geralis[46], L.O. Gerlach[55], P. Gessinger-Befurt[36], M. Ghasemi Bostanabad[163], M. Ghneimat[140], K. Ghorbanian[93], A. Ghosal[140], A. Ghosh[158], A. Ghosh[7], B. Giacobbe[23b], S. Giagu[74a,74b], N. Giangiacomi[154], P. Giannetti[73a], A. Giannini[62a], S.M. Gibson[94], M. Gignac[135], D.T. Gil[84b], A.K. Gilbert[84a], B.J. Gilbert[41], D. Gillberg[34], G. Gilles[113], N.E.K. Gillwald[48], L. Ginabat[126], D.M. Gingrich[2,ac], M.P. Giordani[68a,68c], P.F. Giraud[134], G. Giugliarelli[68a,68c], D. Giugni[70a], F. Giuli[36], I. Gkialas[9,i], L.K. Gladilin[37], C. Glasman[98], G.R. Gledhill[122], M. Glisic[122], I. Gnesi[43b,e], Y. Go[29,af], M. Goblirsch-Kolb[26], B. Gocke[49], D. Godin[107], S. Goldfarb[104], T. Golling[56], M.G.D. Gololo[33g], D. Golubkov[37], J.P. Gombas[106], A. Gomes[129a,129b], G. Gomes Da Silva[140], A.J. Gomez Delegido[161], R. Goncalves Gama[55], R. Gonçalo[129a,129c], G. Gonella[122], L. Gonella[20], A. Gongadze[38], F. Gonnella[20], J.L. Gonski[41], S. González de la Hoz[161], S. Gonzalez Fernandez[13], R. Gonzalez Lopez[91], C. Gonzalez Renteria[17a], R. Gonzalez Suarez[159], S. Gonzalez-Sevilla[56], G.R. Gonzalvo Rodriguez[161], R.Y. González Andana[52], L. Goossens[36], N.A. Gorasia[20], P.A. Gorbounov[37], B. Gorini[36], E. Gorini[69a,69b], A. Gorišek[92], A.T. Goshaw[51], M.I. Gostkin[38], C.A. Gottardo[36], M. Gouighri[35b], V. Goumarre[48], A.G. Goussiou[137], N. Govender[33c], C. Goy[4], I. Grabowska-Bold[84a], K. Graham[34], E. Gramstad[124], S. Grancagnolo[18], M. Grandi[145], V. Gratchev[37,*], P.M. Gravila[27f], F.G. Gravili[69a,69b], H.M. Gray[17a], M. Greco[69a,69b], C. Grefe[24], I.M. Gregor[48], P. Grenier[142], C. Grieco[13], A.A. Grillo[135], K. Grimm[31,m], S. Grinstein[13,t], J.-F. Grivaz[66], E. Gross[167], J. Grosse-Knetter[55], C. Grud[105], A. Grummer[111], J.C. Grundy[125], L. Guan[105], W. Guan[168], C. Gubbels[162], J.G.R. Guerrero Rojas[161], G. Guerrieri[68a,68b], F. Guescini[109], R. Gugel[99], J.A.M. Guhit[105], A. Guida[48], T. Guillemin[4], E. Guilloton[165,133], S. Guindon[36], F. Guo[14a,14d], J. Guo[62c], L. Guo[66], Y. Guo[105], R. Gupta[48], S. Gurbuz[24], S.S. Gurdasani[54], G. Gustavino[36], M. Guth[56], P. Gutierrez[119], L.F. Gutierrez Zagazeta[127], C. Gutschow[95], C. Guyot[134], C. Gwenlan[125], C.B. Gwilliam[91], E.S. Haaland[124], A. Haas[116], M. Habedank[48], C. Haber[17a], H.K. Hadavand[8], A. Hadef[99], S. Hadzic[109], E.H. Haines[95], M. Haleem[164], J. Haley[120], J.J. Hall[138], G.D. Hallewell[101], L. Halser[19], K. Hamano[163], H. Hamdaoui[35e], M. Hamer[24], G.N. Hamity[52], J. Han[62b], K. Han[62a], L. Han[14c], L. Han[62a], S. Han[17a], Y.F. Han[154], K. Hanagaki[82], M. Hance[135], D.A. Hangal[41,z], H. Hanif[141], M.D. Hank[39], R. Hankache[100], J.B. Hansen[42], J.D. Hansen[42], P.H. Hansen[42], K. Hara[156], D. Harada[56], T. Harenberg[169], S. Harkusha[37], Y.T. Harris[125], N.M. Harrison[118], P.F. Harrison[165], N.M. Hartman[142], N.M. Hartmann[108], Y. Hasegawa[139], A. Hasib[52], S. Haug[19], R. Hauser[106], M. Havranek[131], C.M. Hawkes[20], R.J. Hawkings[36], S. Hayashida[110], D. Hayden[106], C. Hayes[105], R.L. Hayes[162], C.P. Hays[125], J.M. Hays[93], H.S. Hayward[91], F. He[62a], Y. He[153], Y. He[126], M.P. Heath[52], V. Hedberg[97], A.L. Heggelund[124], N.D. Hehir[93], C. Heidegger[54], K.K. Heidegger[54], W.D. Heidorn[80], J. Heilman[34], S. Heim[48], T. Heim[17a], J.G. Heinlein[127], J.J. Heinrich[122], L. Heinrich[109], J. Hejbal[130],

JHEP06(2023)036

L. Helary[48], A. Held[168], S. Hellesund[124], C.M. Helling[162], S. Hellman[47a,47b], C. Helsens[36], R.C.W. Henderson[90], L. Henkelmann[32], A.M. Henriques Correia[36], H. Herde[97], Y. Hernández Jiménez[144], L.M. Herrmann[24], M.G. Herrmann[108], T. Herrmann[50], G. Herten[54], R. Hertenberger[108], L. Hervas[36], N.P. Hessey[155a], H. Hibi[83], E. Higón-Rodriguez[161], S.J. Hillier[20], I. Hinchliffe[17a], F. Hinterkeuser[24], M. Hirose[123], S. Hirose[156], D. Hirschbuehl[169], T.G. Hitchings[100], B. Hiti[92], J. Hobbs[144], R. Hobincu[27e], N. Hod[167], M.C. Hodgkinson[138], B.H. Hodkinson[32], A. Hoecker[36], J. Hofer[48], D. Hohn[54], T. Holm[24], M. Holzbock[109], L.B.A.H. Hommels[32], B.P. Honan[100], J. Hong[62c], T.M. Hong[128], J.C. Honig[54], A. Hönle[109], B.H. Hooberman[160], W.H. Hopkins[6], Y. Horii[110], S. Hou[147], A.S. Howard[92], J. Howarth[59], J. Hoya[6], M. Hrabovsky[121], A. Hrynevich[48], T. Hryn'ova[4], P.J. Hsu[65], S.-C. Hsu[137], Q. Hu[41,z], Y.F. Hu[14a,14d,ae], D.P. Huang[95], S. Huang[64b], X. Huang[14c], Y. Huang[62a], Y. Huang[14a], Z. Huang[100], Z. Hubacek[131], M. Huebner[24], F. Huegging[24], T.B. Huffman[125], M. Huhtinen[36], S.K. Huiberts[16], R. Hulsken[103], N. Huseynov[12,a], J. Huston[106], J. Huth[61], R. Hyneman[142], S. Hyrych[28a], G. Iacobucci[56], G. Iakovidis[29], I. Ibragimov[140], L. Iconomidou-Fayard[66], P. Iengo[71a,71b], R. Iguchi[152], T. Iizawa[56], Y. Ikegami[82], A. Ilg[19], N. Ilic[154], H. Imam[35a], T. Ingebretsen Carlson[47a,47b], G. Introzzi[72a,72b], M. Iodice[76a], V. Ippolito[74a,74b], M. Ishino[152], W. Islam[168], C. Issever[18,48], S. Istin[21a,ah], H. Ito[166], J.M. Iturbe Ponce[64a], R. Iuppa[77a,77b], A. Ivina[167], J.M. Izen[45], V. Izzo[71a], P. Jacka[130,131], P. Jackson[1], R.M. Jacobs[48], B.P. Jaeger[141], C.S. Jagfeld[108], G. Jäkel[169], K. Jakobs[54], T. Jakoubek[167], J. Jamieson[59], K.W. Janas[84a], G. Jarlskog[97], A.E. Jaspan[91], M. Javurkova[102], F. Jeanneau[134], L. Jeanty[122], J. Jejelava[148a,y], P. Jenni[54,f], C.E. Jessiman[34], S. Jézéquel[4], J. Jia[144], X. Jia[61], X. Jia[14a,14d], Z. Jia[14c], Y. Jiang[62a], S. Jiggins[52], J. Jimenez Pena[109], S. Jin[14c], A. Jinaru[27b], O. Jinnouchi[153], P. Johansson[138], K.A. Johns[7], D.M. Jones[32], E. Jones[165], P. Jones[32], R.W.L. Jones[90], T.J. Jones[91], R. Joshi[118], J. Jovicevic[15], X. Ju[17a], J.J. Junggeburth[36], A. Juste Rozas[13,t], S. Kabana[136e], A. Kaczmarska[85], M. Kado[74a,74b], H. Kagan[118], M. Kagan[142], A. Kahn[41], A. Kahn[127], C. Kahra[99], T. Kaji[166], E. Kajomovitz[149], N. Kakati[167], C.W. Kalderon[29], A. Kamenshchikov[154], S. Kanayama[153], N.J. Kang[135], Y. Kano[110], D. Kar[33g], K. Karava[125], M.J. Kareem[155b], E. Karentzos[54], I. Karkanias[151], S.N. Karpov[38], Z.M. Karpova[38], V. Kartvelishvili[90], A.N. Karyukhin[37], E. Kasimi[151], C. Kato[62d], J. Katzy[48], S. Kaur[34], K. Kawade[139], K. Kawagoe[88], T. Kawamoto[134], G. Kawamura[55], E.F. Kay[163], F.I. Kaya[157], S. Kazakos[13], V.F. Kazanin[37], Y. Ke[144], J.M. Keaveney[33a], R. Keeler[163], G.V. Kehris[61], J.S. Keller[34], A.S. Kelly[95], D. Kelsey[145], J.J. Kempster[20], K.E. Kennedy[41], P.D. Kennedy[99], O. Kepka[130], B.P. Kerridge[165], S. Kersten[169], B.P. Kerševan[92], S. Keshri[66], L. Keszeghova[28a], S. Ketabchi Haghighat[154], M. Khandoga[126], A. Khanov[120], A.G. Kharlamov[37], T. Kharlamova[37], E.E. Khoda[137], T.J. Khoo[18], G. Khoriauli[164], J. Khubua[148b], Y.A.R. Khwaira[66], M. Kiehn[36], A. Kilgallon[122], D.W. Kim[47a,47b], E. Kim[153], Y.K. Kim[39], N. Kimura[95], A. Kirchhoff[55], D. Kirchmeier[50], C. Kirfel[24], J. Kirk[133], A.E. Kiryunin[109], T. Kishimoto[152], D.P. Kisliuk[154], C. Kitsaki[10], O. Kivernyk[24], M. Klassen[63a], C. Klein[34], L. Klein[164], M.H. Klein[105], M. Klein[91], S.B. Klein[56], U. Klein[91], P. Klimek[36],

JHEP06(2023)036

A. Klimentov[29], F. Klimpel[109], T. Klingl[24], T. Klioutchnikova[36], F.F. Klitzner[108], P. Kluit[113], S. Kluth[109], E. Kneringer[78], T.M. Knight[154], A. Knue[54], D. Kobayashi[88], R. Kobayashi[86], M. Kocian[142], P. Kodyš[132], D.M. Koeck[145], P.T. Koenig[24], T. Koffas[34], M. Kolb[134], I. Koletsou[4], T. Komarek[121], K. Köneke[54], A.X.Y. Kong[1], T. Kono[117], N. Konstantinidis[95], B. Konya[97], R. Kopeliansky[67], S. Koperny[84a], K. Korcyl[85], K. Kordas[151], G. Koren[150], A. Korn[95], S. Korn[55], I. Korolkov[13], N. Korotkova[37], B. Kortman[113], O. Kortner[109], S. Kortner[109], W.H. Kostecka[114], V.V. Kostyukhin[140], A. Kotsokechagia[134], A. Kotwal[51], A. Koulouris[36], A. Kourkoumeli-Charalampidi[72a,72b], C. Kourkoumelis[9], E. Kourlitis[6], O. Kovanda[145], R. Kowalewski[163], W. Kozanecki[134], A.S. Kozhin[37], V.A. Kramarenko[37], G. Kramberger[92], P. Kramer[99], M.W. Krasny[126], A. Krasznahorkay[36], J.A. Kremer[99], T. Kresse[50], J. Kretzschmar[91], K. Kreul[18], P. Krieger[154], F. Krieter[108], S. Krishnamurthy[102], A. Krishnan[63b], M. Krivos[132], K. Krizka[17a], K. Kroeninger[49], H. Kroha[109], J. Kroll[130], J. Kroll[127], K.S. Krowpman[106], U. Kruchonak[38], H. Krüger[24], N. Krumnack[80], M.C. Kruse[51], J.A. Krzysiak[85], O. Kuchinskaia[37], S. Kuday[3a], D. Kuechler[48], J.T. Kuechler[48], S. Kuehn[36], T. Kuhl[48], V. Kukhtin[38], Y. Kulchitsky[37,a], S. Kuleshov[136d,136b], M. Kumar[33g], N. Kumari[101], A. Kupco[130], T. Kupfer[49], A. Kupich[37], O. Kuprash[54], H. Kurashige[83], L.L. Kurchaninov[155a], Y.A. Kurochkin[37], A. Kurova[37], M. Kuze[153], A.K. Kvam[102], J. Kvita[121], T. Kwan[103], K.W. Kwok[64a], N.G. Kyriacou[105], L.A.O. Laatu[101], C. Lacasta[161], F. Lacava[74a,74b], H. Lacker[18], D. Lacour[126], N.N. Lad[95], E. Ladygin[38], B. Laforge[126], T. Lagouri[136e], S. Lai[55], I.K. Lakomiec[84a], N. Lalloue[60], J.E. Lambert[119], S. Lammers[67], W. Lampl[7], C. Lampoudis[151], A.N. Lancaster[114], E. Lançon[29], U. Landgraf[54], M.P.J. Landon[93], V.S. Lang[54], R.J. Langenberg[102], A.J. Lankford[158], F. Lanni[36], K. Lantzsch[24], A. Lanza[72a], A. Lapertosa[57b,57a], J.F. Laporte[134], T. Lari[70a], F. Lasagni Manghi[23b], M. Lassnig[36], V. Latonova[130], T.S. Lau[64a], A. Laudrain[99], A. Laurier[34], S.D. Lawlor[94], Z. Lawrence[100], M. Lazzaroni[70a,70b], B. Le[100], B. Leban[92], A. Lebedev[80], M. LeBlanc[36], T. LeCompte[6], F. Ledroit-Guillon[60], A.C.A. Lee[95], G.R. Lee[16], L. Lee[61], S.C. Lee[147], S. Lee[47a,47b], T.F. Lee[91], L.L. Leeuw[33c], H.P. Lefebvre[94], M. Lefebvre[163], C. Leggett[17a], K. Lehmann[141], G. Lehmann Miotto[36], M. Leigh[56], W.A. Leight[102], A. Leisos[151,s], M.A.L. Leite[81c], C.E. Leitgeb[48], R. Leitner[132], K.J.C. Leney[44], T. Lenz[24], S. Leone[73a], C. Leonidopoulos[52], A. Leopold[143], C. Leroy[107], R. Les[106], C.G. Lester[32], M. Levchenko[37], J. Levêque[4], D. Levin[105], L.J. Levinson[167], M.P. Lewicki[85], D.J. Lewis[4], A. Li[5], B. Li[14b], B. Li[62b], C. Li[62a], C-Q. Li[62c], H. Li[62a], H. Li[62b], H. Li[14c], H. Li[62b], J. Li[62c], K. Li[137], L. Li[62c], M. Li[14a,14d], Q.Y. Li[62a], S. Li[14a,14d], S. Li[62d,62c,d], T. Li[62b], X. Li[103], Z. Li[62b], Z. Li[125], Z. Li[103], Z. Li[91], Z. Li[14a,14d], Z. Liang[14a], M. Liberatore[48], B. Liberti[75a], K. Lie[64c], J. Lieber Marin[81b], K. Lin[106], R.A. Linck[67], R.E. Lindley[7], J.H. Lindon[2], A. Linss[48], E. Lipeles[127], A. Lipniacka[16], A. Lister[162], J.D. Little[4], B. Liu[14a], B.X. Liu[141], D. Liu[62d,62c], J.B. Liu[62a], J.K.K. Liu[32], K. Liu[62d,62c], M. Liu[62a], M.Y. Liu[62a], P. Liu[14a], Q. Liu[62d,137,62c], X. Liu[62a], Y. Liu[48], Y. Liu[14c,14d], Y.L. Liu[105], Y.W. Liu[62a], M. Livan[72a,72b], J. Llorente Merino[141], S.L. Lloyd[93], E.M. Lobodzinska[48], P. Loch[7], S. Loffredo[75a,75b], T. Lohse[18], K. Lohwasser[138], M. Lokajicek[130], J.D. Long[160],

JHEP06(2023)036

I. Longarini[74a,74b], L. Longo[69a,69b], R. Longo[160], I. Lopez Paz[36], A. Lopez Solis[48], J. Lorenz[108], N. Lorenzo Martinez[4], A.M. Lory[108], A. Lösle[54], X. Lou[47a,47b], X. Lou[14a,14d], A. Lounis[66], J. Love[6], P.A. Love[90], J.J. Lozano Bahilo[161], G. Lu[14a,14d], M. Lu[79], S. Lu[127], Y.J. Lu[65], H.J. Lubatti[137], C. Luci[74a,74b], F.L. Lucio Alves[14c], A. Lucotte[60], F. Luehring[67], I. Luise[144], O. Lukianchuk[66], O. Lundberg[143], B. Lund-Jensen[143], N.A. Luongo[122], M.S. Lutz[150], D. Lynn[29], H. Lyons[91], R. Lysak[130], E. Lytken[97], F. Lyu[14a], V. Lyubushkin[38], T. Lyubushkina[38], H. Ma[29], L.L. Ma[62b], Y. Ma[95], D.M. Mac Donell[163], G. Maccarrone[53], J.C. MacDonald[138], R. Madar[40], W.F. Mader[50], J. Maeda[83], T. Maeno[29], M. Maerker[50], V. Magerl[54], H. Maguire[138], D.J. Mahon[41], C. Maidantchik[81b], A. Maio[129a,129b,129d], K. Maj[84a], O. Majersky[28a], S. Majewski[122], N. Makovec[66], V. Maksimovic[15], B. Malaescu[126], Pa. Malecki[85], V.P. Maleev[37], F. Malek[60], D. Malito[43b,43a], U. Mallik[79], C. Malone[32], S. Maltezos[10], S. Malyukov[38], J. Mamuzic[13], G. Mancini[53], G. Manco[72a,72b], J.P. Mandalia[93], I. Mandić[92], L. Manhaes de Andrade Filho[81a], I.M. Maniatis[151], M. Manisha[134], J. Manjarres Ramos[50], D.C. Mankad[167], A. Mann[108], B. Mansoulie[134], S. Manzoni[36], A. Marantis[151], G. Marchiori[5], M. Marcisovsky[130], L. Marcoccia[75a,75b], C. Marcon[70a,70b], M. Marinescu[20], M. Marjanovic[119], E.J. Marshall[90], Z. Marshall[17a], S. Marti-Garcia[161], T.A. Martin[165], V.J. Martin[52], B. Martin dit Latour[16], L. Martinelli[74a,74b], M. Martinez[13,t], P. Martinez Agullo[161], V.I. Martinez Outschoorn[102], P. Martinez Suarez[13], S. Martin-Haugh[133], V.S. Martoiu[27b], A.C. Martyniuk[95], A. Marzin[36], S.R. Maschek[109], L. Masetti[99], T. Mashimo[152], J. Masik[100], A.L. Maslennikov[37], L. Massa[23b], P. Massarotti[71a,71b], P. Mastrandrea[73a,73b], A. Mastroberardino[43b,43a], T. Masubuchi[152], T. Mathisen[159], N. Matsuzawa[152], J. Maurer[27b], B. Maček[92], D.A. Maximov[37], R. Mazini[147], I. Maznas[151], M. Mazza[106], S.M. Mazza[135], C. Mc Ginn[29,af], J.P. Mc Gowan[103], S.P. Mc Kee[105], W.P. McCormack[17a], E.F. McDonald[104], A.E. McDougall[113], J.A. Mcfayden[145], G. Mchedlidze[148b], R.P. Mckenzie[33g], T.C. Mclachlan[48], D.J. Mclaughlin[95], K.D. McLean[163], S.J. McMahon[133], P.C. McNamara[104], C.M. Mcpartland[91], R.A. McPherson[163,v], T. Megy[40], S. Mehlhase[108], A. Mehta[91], B. Meirose[45], D. Melini[149], B.R. Mellado Garcia[33g], A.H. Melo[55], F. Meloni[48], E.D. Mendes Gouveia[129a], A.M. Mendes Jacques Da Costa[20], H.Y. Meng[154], L. Meng[90], S. Menke[109], M. Mentink[36], E. Meoni[43b,43a], C. Merlassino[125], L. Merola[71a,71b], C. Meroni[70a], G. Merz[105], O. Meshkov[37], J.K.R. Meshreki[140], J. Metcalfe[6], A.S. Mete[6], C. Meyer[67], J-P. Meyer[134], M. Michetti[18], R.P. Middleton[133], L. Mijović[52], G. Mikenberg[167], M. Mikestikova[130], M. Mikuž[92], H. Mildner[138], A. Milic[36], C.D. Milke[44], D.W. Miller[39], L.S. Miller[34], A. Milov[167], D.A. Milstead[47a,47b], T. Min[14c], A.A. Minaenko[37], I.A. Minashvili[148b], L. Mince[59], A.I. Mincer[116], B. Mindur[84a], M. Mineev[38], Y. Mino[86], L.M. Mir[13], M. Miralles Lopez[161], M. Mironova[125], M.C. Missio[112], T. Mitani[166], A. Mitra[165], V.A. Mitsou[161], O. Miu[154], P.S. Miyagawa[93], Y. Miyazaki[88], A. Mizukami[82], J.U. Mjörnmark[97], T. Mkrtchyan[63a], T. Mlinarevic[95], M. Mlynarikova[36], T. Moa[47a,47b], S. Mobius[55], K. Mochizuki[107], P. Moder[48], P. Mogg[108], A.F. Mohammed[14a,14d], S. Mohapatra[41], G. Mokgatitswane[33g], B. Mondal[140], S. Mondal[131], K. Mönig[48], E. Monnier[101], L. Monsonis Romero[161], J. Montejo Berlingen[36], M. Montella[118],

JHEP06(2023)036

F. Monticelli[89], N. Morange[66], A.L. Moreira De Carvalho[129a], M. Moreno Llácer[161], C. Moreno Martinez[56], P. Morettini[57b], S. Morgenstern[165], M. Morii[61], M. Morinaga[152], A.K. Morley[36], F. Morodei[74a,74b], L. Morvaj[36], P. Moschovakos[36], B. Moser[36], M. Mosidze[148b], T. Moskalets[54], P. Moskvitina[112], J. Moss[31,n], E.J.W. Moyse[102], S. Muanza[101], J. Mueller[128], D. Muenstermann[90], R. Müller[19], G.A. Mullier[97], J.J. Mullin[127], D.P. Mungo[154], J.L. Munoz Martinez[13], D. Munoz Perez[161], F.J. Munoz Sanchez[100], M. Murin[100], W.J. Murray[165,133], A. Murrone[70a,70b], J.M. Muse[119], M. Muškinja[17a], C. Mwewa[29], A.G. Myagkov[37,a], A.J. Myers[8], A.A. Myers[128], G. Myers[67], M. Myska[131], B.P. Nachman[17a], O. Nackenhorst[49], A. Nag[50], K. Nagai[125], K. Nagano[82], J.L. Nagle[29,af], E. Nagy[101], A.M. Nairz[36], Y. Nakahama[82], K. Nakamura[82], H. Nanjo[123], R. Narayan[44], E.A. Narayanan[111], I. Naryshkin[37], M. Naseri[34], C. Nass[24], G. Navarro[22a], J. Navarro-Gonzalez[161], R. Nayak[150], A. Nayaz[18], P.Y. Nechaeva[37], F. Nechansky[48], L. Nedic[125], T.J. Neep[20], A. Negri[72a,72b], M. Negrini[23b], C. Nellist[112], C. Nelson[103], K. Nelson[105], S. Nemecek[130], M. Nessi[36,g], M.S. Neubauer[160], F. Neuhaus[99], J. Neundorf[48], R. Newhouse[162], P.R. Newman[20], C.W. Ng[128], Y.S. Ng[18], Y.W.Y. Ng[48], B. Ngair[35e], H.D.N. Nguyen[107], R.B. Nickerson[125], R. Nicolaidou[134], J. Nielsen[135], M. Niemeyer[55], N. Nikiforou[36], V. Nikolaenko[37,a], I. Nikolic-Audit[126], K. Nikolopoulos[20], P. Nilsson[29], H.R. Nindhito[56], A. Nisati[74a], N. Nishu[2], R. Nisius[109], J-E. Nitschke[50], E.K. Nkadimeng[33g], S.J. Noacco Rosende[89], T. Nobe[152], D.L. Noel[32], Y. Noguchi[86], T. Nommensen[146], M.A. Nomura[29], M.B. Norfolk[138], R.R.B. Norisam[95], B.J. Norman[34], J. Novak[92], T. Novak[48], O. Novgorodova[50], L. Novotny[131], R. Novotny[111], L. Nozka[121], K. Ntekas[158], N.M.J. Nunes De Moura Junior[81b], E. Nurse[95], F.G. Oakham[34,ac], J. Ocariz[126], A. Ochi[83], I. Ochoa[129a], S. Oerdek[159], A. Ogrodnik[84a], A. Oh[100], C.C. Ohm[143], H. Oide[82], R. Oishi[152], M.L. Ojeda[48], Y. Okazaki[86], M.W. O'Keefe[91], Y. Okumura[152], A. Olariu[27b], L.F. Oleiro Seabra[129a], S.A. Olivares Pino[136e], D. Oliveira Damazio[29], D. Oliveira Goncalves[81a], J.L. Oliver[158], M.J.R. Olsson[158], A. Olszewski[85], J. Olszowska[85,*], Ö.O. Öncel[54], D.C. O'Neil[141], A.P. O'Neill[19], A. Onofre[129a,129e], P.U.E. Onyisi[11], M.J. Oreglia[39], G.E. Orellana[89], D. Orestano[76a,76b], N. Orlando[13], R.S. Orr[154], V. O'Shea[59], R. Ospanov[62a], G. Otero y Garzon[30], H. Otono[88], P.S. Ott[63a], G.J. Ottino[17a], M. Ouchrif[35d], J. Ouellette[29,af], F. Ould-Saada[124], M. Owen[59], R.E. Owen[133], K.Y. Oyulmaz[21a], V.E. Ozcan[21a], N. Ozturk[8], S. Ozturk[21d], J. Pacalt[121], H.A. Pacey[32], K. Pachal[51], A. Pacheco Pages[13], C. Padilla Aranda[13], G. Padovano[74a,74b], S. Pagan Griso[17a], G. Palacino[67], A. Palazzo[69a,69b], S. Palazzo[52], S. Palestini[36], M. Palka[84b], J. Pan[170], T. Pan[64a], D.K. Panchal[11], C.E. Pandini[113], J.G. Panduro Vazquez[94], H. Pang[14b], P. Pani[48], G. Panizzo[68a,68c], L. Paolozzi[56], C. Papadatos[107], S. Parajuli[44], A. Paramonov[6], C. Paraskevopoulos[10], D. Paredes Hernandez[64b], T.H. Park[154], M.A. Parker[32], F. Parodi[57b,57a], E.W. Parrish[114], V.A. Parrish[52], J.A. Parsons[41], U. Parzefall[54], B. Pascual Dias[107], L. Pascual Dominguez[150], V.R. Pascuzzi[17a], F. Pasquali[113], E. Pasqualucci[74a], S. Passaggio[57b], F. Pastore[94], P. Pasuwan[47a,47b], P. Patel[85], J.R. Pater[100], T. Pauly[36], J. Pearkes[142], M. Pedersen[124], R. Pedro[129a], S.V. Peleganchuk[37], O. Penc[36], E.A. Pender[52], C. Peng[64b], H. Peng[62a], K.E. Penski[108],

JHEP06(2023)036

M. Penzin[37], B.S. Peralva[81d,81d], A.P. Pereira Peixoto[60], L. Pereira Sanchez[47a,47b], D.V. Perepelitsa[29,af], E. Perez Codina[155a], M. Perganti[10], L. Perini[70a,70b,*], H. Pernegger[36], S. Perrella[36], A. Perrevoort[112], O. Perrin[40], K. Peters[48], R.F.Y. Peters[100], B.A. Petersen[36], T.C. Petersen[42], E. Petit[101], V. Petousis[131], C. Petridou[151], A. Petrukhin[140], M. Pettee[17a], N.E. Pettersson[36], A. Petukhov[37], K. Petukhova[132], A. Peyaud[134], R. Pezoa[136f], L. Pezzotti[36], G. Pezzullo[170], T.M. Pham[168], T. Pham[104], P.W. Phillips[133], M.W. Phipps[160], G. Piacquadio[144], E. Pianori[17a], F. Piazza[70a,70b], R. Piegaia[30], D. Pietreanu[27b], A.D. Pilkington[100], M. Pinamonti[68a,68c], J.L. Pinfold[2], B.C. Pinheiro Pereira[129a], C. Pitman Donaldson[95], D.A. Pizzi[34], L. Pizzimento[75a,75b], A. Pizzini[113], M.-A. Pleier[29], V. Plesanovs[54], V. Pleskot[132], E. Plotnikova[38], G. Poddar[4], R. Poettgen[97], L. Poggioli[126], I. Pogrebnyak[106], D. Pohl[24], I. Pokharel[55], S. Polacek[132], G. Polesello[72a], A. Poley[141,155a], R. Polifka[131], A. Polini[23b], C.S. Pollard[125], Z.B. Pollock[118], V. Polychronakos[29], E. Pompa Pacchi[74a,74b], D. Ponomarenko[37], L. Pontecorvo[36], S. Popa[27a], G.A. Popeneciu[27d], D.M. Portillo Quintero[155a], S. Pospisil[131], P. Postolache[27c], K. Potamianos[125], I.N. Potrap[38], C.J. Potter[32], H. Potti[1], T. Poulsen[48], J. Poveda[161], M.E. Pozo Astigarraga[36], A. Prades Ibanez[161], M.M. Prapa[46], J. Pretel[54], D. Price[100], M. Primavera[69a], M.A. Principe Martin[98], R. Privara[121], M.L. Proffitt[137], N. Proklova[127], K. Prokofiev[64c], G. Proto[75a,75b], S. Protopopescu[29], J. Proudfoot[6], M. Przybycien[84a], J.E. Puddefoot[138], D. Pudzha[37], P. Puzo[66], D. Pyatiizbyantseva[37], J. Qian[105], D. Qichen[100], Y. Qin[100], T. Qiu[93], A. Quadt[55], M. Queitsch-Maitland[100], G. Quetant[56], G. Rabanal Bolanos[61], D. Rafanoharana[54], F. Ragusa[70a,70b], J.L. Rainbolt[39], J.A. Raine[56], S. Rajagopalan[29], E. Ramakoti[37], K. Ran[48,14d], N.P. Rapheeha[33g], V. Raskina[126], D.F. Rassloff[63a], S. Rave[99], B. Ravina[55], I. Ravinovich[167], M. Raymond[36], A.L. Read[124], N.P. Readioff[138], D.M. Rebuzzi[72a,72b], G. Redlinger[29], K. Reeves[45], J.A. Reidelsturz[169], D. Reikher[150], A. Reiss[99], A. Rej[140], C. Rembser[36], A. Renardi[48], M. Renda[27b], M.B. Rendel[109], F. Renner[48], A.G. Rennie[59], S. Resconi[70a], M. Ressegotti[57b,57a], E.D. Resseguie[17a], S. Rettie[36], B. Reynolds[118], E. Reynolds[17a], M. Rezaei Estabragh[169], O.L. Rezanova[37], P. Reznicek[132], E. Ricci[77a,77b], R. Richter[109], S. Richter[47a,47b], E. Richter-Was[84b], M. Ridel[126], P. Rieck[116], P. Riedler[36], M. Rijssenbeek[144], A. Rimoldi[72a,72b], M. Rimoldi[48], L. Rinaldi[23b,23a], T.T. Rinn[29], M.P. Rinnagel[108], G. Ripellino[143], I. Riu[13], P. Rivadeneira[48], J.C. Rivera Vergara[163], F. Rizatdinova[120], E. Rizvi[93], C. Rizzi[56], B.A. Roberts[165], B.R. Roberts[17a], S.H. Robertson[103,v], M. Robin[48], D. Robinson[32], C.M. Robles Gajardo[136f], M. Robles Manzano[99], A. Robson[59], A. Rocchi[75a,75b], C. Roda[73a,73b], S. Rodriguez Bosca[63a], Y. Rodriguez Garcia[22a], A. Rodriguez Rodriguez[54], A.M. Rodríguez Vera[155b], S. Roe[36], J.T. Roemer[158], A.R. Roepe-Gier[119], J. Roggel[169], O. Røhne[124], R.A. Rojas[163], B. Roland[54], C.P.A. Roland[67], J. Roloff[29], A. Romaniouk[37], E. Romano[72a,72b], M. Romano[23b], A.C. Romero Hernandez[160], N. Rompotis[91], L. Roos[126], S. Rosati[74a], B.J. Rosser[39], E. Rossi[4], E. Rossi[71a,71b], L.P. Rossi[57b], L. Rossini[48], R. Rosten[118], M. Rotaru[27b], B. Rottler[54], D. Rousseau[66], D. Rousso[32], G. Rovelli[72a,72b], A. Roy[160], A. Rozanov[101], Y. Rozen[149], X. Ruan[33g], A. Rubio Jimenez[161], A.J. Ruby[91], V.H. Ruelas Rivera[18],

JHEP06(2023)036

T.A. Ruggeri[1], F. Rühr[54], A. Ruiz-Martinez[161], A. Rummler[36], Z. Rurikova[54], N.A. Rusakovich[38], H.L. Russell[163], J.P. Rutherfoord[7], K. Rybacki[90], M. Rybar[132], E.B. Rye[124], A. Ryzhov[37], J.A. Sabater Iglesias[56], P. Sabatini[161], L. Sabetta[74a,74b], H.F-W. Sadrozinski[135], F. Safai Tehrani[74a], B. Safarzadeh Samani[145], M. Safdari[142], S. Saha[103], M. Sahinsoy[109], M. Saimpert[134], M. Saito[152], T. Saito[152], D. Salamani[36], G. Salamanna[76a,76b], A. Salnikov[142], J. Salt[161], A. Salvador Salas[13], D. Salvatore[43b,43a], F. Salvatore[145], A. Salzburger[36], D. Sammel[54], D. Sampsonidis[151], D. Sampsonidou[62d,62c], J. Sánchez[161], A. Sanchez Pineda[4], V. Sanchez Sebastian[161], H. Sandaker[124], C.O. Sander[48], J.A. Sandesara[102], M. Sandhoff[169], C. Sandoval[22b], D.P.C. Sankey[133], A. Sansoni[53], L. Santi[74a,74b], C. Santoni[40], H. Santos[129a,129b], S.N. Santpur[17a], A. Santra[167], K.A. Saoucha[138], J.G. Saraiva[129a,129d], J. Sardain[7], O. Sasaki[82], K. Sato[156], C. Sauer[63b], F. Sauerburger[54], E. Sauvan[4], P. Savard[154,ac], R. Sawada[152], C. Sawyer[133], L. Sawyer[96], I. Sayago Galvan[161], C. Sbarra[23b], A. Sbrizzi[23b,23a], T. Scanlon[95], J. Schaarschmidt[137], P. Schacht[109], D. Schaefer[39], U. Schäfer[99], A.C. Schaffer[66], D. Schaile[108], R.D. Schamberger[144], E. Schanet[108], C. Scharf[18], M.M. Schefer[19], V.A. Schegelsky[37], D. Scheirich[132], F. Schenck[18], M. Schernau[158], C. Scheulen[55], C. Schiavi[57b,57a], Z.M. Schillaci[26], E.J. Schioppa[69a,69b], M. Schioppa[43b,43a], B. Schlag[99], K.E. Schleicher[54], S. Schlenker[36], J. Schmeing[169], M.A. Schmidt[169], K. Schmieden[99], C. Schmitt[99], S. Schmitt[48], L. Schoeffel[134], A. Schoening[63b], P.G. Scholer[54], E. Schopf[125], M. Schott[99], J. Schovancova[36], S. Schramm[56], F. Schroeder[169], H-C. Schultz-Coulon[63a], M. Schumacher[54], B.A. Schumm[135], Ph. Schune[134], A. Schwartzman[142], T.A. Schwarz[105], Ph. Schwemling[134], R. Schwienhorst[106], A. Sciandra[135], G. Sciolla[26], F. Scuri[73a], F. Scutti[104], C.D. Sebastiani[91], K. Sedlaczek[49], P. Seema[18], S.C. Seidel[111], A. Seiden[135], B.D. Seidlitz[41], T. Seiss[39], C. Seitz[48], J.M. Seixas[81b], G. Sekhniaidze[71a], S.J. Sekula[44], L. Selem[4], N. Semprini-Cesari[23b,23a], S. Sen[51], D. Sengupta[56], V. Senthilkumar[161], L. Serin[66], L. Serkin[68a,68b], M. Sessa[76a,76b], H. Severini[119], S. Sevova[142], F. Sforza[57b,57a], A. Sfyrla[56], E. Shabalina[55], R. Shaheen[143], J.D. Shahinian[127], D. Shaked Renous[167], L.Y. Shan[14a], M. Shapiro[17a], A. Sharma[36], A.S. Sharma[162], P. Sharma[79], S. Sharma[48], P.B. Shatalov[37], K. Shaw[145], S.M. Shaw[100], Q. Shen[62c,5], P. Sherwood[95], L. Shi[95], C.O. Shimmin[170], Y. Shimogama[166], J.D. Shinner[94], I.P.J. Shipsey[125], S. Shirabe[60], M. Shiyakova[38], J. Shlomi[167], M.J. Shochet[39], J. Shojaii[104], D.R. Shope[124], S. Shrestha[118,ag], E.M. Shrif[33g], M.J. Shroff[163], P. Sicho[130], A.M. Sickles[160], E. Sideras Haddad[33g], A. Sidoti[23b], F. Siegert[50], Dj. Sijacki[15], R. Sikora[84a], F. Sili[89], J.M. Silva[20], M.V. Silva Oliveira[36], S.B. Silverstein[47a], S. Simion[66], R. Simoniello[36], E.L. Simpson[59], N.D. Simpson[97], S. Simsek[21d], S. Sindhu[55], P. Sinervo[154], V. Sinetckii[37], S. Singh[141], S. Singh[154], S. Sinha[48], S. Sinha[33g], M. Sioli[23b,23a], I. Siral[36], S.Yu. Sivoklokov[37,*], J. Sjölin[47a,47b], A. Skaf[55], E. Skorda[97], P. Skubic[119], M. Slawinska[85], V. Smakhtin[167], B.H. Smart[133], J. Smiesko[36], S.Yu. Smirnov[37], Y. Smirnov[37], L.N. Smirnova[37,a], O. Smirnova[97], A.C. Smith[41], E.A. Smith[39], H.A. Smith[125], J.L. Smith[91], R. Smith[142], M. Smizanska[90], K. Smolek[131], A. Smykiewicz[85], A.A. Snesarev[37], H.L. Snoek[113], S. Snyder[29], R. Sobie[163,v], A. Soffer[150], C.A. Solans Sanchez[36], E.Yu. Soldatov[37], U. Soldevila[161],

JHEP06(2023)036

A.A. Solodkov[37], S. Solomon[54], A. Soloshenko[38], K. Solovieva[54], O.V. Solovyanov[37], V. Solovyev[37], P. Sommer[36], A. Sonay[13], W.Y. Song[155b], A. Sopczak[131], A.L. Sopio[95], F. Sopkova[28b], V. Sothilingam[63a], S. Sottocornola[72a,72b], R. Soualah[115c], Z. Soumaimi[35e], D. South[48], S. Spagnolo[69a,69b], M. Spalla[109], F. Spanò[94], D. Sperlich[54], G. Spigo[36], M. Spina[145], S. Spinali[90], D.P. Spiteri[59], M. Spousta[132], E.J. Staats[34], A. Stabile[70a,70b], R. Stamen[63a], M. Stamenkovic[113], A. Stampekis[20], M. Standke[24], E. Stanecka[85], M.V. Stange[50], B. Stanislaus[17a], M.M. Stanitzki[48], M. Stankaityte[125], B. Stapf[48], E.A. Starchenko[37], G.H. Stark[135], J. Stark[101], D.M. Starko[155b], P. Staroba[130], P. Starovoitov[63a], S. Stärz[103], R. Staszewski[85], G. Stavropoulos[46], J. Steentoft[159], P. Steinberg[29], A.L. Steinhebel[122], B. Stelzer[141,155a], H.J. Stelzer[128], O. Stelzer-Chilton[155a], H. Stenzel[58], T.J. Stevenson[145], G.A. Stewart[36], M.C. Stockton[36], G. Stoicea[27b], M. Stolarski[129a], S. Stonjek[109], A. Straessner[50], J. Strandberg[143], S. Strandberg[47a,47b], M. Strauss[119], T. Strebler[101], P. Strizenec[28b], R. Ströhmer[164], D.M. Strom[122], L.R. Strom[48], R. Stroynowski[44], A. Strubig[47a,47b], S.A. Stucci[29], B. Stugu[16], J. Stupak[119], N.A. Styles[48], D. Su[142], S. Su[62a], W. Su[62d,137,62c], X. Su[62a,66], K. Sugizaki[152], V.V. Sulin[37], M.J. Sullivan[91], D.M.S. Sultan[77a,77b], L. Sultanaliyeva[37], S. Sultansoy[3b], T. Sumida[86], S. Sun[105], S. Sun[168], O. Sunneborn Gudnadottir[159], M.R. Sutton[145], M. Svatos[130], M. Swiatlowski[155a], T. Swirski[164], I. Sykora[28a], M. Sykora[132], T. Sykora[132], D. Ta[99], K. Tackmann[48,u], A. Taffard[158], R. Tafirout[155a], J.S. Tafoya Vargas[66], R.H.M. Taibah[126], R. Takashima[87], K. Takeda[83], E.P. Takeva[52], Y. Takubo[82], M. Talby[101], A.A. Talyshev[37], K.C. Tam[64b], N.M. Tamir[150], A. Tanaka[152], J. Tanaka[152], R. Tanaka[66], M. Tanasini[57b,57a], J. Tang[62c], Z. Tao[162], S. Tapia Araya[80], S. Tapprogge[99], A. Tarek Abouelfadl Mohamed[106], S. Tarem[149], K. Tariq[62b], G. Tarna[101,27b], G.F. Tartarelli[70a], P. Tas[132], M. Tasevsky[130], E. Tassi[43b,43a], A.C. Tate[160], G. Tateno[152], Y. Tayalati[35e], G.N. Taylor[104], W. Taylor[155b], H. Teagle[91], A.S. Tee[168], R. Teixeira De Lima[142], P. Teixeira-Dias[94], J.J. Teoh[154], K. Terashi[152], J. Terron[98], S. Terzo[13], M. Testa[53], R.J. Teuscher[154,v], A. Thaler[78], O. Theiner[56], N. Themistokleous[52], T. Theveneaux-Pelzer[18], O. Thielmann[169], D.W. Thomas[94], J.P. Thomas[20], E.A. Thompson[48], P.D. Thompson[20], E. Thomson[127], E.J. Thorpe[93], Y. Tian[55], V. Tikhomirov[37,a], Yu.A. Tikhonov[37], S. Timoshenko[37], E.X.L. Ting[1], P. Tipton[170], S. Tisserant[101], S.H. Tlou[33g], A. Tnourji[40], K. Todome[23b,23a], S. Todorova-Nova[132], S. Todt[50], M. Togawa[82], J. Tojo[88], S. Tokár[28a], K. Tokushuku[82], R. Tombs[32], M. Tomoto[82,110], L. Tompkins[142], K.W. Topolnicki[84b], P. Tornambe[102], E. Torrence[122], H. Torres[50], E. Torró Pastor[161], M. Toscani[30], C. Tosciri[39], M. Tost[11], D.R. Tovey[138], A. Traeet[16], I.S. Trandafir[27b], T. Trefzger[164], A. Tricoli[29], I.M. Trigger[155a], S. Trincaz-Duvoid[126], D.A. Trischuk[26], B. Trocmé[60], A. Trofymov[66], C. Troncon[70a], L. Truong[33c], M. Trzebinski[85], A. Trzupek[85], F. Tsai[144], M. Tsai[105], A. Tsiamis[151], P.V. Tsiareshka[37], S. Tsigaridas[155a], A. Tsirigotis[151,s], V. Tsiskaridze[144], E.G. Tskhadadze[148a], M. Tsopoulou[151], Y. Tsujikawa[86], I.I. Tsukerman[37], V. Tsulaia[17a], S. Tsuno[82], O. Tsur[149], D. Tsybychev[144], Y. Tu[64b], A. Tudorache[27b], V. Tudorache[27b], A.N. Tuna[36], S. Turchikhin[38], I. Turk Cakir[3a], R. Turra[70a], T. Turtuvshin[38,w], P.M. Tuts[41], S. Tzamarias[151], P. Tzanis[10], E. Tzovara[99], K. Uchida[152], F. Ukegawa[156],

JHEP06(2023)036

P.A. Ulloa Poblete[136c], G. Unal[36], M. Unal[11], A. Undrus[29], G. Unel[158], J. Urban[28b], P. Urquijo[104], G. Usai[8], R. Ushioda[153], M. Usman[107], Z. Uysal[21b], L. Vacavant[101], V. Vacek[131], B. Vachon[103], K.O.H. Vadla[124], T. Vafeiadis[36], A. Vaitkus[95], C. Valderanis[108], E. Valdes Santurio[47a,47b], M. Valente[155a], S. Valentinetti[23b,23a], A. Valero[161], A. Vallier[101], J.A. Valls Ferrer[161], T.R. Van Daalen[137], P. Van Gemmeren[6], M. Van Rijnbach[124,36], S. Van Stroud[95], I. Van Vulpen[113], M. Vanadia[75a,75b], W. Vandelli[36], M. Vandenbroucke[134], E.R. Vandewall[120], D. Vannicola[150], L. Vannoli[57b,57a], R. Vari[74a], E.W. Varnes[7], C. Varni[17a], T. Varol[147], D. Varouchas[66], L. Varriale[161], K.E. Varvell[146], M.E. Vasile[27b], L. Vaslin[40], G.A. Vasquez[163], F. Vazeille[40], T. Vazquez Schroeder[36], J. Veatch[31], V. Vecchio[100], M.J. Veen[102], I. Veliscek[125], L.M. Veloce[154], F. Veloso[129a,129c], S. Veneziano[74a], A. Ventura[69a,69b], A. Verbytskyi[109], M. Verducci[73a,73b], C. Vergis[24], M. Verissimo De Araujo[81b], W. Verkerke[113], J.C. Vermeulen[113], C. Vernieri[142], P.J. Verschuuren[94], M. Vessella[102], M.C. Vetterli[141,ac], A. Vgenopoulos[151], N. Viaux Maira[136f], T. Vickey[138], O.E. Vickey Boeriu[138], G.H.A. Viehhauser[125], L. Vigani[63b], M. Villa[23b,23a], M. Villaplana Perez[161], E.M. Villhauer[52], E. Vilucchi[53], M.G. Vincter[34], G.S. Virdee[20], A. Vishwakarma[52], C. Vittori[23b,23a], I. Vivarelli[145], V. Vladimirov[165], E. Voevodina[109], F. Vogel[108], P. Vokac[131], J. Von Ahnen[48], E. Von Toerne[24], B. Vormwald[36], V. Vorobel[132], K. Vorobev[37], M. Vos[161], J.H. Vossebeld[91], M. Vozak[113], L. Vozdecky[93], N. Vranjes[15], M. Vranjes Milosavljevic[15], M. Vreeswijk[113], R. Vuillermet[36], O. Vujinovic[99], I. Vukotic[39], S. Wada[156], C. Wagner[102], W. Wagner[169], S. Wahdan[169], H. Wahlberg[89], R. Wakasa[156], M. Wakida[110], V.M. Walbrecht[109], J. Walder[133], R. Walker[108], W. Walkowiak[140], A.M. Wang[61], A.Z. Wang[168], C. Wang[62a], C. Wang[62c], H. Wang[17a], J. Wang[64a], R.-J. Wang[99], R. Wang[61], R. Wang[6], S.M. Wang[147], S. Wang[62b], T. Wang[62a], W.T. Wang[79], X. Wang[14c], X. Wang[160], X. Wang[62c], Y. Wang[62d], Y. Wang[14c], Z. Wang[105], Z. Wang[62d,51,62c], Z. Wang[105], A. Warburton[103], R.J. Ward[20], N. Warrack[59], A.T. Watson[20], H. Watson[59], M.F. Watson[20], G. Watts[137], B.M. Waugh[95], A.F. Webb[11], C. Weber[29], H.A. Weber[18], M.S. Weber[19], S.M. Weber[63a], C. Wei[62a], Y. Wei[125], A.R. Weidberg[125], J. Weingarten[49], M. Weirich[99], C. Weiser[54], C.J. Wells[48], T. Wenaus[29], B. Wendland[49], T. Wengler[36], N.S. Wenke[109], N. Wermes[24], M. Wessels[63a], K. Whalen[122], A.M. Wharton[90], A.S. White[61], A. White[8], M.J. White[1], D. Whiteson[158], L. Wickremasinghe[123], W. Wiedenmann[168], C. Wiel[50], M. Wielers[133], N. Wieseotte[99], C. Wiglesworth[42], L.A.M. Wiik-Fuchs[54], D.J. Wilbern[119], H.G. Wilkens[36], D.M. Williams[41], H.H. Williams[127], S. Williams[32], S. Willocq[102], P.J. Windischhofer[125], F. Winklmeier[122], B.T. Winter[54], J.K. Winter[100], M. Wittgen[142], M. Wobisch[96], R. Wölker[125], J. Wollrath[158], M.W. Wolter[85], H. Wolters[129a,129c], V.W.S. Wong[162], A.F. Wongel[48], S.D. Worm[48], B.K. Wosiek[85], K.W. Woźniak[85], K. Wraight[59], J. Wu[14a,14d], M. Wu[64a], M. Wu[112], S.L. Wu[168], X. Wu[56], Y. Wu[62a], Z. Wu[134,62a], J. Wuerzinger[125], T.R. Wyatt[100], B.M. Wynne[52], S. Xella[42], L. Xia[14c], M. Xia[14b], J. Xiang[64c], X. Xiao[105], M. Xie[62a], X. Xie[62a], S. Xin[14a,14d], J. Xiong[17a], I. Xiotidis[145], D. Xu[14a], H. Xu[62a], H. Xu[62a], L. Xu[62a], R. Xu[127], T. Xu[105], W. Xu[105], Y. Xu[14b], Z. Xu[62b], Z. Xu[14a], B. Yabsley[146], S. Yacoob[33a], N. Yamaguchi[88], Y. Yamaguchi[153],

JHEP06(2023)036

H. Yamauchi[156], T. Yamazaki[17a], Y. Yamazaki[83], J. Yan[62c], S. Yan[125], Z. Yan[25], H.J. Yang[62c,62d], H.T. Yang[62a], S. Yang[62a], T. Yang[64c], X. Yang[62a], X. Yang[14a], Y. Yang[44], Z. Yang[62a,105], W-M. Yao[17a], Y.C. Yap[48], H. Ye[14c], H. Ye[55], J. Ye[44], S. Ye[29], X. Ye[62a], Y. Yeh[95], I. Yeletskikh[38], B.K. Yeo[17a], M.R. Yexley[90], P. Yin[41], K. Yorita[166], C.J.S. Young[54], C. Young[142], M. Yuan[105], R. Yuan[62b,j], L. Yue[95], X. Yue[63a], M. Zaazoua[35e], B. Zabinski[85], E. Zaid[52], T. Zakareishvili[148b], N. Zakharchuk[34], S. Zambito[56], J.A. Zamora Saa[136d], J. Zang[152], D. Zanzi[54], O. Zaplatilek[131], S.V. Zeißner[49], C. Zeitnitz[169], J.C. Zeng[160], D.T. Zenger Jr[26], O. Zenin[37], T. Ženiš[28a], S. Zenz[93], S. Zerradi[35a], D. Zerwas[66], B. Zhang[14c], D.F. Zhang[138], G. Zhang[14b], J. Zhang[62b], J. Zhang[6], K. Zhang[14a,14d], L. Zhang[14c], P. Zhang[14a,14d], R. Zhang[168], S. Zhang[105], T. Zhang[152], X. Zhang[62c], X. Zhang[62b], Y. Zhang[62c,5], Z. Zhang[17a], Z. Zhang[66], H. Zhao[137], P. Zhao[51], T. Zhao[62b], Y. Zhao[135], Z. Zhao[62a], A. Zhemchugov[38], X. Zheng[62a], Z. Zheng[142], D. Zhong[160], B. Zhou[105], C. Zhou[168], H. Zhou[7], N. Zhou[62c], Y. Zhou[7], C.G. Zhu[62b], C. Zhu[14a,14d], H.L. Zhu[62a], H. Zhu[14a], J. Zhu[105], Y. Zhu[62c], Y. Zhu[62a], X. Zhuang[14a], K. Zhukov[37], V. Zhulanov[37], N.I. Zimine[38], J. Zinsser[63b], M. Ziolkowski[140], L. Živković[15], A. Zoccoli[23b,23a], K. Zoch[56], T.G. Zorbas[138], O. Zormpa[46], W. Zou[41], L. Zwalinski[36]

[1] *Department of Physics, University of Adelaide, Adelaide; Australia*
[2] *Department of Physics, University of Alberta, Edmonton AB; Canada*
[3] [(a)] *Department of Physics, Ankara University, Ankara;* [(b)] *Division of Physics, TOBB University of Economics and Technology, Ankara; Türkiye*
[4] *LAPP, Univ. Savoie Mont Blanc, CNRS/IN2P3, Annecy; France*
[5] *APC, Université Paris Cité, CNRS/IN2P3, Paris; France*
[6] *High Energy Physics Division, Argonne National Laboratory, Argonne IL; United States of America*
[7] *Department of Physics, University of Arizona, Tucson AZ; United States of America*
[8] *Department of Physics, University of Texas at Arlington, Arlington TX; United States of America*
[9] *Physics Department, National and Kapodistrian University of Athens, Athens; Greece*
[10] *Physics Department, National Technical University of Athens, Zografou; Greece*
[11] *Department of Physics, University of Texas at Austin, Austin TX; United States of America*
[12] *Institute of Physics, Azerbaijan Academy of Sciences, Baku; Azerbaijan*
[13] *Institut de Física d'Altes Energies (IFAE), Barcelona Institute of Science and Technology, Barcelona; Spain*
[14] [(a)] *Institute of High Energy Physics, Chinese Academy of Sciences, Beijing;* [(b)] *Physics Department, Tsinghua University, Beijing;* [(c)] *Department of Physics, Nanjing University, Nanjing;* [(d)] *University of Chinese Academy of Science (UCAS), Beijing; China*
[15] *Institute of Physics, University of Belgrade, Belgrade; Serbia*
[16] *Department for Physics and Technology, University of Bergen, Bergen; Norway*
[17] [(a)] *Physics Division, Lawrence Berkeley National Laboratory, Berkeley CA;* [(b)] *University of California, Berkeley CA; United States of America*
[18] *Institut für Physik, Humboldt Universität zu Berlin, Berlin; Germany*
[19] *Albert Einstein Center for Fundamental Physics and Laboratory for High Energy Physics, University of Bern, Bern; Switzerland*
[20] *School of Physics and Astronomy, University of Birmingham, Birmingham; United Kingdom*
[21] [(a)] *Department of Physics, Bogazici University, Istanbul;* [(b)] *Department of Physics Engineering, Gaziantep University, Gaziantep;* [(c)] *Department of Physics, Istanbul University, Istanbul;* [(d)] *Istinye University, Sariyer, Istanbul; Türkiye*
[22] [(a)] *Facultad de Ciencias y Centro de Investigaciónes, Universidad Antonio Nariño, Bogotá;* [(b)] *Departamento de Física, Universidad Nacional de Colombia, Bogotá; Colombia*

JHEP06(2023)036

[23] [(a)] Dipartimento di Fisica e Astronomia A. Righi, Università di Bologna, Bologna;[(b)] INFN Sezione di Bologna; Italy
[24] Physikalisches Institut, Universität Bonn, Bonn; Germany
[25] Department of Physics, Boston University, Boston MA; United States of America
[26] Department of Physics, Brandeis University, Waltham MA; United States of America
[27] [(a)] Transilvania University of Brasov, Brasov;[(b)] Horia Hulubei National Institute of Physics and Nuclear Engineering, Bucharest;[(c)] Department of Physics, Alexandru Ioan Cuza University of Iasi, Iasi;[(d)] National Institute for Research and Development of Isotopic and Molecular Technologies, Physics Department, Cluj-Napoca;[(e)] University Politehnica Bucharest, Bucharest;[(f)] West University in Timisoara, Timisoara;[(g)] Faculty of Physics, University of Bucharest, Bucharest; Romania
[28] [(a)] Faculty of Mathematics, Physics and Informatics, Comenius University, Bratislava;[(b)] Department of Subnuclear Physics, Institute of Experimental Physics of the Slovak Academy of Sciences, Kosice; Slovak Republic
[29] Physics Department, Brookhaven National Laboratory, Upton NY; United States of America
[30] Universidad de Buenos Aires, Facultad de Ciencias Exactas y Naturales, Departamento de Física, y CONICET, Instituto de Física de Buenos Aires (IFIBA), Buenos Aires; Argentina
[31] California State University, CA; United States of America
[32] Cavendish Laboratory, University of Cambridge, Cambridge; United Kingdom
[33] [(a)] Department of Physics, University of Cape Town, Cape Town;[(b)] iThemba Labs, Western Cape;[(c)] Department of Mechanical Engineering Science, University of Johannesburg, Johannesburg;[(d)] National Institute of Physics, University of the Philippines Diliman (Philippines);[(e)] University of South Africa, Department of Physics, Pretoria;[(f)] University of Zululand, KwaDlangezwa;[(g)] School of Physics, University of the Witwatersrand, Johannesburg; South Africa
[34] Department of Physics, Carleton University, Ottawa ON; Canada
[35] [(a)] Faculté des Sciences Ain Chock, Réseau Universitaire de Physique des Hautes Energies - Université Hassan II, Casablanca;[(b)] Faculté des Sciences, Université Ibn-Tofail, Kénitra;[(c)] Faculté des Sciences Semlalia, Université Cadi Ayyad, LPHEA-Marrakech;[(d)] LPMR, Faculté des Sciences, Université Mohamed Premier, Oujda;[(e)] Faculté des sciences, Université Mohammed V, Rabat;[(f)] Institute of Applied Physics, Mohammed VI Polytechnic University, Ben Guerir; Morocco
[36] CERN, Geneva; Switzerland
[37] Affiliated with an institute covered by a cooperation agreement with CERN
[38] Affiliated with an international laboratory covered by a cooperation agreement with CERN
[39] Enrico Fermi Institute, University of Chicago, Chicago IL; United States of America
[40] LPC, Université Clermont Auvergne, CNRS/IN2P3, Clermont-Ferrand; France
[41] Nevis Laboratory, Columbia University, Irvington NY; United States of America
[42] Niels Bohr Institute, University of Copenhagen, Copenhagen; Denmark
[43] [(a)] Dipartimento di Fisica, Università della Calabria, Rende;[(b)] INFN Gruppo Collegato di Cosenza, Laboratori Nazionali di Frascati; Italy
[44] Physics Department, Southern Methodist University, Dallas TX; United States of America
[45] Physics Department, University of Texas at Dallas, Richardson TX; United States of America
[46] National Centre for Scientific Research "Demokritos", Agia Paraskevi; Greece
[47] [(a)] Department of Physics, Stockholm University;[(b)] Oskar Klein Centre, Stockholm; Sweden
[48] Deutsches Elektronen-Synchrotron DESY, Hamburg and Zeuthen; Germany
[49] Fakultät Physik , Technische Universität Dortmund, Dortmund; Germany
[50] Institut für Kern- und Teilchenphysik, Technische Universität Dresden, Dresden; Germany
[51] Department of Physics, Duke University, Durham NC; United States of America
[52] SUPA - School of Physics and Astronomy, University of Edinburgh, Edinburgh; United Kingdom
[53] INFN e Laboratori Nazionali di Frascati, Frascati; Italy
[54] Physikalisches Institut, Albert-Ludwigs-Universität Freiburg, Freiburg; Germany
[55] II. Physikalisches Institut, Georg-August-Universität Göttingen, Göttingen; Germany
[56] Département de Physique Nucléaire et Corpusculaire, Université de Genève, Genève; Switzerland
[57] [(a)] Dipartimento di Fisica, Università di Genova, Genova;[(b)] INFN Sezione di Genova; Italy

JHEP06(2023)036

[58] II. Physikalisches Institut, Justus-Liebig-Universität Giessen, Giessen; Germany
[59] SUPA - School of Physics and Astronomy, University of Glasgow, Glasgow; United Kingdom
[60] LPSC, Université Grenoble Alpes, CNRS/IN2P3, Grenoble INP, Grenoble; France
[61] Laboratory for Particle Physics and Cosmology, Harvard University, Cambridge MA; United States of America
[62] [(a)] Department of Modern Physics and State Key Laboratory of Particle Detection and Electronics, University of Science and Technology of China, Hefei;[(b)] Institute of Frontier and Interdisciplinary Science and Key Laboratory of Particle Physics and Particle Irradiation (MOE), Shandong University, Qingdao;[(c)] School of Physics and Astronomy, Shanghai Jiao Tong University, Key Laboratory for Particle Astrophysics and Cosmology (MOE), SKLPPC, Shanghai;[(d)] Tsung-Dao Lee Institute, Shanghai; China
[63] [(a)] Kirchhoff-Institut für Physik, Ruprecht-Karls-Universität Heidelberg, Heidelberg;[(b)] Physikalisches Institut, Ruprecht-Karls-Universität Heidelberg, Heidelberg; Germany
[64] [(a)] Department of Physics, Chinese University of Hong Kong, Shatin, N.T., Hong Kong;[(b)] Department of Physics, University of Hong Kong, Hong Kong;[(c)] Department of Physics and Institute for Advanced Study, Hong Kong University of Science and Technology, Clear Water Bay, Kowloon, Hong Kong; China
[65] Department of Physics, National Tsing Hua University, Hsinchu; Taiwan
[66] IJCLab, Université Paris-Saclay, CNRS/IN2P3, 91405, Orsay; France
[67] Department of Physics, Indiana University, Bloomington IN; United States of America
[68] [(a)] INFN Gruppo Collegato di Udine, Sezione di Trieste, Udine;[(b)] ICTP, Trieste;[(c)] Dipartimento Politecnico di Ingegneria e Architettura, Università di Udine, Udine; Italy
[69] [(a)] INFN Sezione di Lecce;[(b)] Dipartimento di Matematica e Fisica, Università del Salento, Lecce; Italy
[70] [(a)] INFN Sezione di Milano;[(b)] Dipartimento di Fisica, Università di Milano, Milano; Italy
[71] [(a)] INFN Sezione di Napoli;[(b)] Dipartimento di Fisica, Università di Napoli, Napoli; Italy
[72] [(a)] INFN Sezione di Pavia;[(b)] Dipartimento di Fisica, Università di Pavia, Pavia; Italy
[73] [(a)] INFN Sezione di Pisa;[(b)] Dipartimento di Fisica E. Fermi, Università di Pisa, Pisa; Italy
[74] [(a)] INFN Sezione di Roma;[(b)] Dipartimento di Fisica, Sapienza Università di Roma, Roma; Italy
[75] [(a)] INFN Sezione di Roma Tor Vergata;[(b)] Dipartimento di Fisica, Università di Roma Tor Vergata, Roma; Italy
[76] [(a)] INFN Sezione di Roma Tre;[(b)] Dipartimento di Matematica e Fisica, Università Roma Tre, Roma; Italy
[77] [(a)] INFN-TIFPA;[(b)] Università degli Studi di Trento, Trento; Italy
[78] Universität Innsbruck, Department of Astro and Particle Physics, Innsbruck; Austria
[79] University of Iowa, Iowa City IA; United States of America
[80] Department of Physics and Astronomy, Iowa State University, Ames IA; United States of America
[81] [(a)] Departamento de Engenharia Elétrica, Universidade Federal de Juiz de Fora (UFJF), Juiz de Fora;[(b)] Universidade Federal do Rio De Janeiro COPPE/EE/IF, Rio de Janeiro;[(c)] Instituto de Física, Universidade de São Paulo, São Paulo;[(d)] Rio de Janeiro State University, Rio de Janeiro; Brazil
[82] KEK, High Energy Accelerator Research Organization, Tsukuba; Japan
[83] Graduate School of Science, Kobe University, Kobe; Japan
[84] [(a)] AGH University of Science and Technology, Faculty of Physics and Applied Computer Science, Krakow;[(b)] Marian Smoluchowski Institute of Physics, Jagiellonian University, Krakow; Poland
[85] Institute of Nuclear Physics Polish Academy of Sciences, Krakow; Poland
[86] Faculty of Science, Kyoto University, Kyoto; Japan
[87] Kyoto University of Education, Kyoto; Japan
[88] Research Center for Advanced Particle Physics and Department of Physics, Kyushu University, Fukuoka ; Japan
[89] Instituto de Física La Plata, Universidad Nacional de La Plata and CONICET, La Plata; Argentina
[90] Physics Department, Lancaster University, Lancaster; United Kingdom
[91] Oliver Lodge Laboratory, University of Liverpool, Liverpool; United Kingdom
[92] Department of Experimental Particle Physics, Jožef Stefan Institute and Department of Physics, University of Ljubljana, Ljubljana; Slovenia

JHEP06(2023)036

[93] School of Physics and Astronomy, Queen Mary University of London, London; United Kingdom
[94] Department of Physics, Royal Holloway University of London, Egham; United Kingdom
[95] Department of Physics and Astronomy, University College London, London; United Kingdom
[96] Louisiana Tech University, Ruston LA; United States of America
[97] Fysiska institutionen, Lunds universitet, Lund; Sweden
[98] Departamento de Física Teorica C-15 and CIAFF, Universidad Autónoma de Madrid, Madrid; Spain
[99] Institut für Physik, Universität Mainz, Mainz; Germany
[100] School of Physics and Astronomy, University of Manchester, Manchester; United Kingdom
[101] CPPM, Aix-Marseille Université, CNRS/IN2P3, Marseille; France
[102] Department of Physics, University of Massachusetts, Amherst MA; United States of America
[103] Department of Physics, McGill University, Montreal QC; Canada
[104] School of Physics, University of Melbourne, Victoria; Australia
[105] Department of Physics, University of Michigan, Ann Arbor MI; United States of America
[106] Department of Physics and Astronomy, Michigan State University, East Lansing MI; United States of America
[107] Group of Particle Physics, University of Montreal, Montreal QC; Canada
[108] Fakultät für Physik, Ludwig-Maximilians-Universität München, München; Germany
[109] Max-Planck-Institut für Physik (Werner-Heisenberg-Institut), München; Germany
[110] Graduate School of Science and Kobayashi-Maskawa Institute, Nagoya University, Nagoya; Japan
[111] Department of Physics and Astronomy, University of New Mexico, Albuquerque NM; United States of America
[112] Institute for Mathematics, Astrophysics and Particle Physics, Radboud University/Nikhef, Nijmegen; Netherlands
[113] Nikhef National Institute for Subatomic Physics and University of Amsterdam, Amsterdam; Netherlands
[114] Department of Physics, Northern Illinois University, DeKalb IL; United States of America
[115] [(a)] New York University Abu Dhabi, Abu Dhabi;[(b)] United Arab Emirates University, Al Ain;[(c)] University of Sharjah, Sharjah; United Arab Emirates
[116] Department of Physics, New York University, New York NY; United States of America
[117] Ochanomizu University, Otsuka, Bunkyo-ku, Tokyo; Japan
[118] Ohio State University, Columbus OH; United States of America
[119] Homer L. Dodge Department of Physics and Astronomy, University of Oklahoma, Norman OK; United States of America
[120] Department of Physics, Oklahoma State University, Stillwater OK; United States of America
[121] Palacký University, Joint Laboratory of Optics, Olomouc; Czech Republic
[122] Institute for Fundamental Science, University of Oregon, Eugene, OR; United States of America
[123] Graduate School of Science, Osaka University, Osaka; Japan
[124] Department of Physics, University of Oslo, Oslo; Norway
[125] Department of Physics, Oxford University, Oxford; United Kingdom
[126] LPNHE, Sorbonne Université, Université Paris Cité, CNRS/IN2P3, Paris; France
[127] Department of Physics, University of Pennsylvania, Philadelphia PA; United States of America
[128] Department of Physics and Astronomy, University of Pittsburgh, Pittsburgh PA; United States of America
[129] [(a)] Laboratório de Instrumentação e Física Experimental de Partículas - LIP, Lisboa;[(b)] Departamento de Física, Faculdade de Ciências, Universidade de Lisboa, Lisboa;[(c)] Departamento de Física, Universidade de Coimbra, Coimbra;[(d)] Centro de Física Nuclear da Universidade de Lisboa, Lisboa;[(e)] Departamento de Física, Universidade do Minho, Braga;[(f)] Departamento de Física Teórica y del Cosmos, Universidad de Granada, Granada (Spain);[(g)] Departamento de Física, Instituto Superior Técnico, Universidade de Lisboa, Lisboa; Portugal
[130] Institute of Physics of the Czech Academy of Sciences, Prague; Czech Republic
[131] Czech Technical University in Prague, Prague; Czech Republic
[132] Charles University, Faculty of Mathematics and Physics, Prague; Czech Republic
[133] Particle Physics Department, Rutherford Appleton Laboratory, Didcot; United Kingdom

JHEP06(2023)036

[134] IRFU, CEA, Université Paris-Saclay, Gif-sur-Yvette; France
[135] Santa Cruz Institute for Particle Physics, University of California Santa Cruz, Santa Cruz CA; United States of America
[136] [(a)] Departamento de Física, Pontificia Universidad Católica de Chile, Santiago; [(b)] Millennium Institute for Subatomic physics at high energy frontier (SAPHIR), Santiago; [(c)] Instituto de Investigación Multidisciplinario en Ciencia y Tecnología, y Departamento de Física, Universidad de La Serena; [(d)] Universidad Andres Bello, Department of Physics, Santiago; [(e)] Instituto de Alta Investigación, Universidad de Tarapacá, Arica; [(f)] Departamento de Física, Universidad Técnica Federico Santa María, Valparaíso; Chile
[137] Department of Physics, University of Washington, Seattle WA; United States of America
[138] Department of Physics and Astronomy, University of Sheffield, Sheffield; United Kingdom
[139] Department of Physics, Shinshu University, Nagano; Japan
[140] Department Physik, Universität Siegen, Siegen; Germany
[141] Department of Physics, Simon Fraser University, Burnaby BC; Canada
[142] SLAC National Accelerator Laboratory, Stanford CA; United States of America
[143] Department of Physics, Royal Institute of Technology, Stockholm; Sweden
[144] Departments of Physics and Astronomy, Stony Brook University, Stony Brook NY; United States of America
[145] Department of Physics and Astronomy, University of Sussex, Brighton; United Kingdom
[146] School of Physics, University of Sydney, Sydney; Australia
[147] Institute of Physics, Academia Sinica, Taipei; Taiwan
[148] [(a)] E. Andronikashvili Institute of Physics, Iv. Javakhishvili Tbilisi State University, Tbilisi; [(b)] High Energy Physics Institute, Tbilisi State University, Tbilisi; [(c)] University of Georgia, Tbilisi; Georgia
[149] Department of Physics, Technion, Israel Institute of Technology, Haifa; Israel
[150] Raymond and Beverly Sackler School of Physics and Astronomy, Tel Aviv University, Tel Aviv; Israel
[151] Department of Physics, Aristotle University of Thessaloniki, Thessaloniki; Greece
[152] International Center for Elementary Particle Physics and Department of Physics, University of Tokyo, Tokyo; Japan
[153] Department of Physics, Tokyo Institute of Technology, Tokyo; Japan
[154] Department of Physics, University of Toronto, Toronto ON; Canada
[155] [(a)] TRIUMF, Vancouver BC; [(b)] Department of Physics and Astronomy, York University, Toronto ON; Canada
[156] Division of Physics and Tomonaga Center for the History of the Universe, Faculty of Pure and Applied Sciences, University of Tsukuba, Tsukuba; Japan
[157] Department of Physics and Astronomy, Tufts University, Medford MA; United States of America
[158] Department of Physics and Astronomy, University of California Irvine, Irvine CA; United States of America
[159] Department of Physics and Astronomy, University of Uppsala, Uppsala; Sweden
[160] Department of Physics, University of Illinois, Urbana IL; United States of America
[161] Instituto de Física Corpuscular (IFIC), Centro Mixto Universidad de Valencia - CSIC, Valencia; Spain
[162] Department of Physics, University of British Columbia, Vancouver BC; Canada
[163] Department of Physics and Astronomy, University of Victoria, Victoria BC; Canada
[164] Fakultät für Physik und Astronomie, Julius-Maximilians-Universität Würzburg, Würzburg; Germany
[165] Department of Physics, University of Warwick, Coventry; United Kingdom
[166] Waseda University, Tokyo; Japan
[167] Department of Particle Physics and Astrophysics, Weizmann Institute of Science, Rehovot; Israel
[168] Department of Physics, University of Wisconsin, Madison WI; United States of America
[169] Fakultät für Mathematik und Naturwissenschaften, Fachgruppe Physik, Bergische Universität Wuppertal, Wuppertal; Germany
[170] Department of Physics, Yale University, New Haven CT; United States of America

[a] Also Affiliated with an institute covered by a cooperation agreement with CERN

JHEP06(2023)036

[b] Also at Borough of Manhattan Community College, City University of New York, New York NY; United States of America
[c] Also at Bruno Kessler Foundation, Trento; Italy
[d] Also at Center for High Energy Physics, Peking University; China
[e] Also at Centro Studi e Ricerche Enrico Fermi; Italy
[f] Also at CERN, Geneva; Switzerland
[g] Also at Département de Physique Nucléaire et Corpusculaire, Université de Genève, Genève; Switzerland
[h] Also at Departament de Fisica de la Universitat Autonoma de Barcelona, Barcelona; Spain
[i] Also at Department of Financial and Management Engineering, University of the Aegean, Chios; Greece
[j] Also at Department of Physics and Astronomy, Michigan State University, East Lansing MI; United States of America
[k] Also at Department of Physics and Astronomy, University of Louisville, Louisville, KY; United States of America
[l] Also at Department of Physics, Ben Gurion University of the Negev, Beer Sheva; Israel
[m] Also at Department of Physics, California State University, East Bay; United States of America
[n] Also at Department of Physics, California State University, Sacramento; United States of America
[o] Also at Department of Physics, King's College London, London; United Kingdom
[p] Also at Department of Physics, University of Fribourg, Fribourg; Switzerland
[q] Also at Department of Physics, University of Thessaly; Greece
[r] Also at Department of Physics, Westmont College, Santa Barbara; United States of America
[s] Also at Hellenic Open University, Patras; Greece
[t] Also at Institucio Catalana de Recerca i Estudis Avancats, ICREA, Barcelona; Spain
[u] Also at Institut für Experimentalphysik, Universität Hamburg, Hamburg; Germany
[v] Also at Institute of Particle Physics (IPP); Canada
[w] Also at Institute of Physics and Technology, Ulaanbaatar; Mongolia
[x] Also at Institute of Physics, Azerbaijan Academy of Sciences, Baku; Azerbaijan
[y] Also at Institute of Theoretical Physics, Ilia State University, Tbilisi; Georgia
[z] Also at Lawrence Livermore National Laboratory, Livermore; United States of America
[aa] Also at RWTH Aachen University, III. Physikalisches Institut A, Aachen; Germany
[ab] Also at The Collaborative Innovation Center of Quantum Matter (CICQM), Beijing; China
[ac] Also at TRIUMF, Vancouver BC; Canada
[ad] Also at Università di Napoli Parthenope, Napoli; Italy
[ae] Also at University of Chinese Academy of Sciences (UCAS), Beijing; China
[af] Also at University of Colorado Boulder, Department of Physics, Colorado; United States of America
[ag] Also at Washington College, Maryland; United States of America
[ah] Also at Yeditepe University, Physics Department, Istanbul; Türkiye
[ai] Also at Physics Department, An-Najah National University, Nablus; Palestine
[*] Deceased

JHEP06(2023)036